

# COMPUTER AIDED DESIGN OF CAM MODULATED LINKAGES

*A Thesis Submitted  
in Partial Fulfilment of the Requirements  
for the Degree of  
MASTER OF TECHNOLOGY*

**126601**

*by*

**SANDEEP KULKARNI**

*to the*

**DEPARTMENT OF MECHANICAL ENGINEERING  
INDIAN INSTITUTE OF TECHNOLOGY, KANPUR**

**MAY, 1989**

5 OCT 1989

CENTRAL LIBRARY

Doc. No. 105929

TH

621.838

K 959 c

ME-1989-M-KUL-COM.

CERTIFICATE.

8/5/89

This is to certify that the work entitled *Computer Aided Design of Cam Modulated Linkages* by Sandeep Kulkarni has been carried out under our supervision and has not been submitted elsewhere for the award of a degree.

*A. K. Mallik*  
6/5/89

Dr. A.K. Mallik,

Professor,

Dept. of Mech. Engg.,

I.I.T. Kanpur.

*B. Sahay*

Dr. B. Sahay,

Professor,

Dept. of Mech. Engg.,

I.I.T. Kanpur.

With all the formalism in the work tied up neatly, I pause for a while with thoughts beyond the reach of words.

It was Prof. Dhande who laid the roots of this work. Discussions with him - first in person, and then through letters - have given me a lot of confidence all-throughout.

The work stands in the ground of various facilities made available by Prof. Sahay. His continual help and the concern for me - even about things apart from the work, are unforgettable.

In the work are dissolved, inseperable suggestions and guide-lines from Prof. Mallik, with whom the time for me seemed to be infinite. Pains taken by him, especially in the later stages, have greatly helped in bringing out my ideas effectively.

There are many things I learned from my friends at IIT-K. Moments with them will reside in my memory forever.

Sandeep.

# CONTENTS.

|      |   |    |
|------|---|----|
|      | ABSTRACT  |    |
| I    | INTRODUCTION                                    | 1  |
| 1.1  | Introduction.                                   | 1  |
| 1.2. | Scope and objective of the work.                | 5  |
| II   | DESIGN PROCEDURE                                | 8  |
| 2.1  | Preliminaries.                                  | 8  |
| 2.2  | Systems of coordinates.                         | 8  |
| 2.3  | Trajectory specification.                       | 10 |
| 2.4  | Synthesis of CMLs.                              | 11 |
| 2.5  | Assembly of motion components.                  | 20 |
| 2.6  | Analysis.                                       | 23 |
| III  | COMPUTATIONAL ASPECTS.                          | 26 |
| 3.1  | Linkage analysis.                               | 26 |
| 3.2  | Linkage synthesis.                              | 29 |
| 3.3  | Cam design.                                     | 32 |
| 3.4  | Application to a non-differentiable trajectory. | 32 |
| 3.5  | Application to a differentiable trajectory.     | 41 |
| IV   | PRACTICAL CONSIDERATIONS.                       | 51 |
| 4.1  | Considerations in the motion assembly.          | 51 |
| 4.2  | Generation of higher degrees of freedom.        | 57 |
| 4.3  | Summary.  | 60 |
| V    | OPTIMUM DESIGN OF CAM-FOLLOWER SYSTEMS.         | 62 |
| 5.1  | Introduction.                                   | 62 |
| 5.2  | Formulation of the optimization problem.        | 64 |
| 5.3  | Solution of the optimization problem.           | 66 |
| 5.4  | Zoutendijk's method for nonlinear optimization. | 68 |
| 5.5  | Application of the Zoutendijk's procedure.      | 71 |
| 5.6  | Limitations of the Zoutendijk's procedure.      | 80 |

|     |   |     |
|-----|---|-----|
| VI  | APPLICATION TO TYPICAL CAM-FOLLOWERS.             | 82  |
| 6.1 | Preliminaries.                                    | 82  |
| 6.2 | Translating roller follower mechanism.            | 85  |
| 6.3 | Oscillating roller follower mechanism.            | 95  |
| 6.4 | Flat faced followers.                             | 100 |
| 6.4 | General discussion on the optimization procedure. | 100 |

|     |                         |     |
|-----|-------------------------|-----|
| VII | IMPLEMENTATION.         | 105 |
| 7.1 | Scope and assumptions.  | 105 |
| 7.2 | Data structures.        | 106 |
| 7.3 | Programme structure.    | 109 |
| 7.4 | User interaction.       | 111 |
| 7.5 | Programme control flow. | 114 |

|      |                               |     |
|------|-------------------------------|-----|
| VIII | CONCLUSIONS AND FURTHER WORK. | 117 |
| 8.1  | Conclusions                   | 117 |
| 8.2  | Scope for further work.       | 118 |

## REFERENCES

|              |  |      |
|--------------|--|------|
| Appendix — A | The Newton-Raphson's method.                 | A- 1 |
| Appendix — B | Expressions used for cam design.             | A- 4 |
| Appendix — C | Expressions used for the assembly of motion. | A-13 |
| Appendix — D | Further computational aspects of analysis.   | A-16 |

## ABSTRACT

Industry often demands the generation of preprogrammed motion. In fixed automation, it becomes necessary many a times to have a mechanism which generates a predefined motion with high accuracy and repeatability, and at a high speed. Computer controlled robots become unsuitable in such cases owing to their relatively lesser motion resolution, low repeatability, and high cost. A multi-degree-of-freedom mechanism, composed of cam modulated linkages, is proposed as a means of achieving the above requirements. The simplicity in the design and manufacture, and capability to generate precisely controlled motion including the generation of non-differentiable paths, makes these mechanisms very useful. An attempt is made in the present work to develop a procedure for the design of these mechanisms.

The present work comprises of three parts. In the first part, a strategy for the design of cam modulated linkages capable of generating a given trajectory, has been developed. Along with a procedure to synthesise and analyse the mechanisms, critical hardware and practical design issues are also discussed. Examples supporting the proposed method are presented.

The second part is an extension of the design of cam modulated linkages, in which, a method is proposed for the optimal synthesis of cam follower mechanisms, to minimize the cam size in consideration of operational constraints.

In the third part, software to assist the design of the cam modulated linkages incorporating the above two parts has been developed.

## chapter 1. INTRODUCTION

### 1.1 Introduction.

In fixed automation, it is frequently necessary to generate programmed motion which remains unchanged for a large number of operation cycles. Typical applications include mechanical part handlers on assembly lines, and profile cutting machines operating at a mass production rate. The demands on the machines producing such a motion are that they should be inexpensive, accurate, and preprogrammable. Though computer controlled reprogrammable robots can be used in such cases, they have certain limitations in that they are expensive, have lower repeatability, and lower motion resolution. Also, they cannot be made to operate at very high speeds. In such cases, mechanical devices termed as *mechanical robots*, can be employed. In these devices, the output motion is governed through mechanical elements like cams and linkages, and is achieved by pre-designing the geometry of these elements.

Many of these applications generally demand more than one degree-of-freedom in the output motion. The profile cutters for example, require a feed rate control, and a speed or depth of cut rate control, independent of each other. Similarly, the assembly part handlers may need a *stroke* and a *lift*, or *swing* about some axis, and a *lift*, which again may be independent of each other. There is generally one single prime mover in mechanical devices from which power is extracted. To have more than a single degree-of-freedom motion, it becomes necessary to have as many number of constrained mechanisms as the number of degrees-of-freedom, each taking power from the same shaft, and each controlling

one component of motion. Thus the  $n$  dimensional motion gets divided into  $n$  components, each generated independently by one mechanism according to specified requirements. Planar mechanisms can be used to govern the motion in each direction, and this proves to be a simpler choice from design and manufacturing point of view.

In as far as the generation of planar motion is concerned, linkages will be the first choice. However, when a precise control over the output position and velocity or acceleration throughout the motion is needed, linkages become unsuitable. For each specified point of the output motion, there will be one mathematical condition in terms of the geometric parameters of the mechanism. Therefore, to have an infinite point accurate motion, the mechanism requires an infinite number of geometric parameters to specify its dimensions. The cam mechanism is such a mechanism; the points on the cam profile being the design parameters. However, as is shown in the present work, the use of just a cam mechanism is not sufficient in most of the cases, since the range of motion that can be extracted out of a cam is generally small, unless the cam itself happens to be large. Also, most of the time, it is better to use an oscillating roller follower since it permits the use of a larger pressure angle. In such cases, there would be a necessity of converting angular motion to linear. Moreover, in some cases, the cam profile may turn out to be too complex to be of any practical use. In all such situations, if this higher pair could be used as a part of a cam modulated linkage (CML for short), all purposes - viz. magnification of motion, conversion from angular to linear (and vice-versa), and alleviating the demands on the cam profile through the input output relationships of the linkage - would be served. Hence a cam modulated linkage becomes a better choice in this application. A multi degree-of-freedom mechanism with planar cam modulated linkages governing one degree of

freedom each, is proposed in the present work.

A large number of methods for the design of linkages and cams taken as individual elements have been developed. (Ref [1], [2], [5], [6], [7], [11]) However, only a few methods exist for the design of cam modulated linkages. Number synthesis of CMLs has been done by Kohli and Singh [8], and Sandor and Erdman [11]. Sandor and Erdman [11] have discussed the necessity and sufficiency criterion for a simple linkage to be converted to a cam modulated linkage. A few analytical methods for the design of CMLs have been proposed by Kohli and Singh [8].

The first important step in the design of CMLs is that of number synthesis in which either by the enumeration and classification technique [11] or otherwise, all CMLs having the same constructional features are evaluated, and a selection from these based on the application is made. In our case, it can be seen that the cams and linkages used in the mechanism actually serve two different purposes. Cams in particular are used to have a programmed output motion in which the displacements, velocities, accelerations and dwells if any, take place in a kinematically controlled manner. Linkages on the other hand serve the purpose of motion magnification, and conversion of motion from one type to another. (Angular to linear, etc.) This shows that a modularity exists between the linkages and cams. Hence it should be easier to design and manufacture these units if cams be used in the first stage of motion transfer and linkages in the second. The input from the shaft at a constant angular velocity, can be converted to a desired time function of the follower displacement, velocity etc. by the cam; and the linkage may further magnify or convert this motion to a desired type, prior to passing it to the output end. Coordination and combination of individual motion components form an important part of design and is achieved through elements termed as *motion assemblers*.

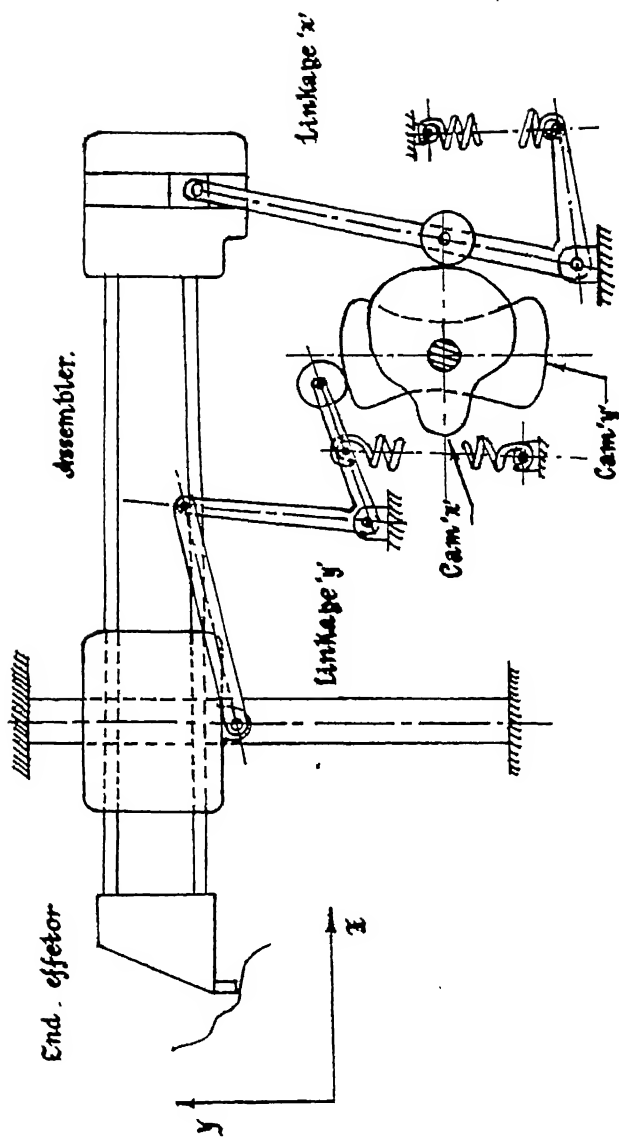


Fig 1.1. A schematic layout of a typical  
CMD - type mechanical robot.

Fig. 1.1 shows a schematic sketch of a 2 degrees-of-freedom motion generating mechanism based on the above principle, producing motion in the x-y plane as a combination of motions along x and y directions. As can be seen from the figure, both the motions are independent of each other, and are finally coupled by means of the assembler.

The second step in the design of mechanisms comprises of dimensional synthesis in which geometric parameters of all the components in the system are designed. To restrict the size of the cam within reasonable limits, it becomes necessary to limit the cam-follower displacements within a certain range. Linkage synthesis primarily comprises of coordinating this range with the end effector motion range in that particular direction.

Cam design comprises of designing the follower parameters, (e.g. the arm length, roller radius etc., for an oscillating roller follower) and the synthesis of the cam profile. In designing the follower parameters, the approach is to reduce the cam size to the maximum possible extent, and an optimizing algorithm has been used for this purpose. Cam profile design is based on these follower parameters, and the follower motion which can be determined by performing the inverse analysis of the designed linkage.

## 1.2 Scope and objective of the work.

Industry has been using the type of mechanisms described above. However, a formal study regarding the different design issues remained to be done. It was sought at the commencement of this work to explore these aspects, and to implement them in the form of an interactive programme.

A generalised approach for cam and linkage design was felt necessary to facilitate computation. Most of the methods for linkage design use analytical expressions needed for the particular linkage under consideration. However, since here, a large number of such linkages would be involved, it would not be feasible to use analytical expressions for each of the possible linkages. Also, doing so would limit the application of the procedure to only those linkages which were considered at the stage of implementation.

Since the design primarily involves the determination of all the geometric parameters of the mechanism, a need was felt to develop a strategy for the design of the cam-follower parameters which are normally based on general judgement, considerations of space etc., or deduced from some standard nomograms.

In view of the above aspects, the following points reflect the objectives of the present work.

- Formulation of the linkage synthesis and analysis problem in a generalised form.
- Development of a design scheme suitable for the mechanisms described earlier, by bringing together existing methods of cam and linkage design.
- A general study as regards the applicability and limitations of these mechanisms, including some related practical issues.
- Building up a strategy for the optimal design of the follower parameters.
- Development of a software incorporating all these ideas, followed by the testing with a few possible mechanisms.

#### Scope.

In the present work only 2 degrees-of-freedom systems have been dealt with,

and the resulting motion of two, and two and half dimensions of space (Sect. 4.2.1) has been discussed. The principle remains the same for a larger number of degrees-of-freedom. The cams considered are of the *disc* type. The method for design however, is developed in such a way that 3-d cams can also be included. Linkages are assumed to be of four joints only, with any combination of revolute and prismatic joints. In most of the cases these will suffice and it will be rarely necessary to go beyond what is offered by a four bar chain for this application.

#### Division of the work.

With the objectives as mentioned above, the work has been subdivided into the following parts.

1. CML design.
2. Follower parameter optimization.
3. Software development incorporating (1) and (2) above.

CML design has been discussed in chapters 2, 3, and 4. The design procedure is developed in Chapter 2. Chapter 3 discusses the details of the computational and other details of the design. Chapter 4 deals with the hardware, and practical issues. Chapters 5 and 6 are devoted to the design of the follower parameters in view of optimization of the cam size. Details of the implementation appear in chapter 7. Finally, the conclusions and possibilities of further work are mentioned in chapter 8.

## chapter 2. DESIGN PROCEDURE

### 2.1 Preliminaries.

The design problem under consideration can be stated as:

"Given an arbitrary trajectory expressible in two planar independent variables (angular or linear), to design cam modulated linkages which will be capable of generating this trajectory."

The procedure consists of the following steps:

1. Trajectory specification, in which the path to be followed and the end effector kinematics are represented in a way so as to facilitate the subsequent synthesis.
2. Synthesis of Cam Modulated Linkages (CML) for each independent direction. i.e for each degree of freedom.
3. Assembly and coordination of the motion generated by the CML for each direction.
4. Analysis of the designed mechanism to test its performance, and resynthesis if needed.

These are explained in the following paragraphs.

### 2.2 Systems of coordinates.

We shall in general have  $D_f + 2$  permanently fixed coordinate systems, (Fig. 2.1) where  $D_f$  is the number of CMLs in the mechanism i.e. the number of degrees-of-

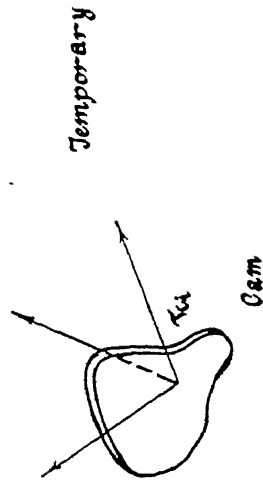
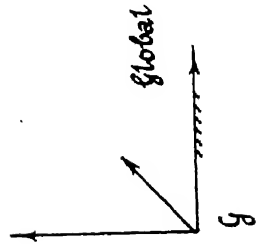
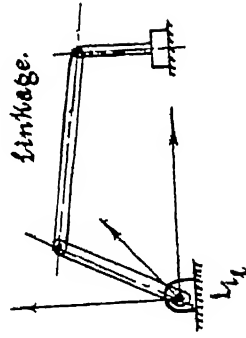
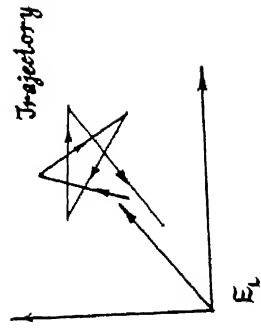


Fig 2.1. Systems of Coordinates.

freedom (2 in our case). These will be as follows.

- One global coordinate system  $G$ .
- One local coordinate system  $E_i$  for the expression of end effector displacements.
- $D$ , fixed local coordinate systems  $L_{i,j}$  for the description of linkage configurations. (One coordinate system per linkage)

-  $D$ , temporarily fixed coordinate systems  $T_c$ . These are fixed at the cam centre. They are termed as temporary since the location of the cam centre is unknown at the commencement of design. The temporary coordinate system is used to design the cam-follower mechanism, and after all the cams in the system are synthesised, it is transported to a permanent position during the assembly of the CMLs.

In addition to these, we will have local moving coordinate systems used in the cam profile synthesis; which are explained later.

### 2.3 Trajectory specification.

The trajectory is the motion generated at the end effector of the mechanism. Curves in space are generally represented in terms of  $D-1$  simultaneous equations, where  $D$  is the number of dimensions of the space under consideration. In our case, let  $X_1$  and  $X_2$  be the two dimensions, with time ( $t$ ) as the third dimension. Then the following forms of representations hold.

1. Explicit specification of  $X_2$  and  $X_1$  as functions of  $t$ .

$$X_1 = f_1(t), \quad X_2 = f_2(t).$$

2. Explicit parametric equations.

$$X_1 = f_1(u), \quad X_2 = f_2(u), \quad t = f_3(u).$$

3. One space function, one space-time function.

$$f_1(X_1, X_2) = 0, \quad f_2(X_1, X_2) = g(t).$$

Typically,  $f_1$  will represent the path generated in space,  $f_2$  the length along the curve, and  $g$ , its time variation.

4. Implicit relations in  $X_1$ ,  $X_2$  and  $t$ .

$$f_1(X_1, X_2, t) = 0, \quad f_2(X_1, X_2, t) = 0.$$

These are generally not encountered in practice.

5. In the form of numerical tables over the cycle time.

The actual trajectory followed may be a single continuous function, a piecewise continuous function, or a discrete numeric function. In any of the above forms of representation, the values of  $X_1$ , and  $X_2$  at any given time instant can be determined by the solution of simultaneous equations, or by direct substitution. A search in these directions gives the extreme values of the displacement needed for linkage design.

It can be seen that since  $X_1(t)$ , or  $X_2(t)$  are the motions generated by one single CML, the higher derivatives of these with respect to time need to be continuous for a smooth performance. However, there is no such restriction on  $X_1(X_2)$ . Thus it is possible to generate motion which can be non-differentiable at intermediate points i.e., sharp corners may as well be incorporated in the trajectory.

The trajectory is always represented as a curve in the fixed frame of reference  $E_1$ .

## 2.4 Synthesis of CMLs.

Synthesis comprises of the following:

1. Linkage synthesis, based on the needed range of the output motion and desired range of input motion to the linkage.
2. Inverse analysis of this linkage, to determine the input motion needed over a complete cycle.
3. Design of the cam follower system based on the input motion to the linkage.

#### 2.4.1 Linkage synthesis.

Objective of the linkage synthesis is to coordinate the required range of output motion and desired range of input motion. A generalised method for the design of four bar linkages is presented.

##### Scheme of representation.

Representation in the form of vectors has been used here. (Fig. 2.2) Though we have only four link mechanisms under consideration, an  $n$  vector model with one degree-of-freedom has been used. This is to facilitate the representation of links which can be expressed in the form of more than one vector. eg. a bell crank lever. This is closer to the physical solution in the first place, and is especially useful when a slider joint is involved. Though kinematically the two are equivalent to a single vector, at times the results obtained by treating them so are not of much physical significance. This will be clear from Fig. 2.3.

The linkage is represented as a closed polygon of  $n$  vectors, with the head of one vector at the tail of its following vector. The vectors are termed *links* and the common point of 2 consecutive vectors, a *joint*. The length of each vector if constant, represents the link length, and if variable, is a measure of the displacement of the slider which may be at one of its ends. There will always be a

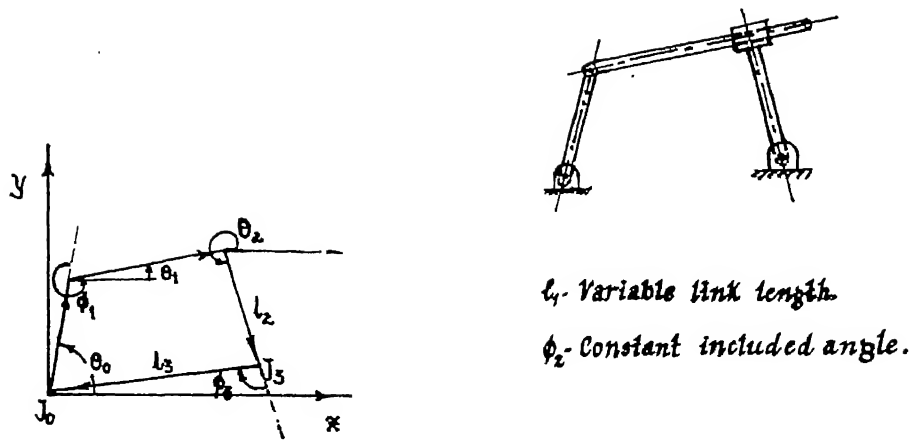
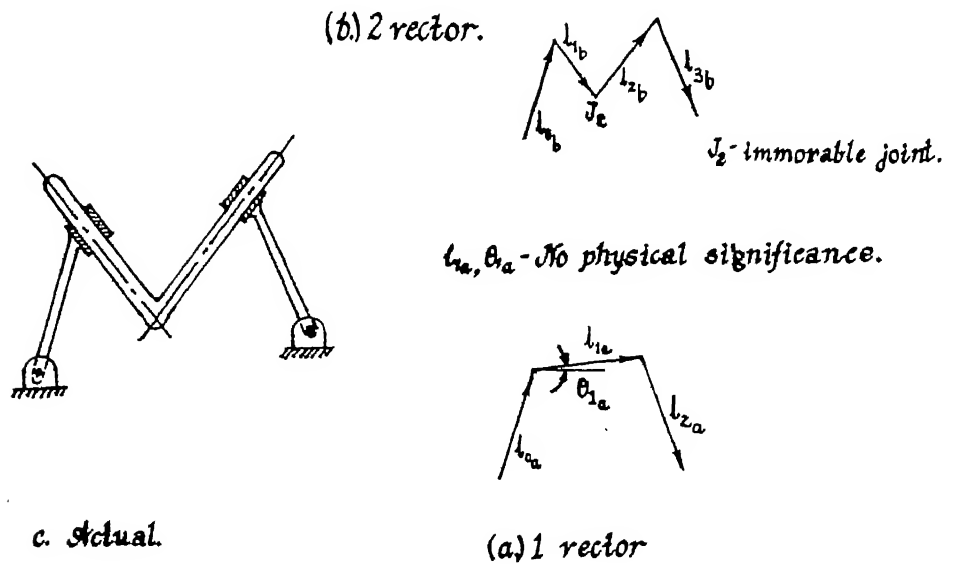


Fig 2.2. Vector representation of linkages.

Fig 2.3. Representation of a slider link.



vector in the direction of reciprocation of a sliding joint.

The links are numbered starting from 0, which is the input link, through  $n-1$ . (  $n \equiv$  the number of links in the loop. ) Link  $n-1$  or  $n-2$  is the output link depending upon whether or not a fixed link (i.e. a vector with fixed length and fixed orientation.) is present in the linkage. The fixed link if present, is numbered as  $n - 1$ . Joints  $i$  are the joints at the tail of the  $i$  th vector.  $\theta_i$  is the angle made by the link  $i$  ( i.e. the directed vector from joint  $i$  to  $i+1$  ) with the positive direction of the reference line. (e.g. X axis if linkage is in the X-Y plane) .  $\phi_i$  is the angle traversed by the extended link  $i-1$  rotated in anticlockwise direction ( positive direction of the axis perpendicular to the plane of the linkage ) about the joint  $i$  to get aligned along the link  $i$ . For all such cases, the following relation holds:

$$\theta_i = \theta_{i-1} + \phi_i \quad (2.0)$$

The angle  $\phi_i$  is constant for sliding and immovable joints and variable for rotating joints. It essentially is the the angle between the links  $i$  and  $i-1$ .

### Number synthesis.

This involves the selection of a particular combination of revolute and prismatic joints from different possible structural configurations. Primary consideration is that of the nature of the input and output motion which decides the nature of the first and last joint of the linkage. viz., rotational or translational. The nature of the input decides the type of cam-follower mechanism to be used, i.e. whether an oscillating or translating follower needs to be employed. Oscillating followers generally prove to be better due to the simplicity of operation and manufacture. The remaining joints can be selected depending on the application.

### Dimensional synthesis.

The loop closure equations for the vector representation of the linkages can be written as :

$$\sum_{i=0}^{n-1} \underline{L}_i = \underline{\bar{0}}. \quad (2.1)$$

where  $\underline{L}_i$  is one of the vectors, and  $\underline{\bar{0}}$ , a null vector.

In terms of the scalar components,

$$\sum_{i=0}^{n-1} l_i \cos(\theta_i) = 0, \quad (2.2a)$$

and

$$\sum_{i=0}^{n-1} l_i \sin(\theta_i) = 0 \quad (2.2b)$$

where  $l_i = |\underline{L}_i|$ , and  $\theta_i$  is the orientation of  $\underline{L}_i$  from the reference axis in the plane of the linkage.

The two extremities of the output motion are the two points at which the input and output is coordinated. There can be additional points, the total number being equal to the number of design parameters. Any number of parameters ( $p_{des}$ ) which can be either  $l_i$ ,  $\theta_i$ , or  $\phi_i$  can be designed, (generally 2 or 3) depending upon the linkage being used.

Let  $p_{out}$  be the output parameter,  $p_{in}$  be the input parameter, and  $p_{sec}$  be the secondary parameter which determines the motion of an intermediate link of the linkage. Let  $p_{out_j}$  and  $p_{in_j}$  ( $j = 1, \dots, m$ ) be the coordinated input-output points. ( $m$  is the number of design variables). Then the loop closure equations at these points are represented as:

$$\left[ \sum_{i=0}^{n-1} l_i \cos(\theta_i) \mid (p_{out} = p_{out_j}, p_{in} = p_{in_j}) \right] = 0, \quad (2.3a)$$

and

$$\left[ \sum_{i=0}^{n-1} l_i \sin(\theta_i) \mid (p_{out} = p_{out_j}, p_{in} = p_{in_j}) \right] = 0. \quad (2.3b)$$

for  $j = 1, \dots, m$ .

These are  $2m$  equations in  $2m$  unknowns ( $p_{des,j}$  and  $p_{sec,j}$ ) which can be solved to get the values of these unknowns. The actual equations which are formed from the substitution of the above constants ( $p_{out,j}$  and  $p_{in,j}$ ) are dependent on the nature of the input, output and the secondary variable. However, the general method of solution remains the same irrespective of these and can be easily taken care of in the computational phase. (Section 3.2).

Note : With a slider joint, it is possible to design the angle  $\phi_i$  also, if needed, and can be incorporated in equations (2.3) by means of equation (2.0).

Inverse analysis of the linkage is done by analysing the linkage formed by reversing the sequence of joints in the designed linkage. Analysis of linkages is discussed in section 2.6.

#### 2.4.2 Cam synthesis.

Objective of the cam synthesis is to determine the follower parameters and the cam profile which will generate a programmed motion serving as the input motion to the linkage. Design of the follower parameters is dealt with in chapters 5 and 6. Cam profile synthesis assuming that the follower parameters are already designed, is discussed here.

#### Systems of coordinates.

Cam design is done in a temporarily fixed frame of reference, the final position of which is decided during the assembly. Here, for convenience, we

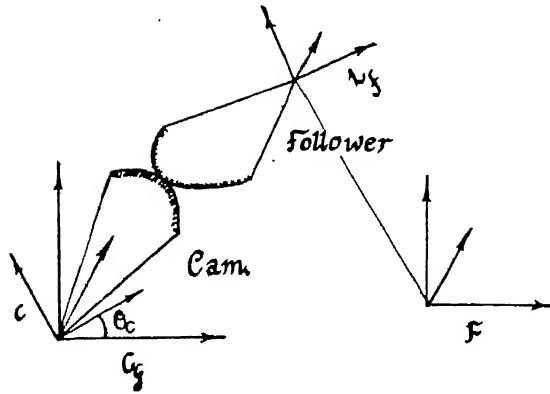
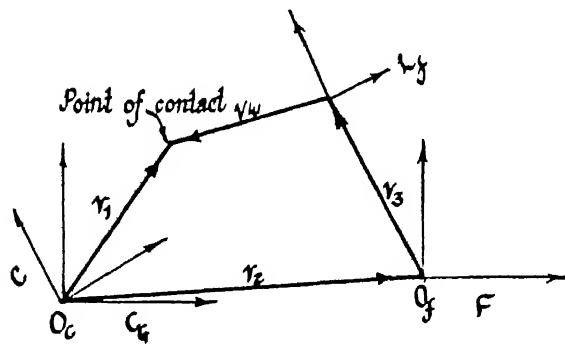
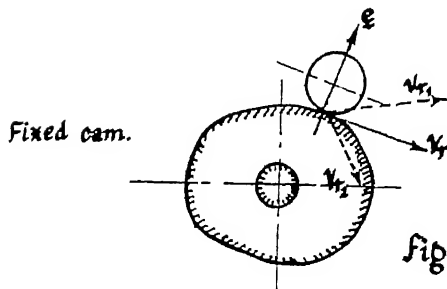


Fig 2.4. Cam design: Systems of Coordinates.



$$\tilde{v}_1 = \tilde{v}_2 + \tilde{v}_3 + \tilde{v}_4$$

Fig 2.5. Cam synthesis as vector addition.



$v_r$ : orthogonal relative velocity

$v_{r1}$ : follower losing contact

$v_{r2}$ : follower cutting inside the cam

Fig 2.6. Condition of contact

assume that this temporary frame is the global frame of reference as far as the cam is concerned.

The follower and the cam are represented in two different frames of reference, and the motion of one is mapped onto another. (Fig. 2.4).  $C_g$  (same as  $T_c$ ) is the global coordinate system stationed at the cam centre.  $L_f$  is the local coordinate system at the follower and moving with it.  $C$  is the coordinate system fixed to the cam and rotating with it.  $F$  is the coordinate system fixed in space and used to express the follower displacements ( same as  $L_f$  ).

#### Cam profile synthesis.

Consider cam and follower surfaces in the systems of coordinates described above as shown in Fig. 2.4. The mapping of motion from one frame to another is done on the basis of the following principle.

"The position vectors at the point of contact expressed in the global coordinate system are equal on the cam and follower surfaces. "

This also amounts to a simple addition of vectors as shown in Fig. 2.5. Along with this, the following *condition of contact* [2] needs to be satisfied.

"The relative velocity of the follower with respect to the cam at the point of contact should be orthogonal to the common normal to the cam and follower surface at the point of contact. "

This will be clear from Fig. 2.6.

Using these two principles, the cam profile can be synthesised as follows:  
For the point of contact, the globally expressed position vectors are equal.

$$\vec{R}_{gc} = \vec{R}_{gf} \quad (2.4)$$

where

$$\tilde{R}_{gc} \equiv (R)_{gc} \quad \text{and} \quad \tilde{R}_{gf} \equiv (R)_{gf}$$

are the position vectors of the point of contact expressed in the global frame from the cam coordinate system and the follower coordinate system respectively. ( ' $\sim$ ' represents a vector, and ' $()$ ' represent column vectors.

Now,

$$(R)_{gc} = [M_c]_g (R)_{1c} \quad (2.5)$$

$$\text{and} \quad (R)_{gf} = [M_f]_g (R)_{1f} \quad (2.6)$$

where

$$\begin{aligned} (R)_{1f} &\equiv \text{position vector of the contact point in frame } L_f, \\ [M_f]_g &\equiv \text{transformation matrix from frame } L_f \text{ to } C_G, \\ (R)_{1c} &\equiv \text{position vector of the contact point in frame } C, \\ [M_f]_g &\equiv \text{transformation matrix from frame } C \text{ to } C_G. \end{aligned}$$

Thus,

$$[M_c]_g (R)_{1c} = [M_f]_g (R)_{1f} \quad (2.7)$$

$$(R)_{1c} = [M_c]_g^{-1} [M_f]_g (R)_{1f} \quad (2.8)$$

The above equation gives the position coordinates (x, y, z) of a point on the cam profile in terms of the follower displacement and velocity.

We assume that the global coordinate system  $C_G$  is fixed at the cam centre. The cam local coordinate system  $C$  has its origin at the cam centre and is fixed to the cam.

$$[M_c]_g = \begin{bmatrix} \cos\theta_c & -\sin\theta_c & 0 & 0 \\ \sin\theta_c & \cos\theta_c & 0 & 0 \\ 0 & 0 & 1 & 0 \\ 0 & 0 & 0 & 1 \end{bmatrix} \quad (2.9)$$

where  $\theta_c$  is the cam rotation angle, i.e. the angle by which C is displaced from  $C_G$ .

Thus,

$$[M_c]_g^{-1} = \begin{bmatrix} \cos\theta_c & \sin\theta_c & 0 & 0 \\ -\sin\theta_c & \cos\theta_c & 0 & 0 \\ 0 & 0 & 1 & 0 \\ 0 & 0 & 0 & 1 \end{bmatrix} \quad (2.10)$$

It may be noted here that on the L.H.S. of equation (2.7),  $[M_c]_g$  is dependent on  $\theta_c$ , whereas the R.H.S depends upon the follower displacement and velocity, and consequently on the type of the follower being used.  $[M_c]_g$  and  $\{R\}_{1f}$  are determined for various types of followers in appendix B.

#### Determination of cam speed.

The angular speed at which the cam rotates, is determined by the total cycle time of the end effector motion. Let  $T$  be the cycle time. Then, the angular speed is

$$\omega = \frac{2\pi N_c}{T} \quad (2.11)$$

where  $N_c$  is the number of cam rotations for one cycle of motion. (Usually,  $N_c = 1$ )

#### 2.5 Assembly of motion.

The following are the objectives of the assembly.

1. Combination of the motions generated by each CML at the output end.
2. Coordination of the motions generated by each cam at the input end.
3. Determination of the assembly dependent parameters.

Motion combination is achieved through elements known as assemblers, and is

essentially a hardware problem. This is discussed in the section 4.1.2 .

#### **Motion coordination.**

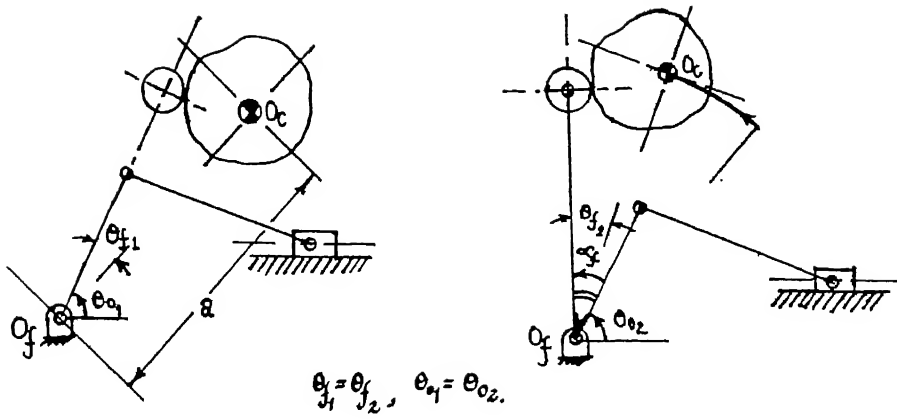
Since the motion in each direction is generated independently, if all the motion components at any instant are not appropriately matched, all the CMLs will be generating the desired motion individually, but there will be a lack of coordination, and the trajectory will appear distorted. This can be controlled by maintaining the appropriate phase angle between two cams. (Sect. 4.1.3)

#### **Determination of assembly dependent parameters.**

Once all the cams in the system are designed, it becomes possible to locate the cam centre, or the cam axis. All the temporary frames of reference can be then transported to appropriate points on the camshaft axis.

The location of the cam axis depends upon the parameters designed in the earlier stages of design, typically, the cam-follower pivot distance, or the offset. Generally, the global coordinates of  $O_{r_i}$  (Fig. 2.1) will be known, whereas the location of the cam centre  $O_{c_i}$  will be known in terms of  $O_{r_i}$ . This information for each cam needs to be coordinated since the global coordinates of all the cam centres should be such that they lie on a straight line.

Since only two points in space decide a straight line, this process of location of the centres has to be carried out with two cams only. For mechanisms with more than two cams, an adjustment in the values of the centre distance etc. has to be made in order to maintain a consistency between the mechanisms. With



Temporary location.

Finalised location.

Fig 27 Significance of ' $\alpha_f$ '.

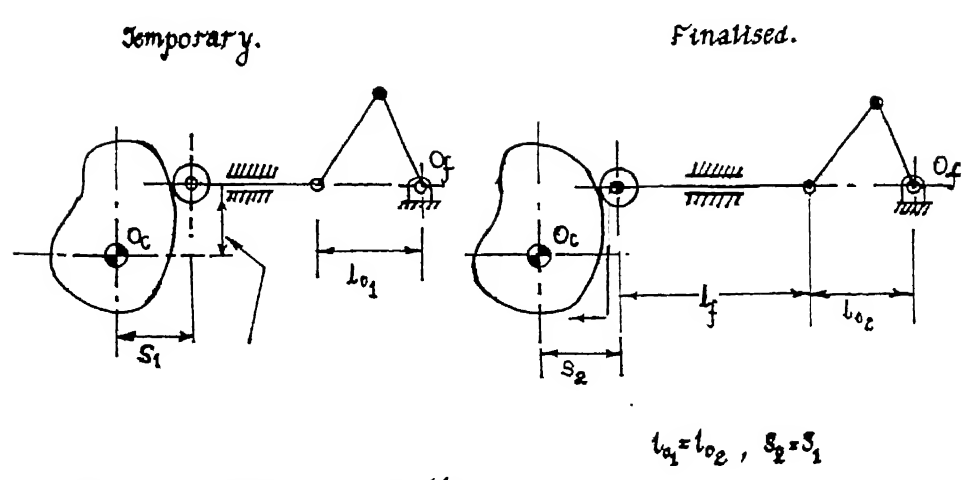


Fig 28. Significance of ' $l_f$ '.

two planar disc cam mechanisms, this problem reduces to a simple geometric problem of location of the points of intersection of a circle and a straight line, or two circles, etc. depending upon the type of the follower that is being used. (Appendix C.)

A point to be noted here is that when the origin of the cam coordinate system is transported to some other point by either rotation about or translation from the point  $O_{f_1}$ , since the position of the linkage remains unchanged, the absolute values of the follower displacements may get altered. To take care of this, the parameters  $\alpha_f$  and  $l_f$  (Fig. 2.7, 2.8) are assigned values at this stage. The analytical expressions for the determination of these parameters depend upon the location of the cam centre. (Appendix C).

## 2.6 Analysis.

Following are the two objectives of the analysis:

1. To check the accuracy of the motion produced by the generated mechanism.
2. To test the performance of the system in terms of
  - (i) the peak values of acceleration reached for each member in the mechanism.
  - (ii) cyclic transmission efficiency.

The following three step procedure is employed.

1. Determination at any given instant of the follower kinematics of each CML.
2. Determination of the output kinematics of the linkage at any given instant.
3. Combination of motion (displacement) in individual directions to determine the path followed by the end effector .

### Determination of the follower kinematics.

From equation 2.7, we know that

$$[M_f]_g (R)_{1f} = [M_c]_g (R)_{1c}. \quad (2.12)$$

The R.H.S. of this equation is known since  $[M_c]_g = f(\theta_c)$ , and  $\theta_c$  depends on the time instant under consideration. Also, the cam profile being already designed,  $(R)_{1c}$  is known. The L.H.S. is in terms of the follower displacement ( $s$ ) and velocity ( $\dot{s}$ ). The above matrix equation is formed of two independent scalar equations with two unknowns  $s$ , and  $\dot{s}$  and can be solved for the two unknowns.

Actually, this analysis amounts to solving the loop closure equations of a 4 vector loop and can be achieved by treating it as a linkage and using the principle for linkage analysis, explained in the next section.

### Linkage analysis.

The loop closure equations for a linkage are written as

$$\sum_{i=0}^{n-1} l_i \cos(\theta_i) = 0, \quad (2.13a)$$

and

$$\sum_{i=0}^{n-1} l_i \sin(\theta_i) = 0. \quad (2.13b)$$

With all the dimensions of the linkage being designed, for a given value of  $p_{in}$ , the above two form simultaneous equations in 2 variables,  $p_{out}$  and  $p_{sec}$ , and can be solved using the same technique as for the synthesis with the help of equation 2.0. Differentiating equations 2.13 with respect to time, we get the loop closure equation for the velocity as:

$$\sum_{i=0}^{n-1} \dot{l}_i \cos(\theta_i) - l_i \sin(\theta_i) \cdot \dot{\theta}_i = 0, \quad (2.14a)$$

and

$$\sum_{i=0}^{n-1} \dot{l}_i \sin(\theta_i) + l_i \cos(\theta_i) \cdot \dot{\theta}_i = 0 \quad (2.14b)$$

Also differentiating equation 2.0,

$$\dot{\theta}_i = \dot{\theta}_{i-1} + \dot{\phi}_i. \quad (2.15)$$

Equations (2.14) are linear in nature, since all the  $\theta_i$ s are determined previously from the displacement analysis, and for a specified value of  $\dot{p}_{in}$ , can be solved for  $\dot{p}_{out}$  and  $\dot{p}_{sec}$ .

Similarly, differentiating equations 2.14 and 2.15 with respect to time, we get the loop closure equations for the acceleration as:

$$\sum_{i=0}^{n-1} \ddot{l}_i \cos(\theta_i) - 2 \dot{l}_i \sin(\theta_i) \cdot \dot{\theta}_i - l_i \cos(\theta_i) \dot{\theta}_i^2 - l_i \sin(\theta_i) \ddot{\theta}_i = 0, \quad (2.16a)$$

and

$$\sum_{i=0}^{n-1} \ddot{l}_i \sin(\theta_i) + 2 \dot{l}_i \cos(\theta_i) \cdot \dot{\theta}_i - l_i \sin(\theta_i) \dot{\theta}_i^2 - l_i \cos(\theta_i) \ddot{\theta}_i = 0, \quad (2.16b)$$

and

$$\ddot{\theta}_i = \ddot{\theta}_{i-1} + \ddot{\phi}_i. \quad (2.17)$$

These are also linear equations, and for a specified value of  $\ddot{p}_{in}$ , can be solved for  $\ddot{p}_{out}$  and  $\ddot{p}_{sec}$ .

## chapter 3. COMPUTATIONAL ASPECTS.

In the previous chapter, a scheme was developed to design the CMLs in different directions as per the motion components of the trajectory. Various aspects of this procedure are discussed in the present chapter. These are:

- Method of solving simultaneous equations.
- Details of Linkage analysis.
- Details of Linkage synthesis.
- Cam profile design details.

By far, the most common method for solving nonlinear simultaneous equations is the Newton-Raphson's method. A few aspects of this are discussed in appendix A, and the relevant issues are referred to in the following sections. Finally, two examples illustrating the application of this procedure are presented.

### 3.1 Linkage analysis.

The underlying principle of linkage analysis was discussed in section 2.6. The Newton-Raphson's method is applied to 2 equations in 2 unknowns, and comprises of the following steps.

1. Identification of the variables.
2. Selection of an initial point..
3. Formation of approximated linear equations in terms of the coefficients of the variables and the constants in the equations.
4. Solution of the linear equations followed by updating the variables, and

reformulation till a satisfactory solution of the nonlinear equations is reached.

#### Identification of variables.

The loop closure equations for the displacement are represented as:

$$\sum_{i=0}^{n-1} l_i \cos(\theta_i) = 0, \quad (3.1a)$$

and

$$\sum_{i=0}^{n-1} l_i \sin(\theta_i) = 0. \quad (3.1b)$$

Also,

$$\theta_i = \theta_{i-1} + \phi_i, \quad i = 0, \dots, n-1 \quad (3.2)$$

The structural parameters of the mechanism are the lengths  $l_i$  of the links and the angle  $\phi_i$  between two successive links (if constant). Variables of motion are the lengths  $l_i$  of the sliding links and orientations  $\theta_i$  of the rotating links. These are dependent of the joint configuration of the linkage. There will be two variables which can be evaluated with the two loop closure equations for a specified input value. When vectors with varying lengths, and orientations are encountered, it is helpful to determine length, rather than the orientation from the loop closure equation, and then determine the orientation from equation (3.2).

#### An initial point.

Some initial approximate values need to be specified to start the procedure for the solution of simultaneous equations. For simplicity, one of the points at which the input-output motion is coordinated during the synthesis, may be stored and be used as the initial point. For analysis over the complete cycle, the configuration obtained for every small interval may be stored, and given as an initial point for the determination of the next configuration. This saves the

number of iterations to be performed before the solution is reached.

#### Formation of linear equations.

At any stage of the solution, each term of the coefficient matrix is given as: (Appendix A)

$$c_{ij} = \frac{\partial e_i}{\partial v_j} \quad (3.3)$$

where  $e_i$  is the expression for equation  $i$ ,

and  $v_j$  is the  $j$  th variable of analysis.

There will be two possible types of values for  $v_j$ . It will either be the length  $l_r$  of the link  $r$  or the orientation  $\theta_r$  of the the link  $r$ .

If  $v_j \equiv l_r$ ,

$$c_{1j} = \frac{\partial e_1}{\partial l_r} = \cos \theta_r, \quad (3.4a)$$

$$\text{and} \quad c_{2j} = \frac{\partial e_2}{\partial l_r} = \sin \theta_r, \quad (3.4b)$$

from equations (3.1).

Similarly, if  $v_j \equiv \theta_r$ , then from equations (3.1) and (3.2),

$$c_{1j} = \frac{\partial e_1}{\partial \theta_r} = - \sum_{p=0}^z l_{r+p} \sin(\theta_{r+p}) \quad (3.5a)$$

$$\text{and} \quad c_{2j} = \frac{\partial e_2}{\partial \theta_r} = - \sum_{p=0}^z l_{r+p} \cos(\theta_{r+p}) \quad (3.5b)$$

where  $z \equiv$  the number of successive constant  $\phi_p$ s following  $\theta_r$  till  $r + p < n$ , the number of vectors in the loop, and  $\theta_{r+p}$  are determined from equation 3.2.

Similarly, the constants of the linear equations are given as:

$$b_1 = - \sum_{p=0}^{n-1} l_p \cos(\theta_p) , \quad (3.6a)$$

$$\text{and} \quad b_2 = - \sum_{p=0}^{n-1} l_p \sin(\theta_p) . \quad (3.6b)$$

All the  $b_i$ s and  $c_{ij}$ s are evaluated at current values of  $(l_0, \dots, l_{n-1})$ ,  $(\theta_0, \dots, \theta_{n-1})$ , and  $(\phi_0, \dots, \phi_{n-1})$ .

### Solution of equations.

The constants  $b_j$  will not be zero unless the solution is reached, and act as corrections to the values of the variables  $v_j$ .

Thus,

$$v_{j,next} = v_{j,current} + b_j$$

for the next iteration, where  $b_j$  is as evaluated at the end of the solution of the linear approximate equations. The condition that  $\sum b_j^2 \approx 0$ , provides a check for the termination of the procedure.

Inconsistent or divergent solutions reflect that no loop closure with the specified values can be struck at. This usually happens when the value of the input variable goes out of range of its possible values giving imaginary solutions.

A few more aspects of the analysis appear in appendix D.

## 3.2. Linkage synthesis.

The principle on which linkage synthesis is based, was explained in section 2.4.1. To solve the simultaneous equations, the Newton-Raphson's method is employed with  $2m$  equations in  $2m$  unknowns. ( $m \equiv$  the number of design variables) The solution is identified when all the  $m$  loop closures are simultaneously satisfied. The four step procedure described earlier for analysis holds.

### Identification of the variables.

The first  $m$  variables will be the variables to be synthesised. The remaining  $m$  variables will be the variables  $p_{sec,j}$ , representing the motion of the intermediate link for each configuration  $j$ . This also is one of the variables in the analysis, and can be found from the method described in the previous section.

### Initial point.

Initial values are the approximate values close to which the solution is expected to lie. In most of the cases, these are formed on the basis of judgement, a scaled drawing, or some sort of approximation. The initial values of the secondary variables may also be specified in a similar manner. Even if arbitrary values are assigned, most of the time, solutions will be obtained on the basis of the initial values of the other variables. However, at times, inconsistencies or divergent solutions may be obtained. Usually, with a little trial and error, it is possible to reach initial values giving satisfactory results.

### Formation of linear equations.

The primary variables can either be lengths  $l_r$  of the links  $r$ , or the angle  $\phi_r$  between two links  $r$  and  $(r - 1)$ . If the design parameter  $p_{des} \equiv l_r$ , the terms in the coefficient matrix will be:

$$c_{kj} = \frac{\partial a_k}{\partial l_r} = \cos \theta_{ri} \quad (3.8a)$$

$$c_{kj} = \frac{\partial a_k}{\partial l_r} = \sin \theta_{ri} \quad (3.8b)$$

$$c_{kj} = \frac{\partial e_k}{\partial l_r} = \sin \theta_{r,i} \quad (3.b)$$

where  $i = 1, \dots, m$  represents the numbers of configurations, and  $(k = 2i - 1, k+1 = 2i)$ , the number of corresponding loop closure equations.

Similarly, if  $p_{des} \equiv \phi_r$ , then from equations (3.1) and (3.2),

$$c_{kj} = \frac{\partial e_k}{\partial \phi_r} = - \sum_{p=0}^z l_{r+p} \sin(\theta_{r+p}) \Big|_i \quad (3.9a)$$

$$c_{k+1,j} = \frac{\partial e_{k+1}}{\partial \phi_r} = \sum_{p=0}^z l_{r+p} \cos(\theta_{r+p}) \Big|_i \quad (3.9b)$$

where  $z \equiv$  the number of successive constant  $\phi_p$ s following  $\theta_r$  till  $r + p < n$ , and  $\theta_{r+p}$  are determined from equation (3.2).

Similarly, the constants of the linear equations are given as:

$$b_k = - \sum_{p=1}^n l_{p,i} \cos(\theta_{p,i}) , \quad (3.10a)$$

$$\text{and} \quad b_{k+1} = - \sum_{p=1}^n l_{p,i} \sin(\theta_{p,i}) . \quad (3.10b)$$

All the  $b_k$ s and  $c_{kj}$ s are evaluated at current values of  $(l_0, \dots, l_{n-1})_i$ ,  $(\theta_0, \dots, \theta_{n-1})_i$ , and  $(\phi_0, \dots, \phi_{n-1})_i$  for the corresponding configurations  $i$ .

### Solution of equations.

The equations are solved in a manner similar to that described for analysis. Inconsistent solutions here reflect that with the specified initial values and / or coordinated input output values, no consistent set of values of the design variables can be arrived at. In such cases, either the input output coordination, or the initial values need to be modified.

### Discussion.

There are chances of the occurrence of multiple solutions for synthesis, more so than analysis, since a larger number of variables are involved. However, it

usually works out to our advantage that solutions in the vicinity of the initial values are obtained. Different initial points may be tried to get different possible solutions, and the best one amongst them may be selected depending upon the application. Generally, the criteria of space, weight, maximum allowable link lengths, etc. will be the deciding factors. Also, the peak values of the acceleration, velocity, and transmission angle will be important.

### 3.3 Cam design.

Cam profile synthesis theoretically comprises of generating infinite points that constitute the profile. In practice, a large number of points sufficient enough to describe the details of the surface are used. The number depends primarily upon the the complexity of the profile, and secondly on the size of the cam. For most of the cases, 100 to 150 divisions of the cam surface are sufficient. Localised clustering of more points in order to capture the details may be necessary in some of the cases.

Since the profile synthesis equations turn out to be explicit equations of  $x$  and  $y$  in terms of the parameter  $\theta_c$ , (Ref. section 2.4.2) these are determined in the form of analytical expressions, and quoted in appendix B .

Analysis of the follower motion can be based on a principle similar to linkage analysis described above.

### 3.5 Application to a segmented trajectory of straight lines. (Example 1)

One of the advantages of using the CML type mechanical robots is that non-smooth trajectories can be very easily generated. The present example relates to a trajectory comprising of a segmented path of straight lines connected to each

other. This is shown in Fig. 3.1. The right angled turns present on it, make it impossible to be generated with a single cam drive. However, with two CMLs, one governing the motion in the X axis, and the other in the Y axis, the trajectory gets resolved into simple periods of rise, return and dwell for the cam in each CML.

The resolved components of the trajectory are shown in Figs 3.2, and 3.3. The time variation in each section of the motion is assumed to be cycloidal, resulting into smooth acceleration curves. The range of the motion in each direction shows that if a simple cam be used to generate these motions, it would require an enormous one. This will clarify the use of a linkage.

The linkage used for motion transmission in the Y direction is an RRRP mechanism. In most of the applications, these will be used on account of their simplicity, and the fact that it is preferable to have an oscillating follower to the cam. The input link of the linkage may be a crank or a rocker. In the X direction, an RRPP linkage with a movable support type of assembler (Sect. 4.1.2) is used. The output displacement simply becomes a sine component of the input link length (Fig. 3.4).

The input to the linkage synthesis is shown in tables 3.2 and 3.4 for x and y directions. The range of the input motion is based on the judgement of the follower motion range in that direction. The resulting linkages are shown in Figs 3.4 and 3.5. The inverse analysis of these linkages is done based on the output required from the linkages, and is shown in Figs 3.6 and 3.8. This forms the input to the linkages, and the motion of the follower.

Both the cams are of the oscillating follower type, and the follower parameters have been optimized using the method explained in chapters 5 and 6. The values of these parameters are shown in tables 3.6 and 3.5. Cam profile is

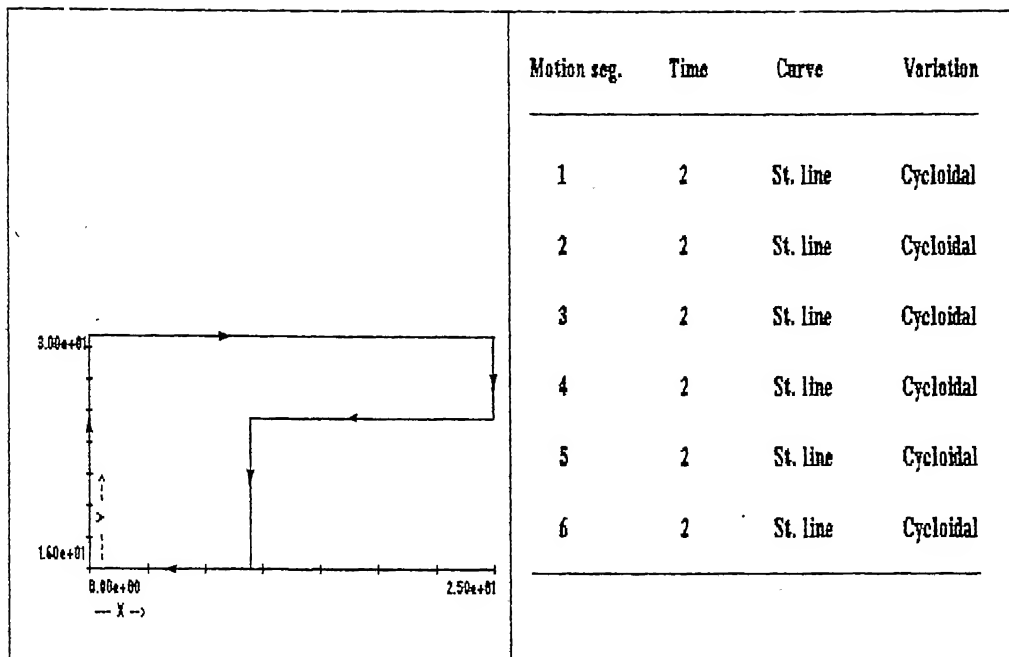


Fig.3.1. Trajectory. ( Prob. 1 )

Table 3.1. Input data for trajectory. ( Prob. 1 )

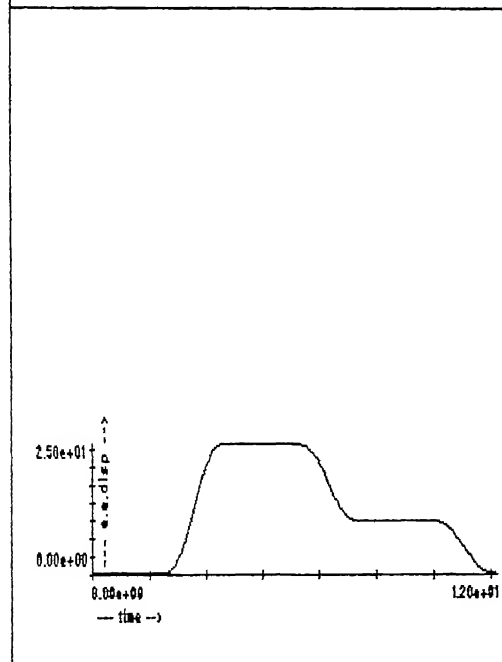


Fig.3.2. X' displacement variation. ( Prob.1 )

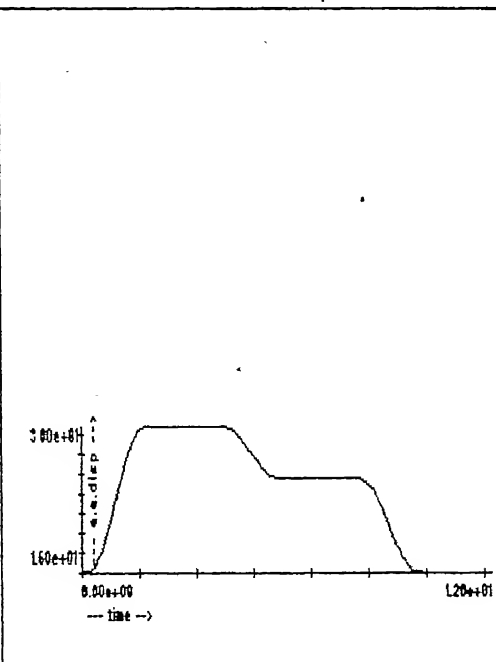
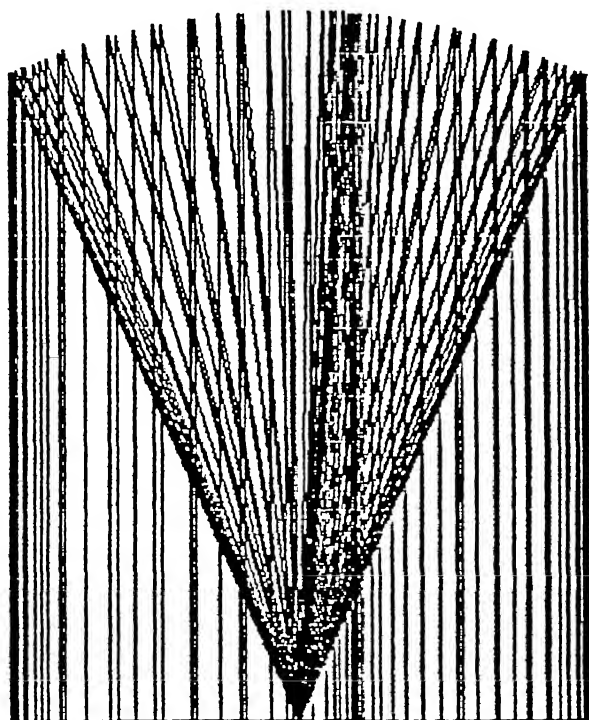


Fig.3.3. Y' displacement variation. ( Prob.1 )



*Fig3.4. Display of 'X' linkage throughout the input motion range. ( Prob. 1 )*

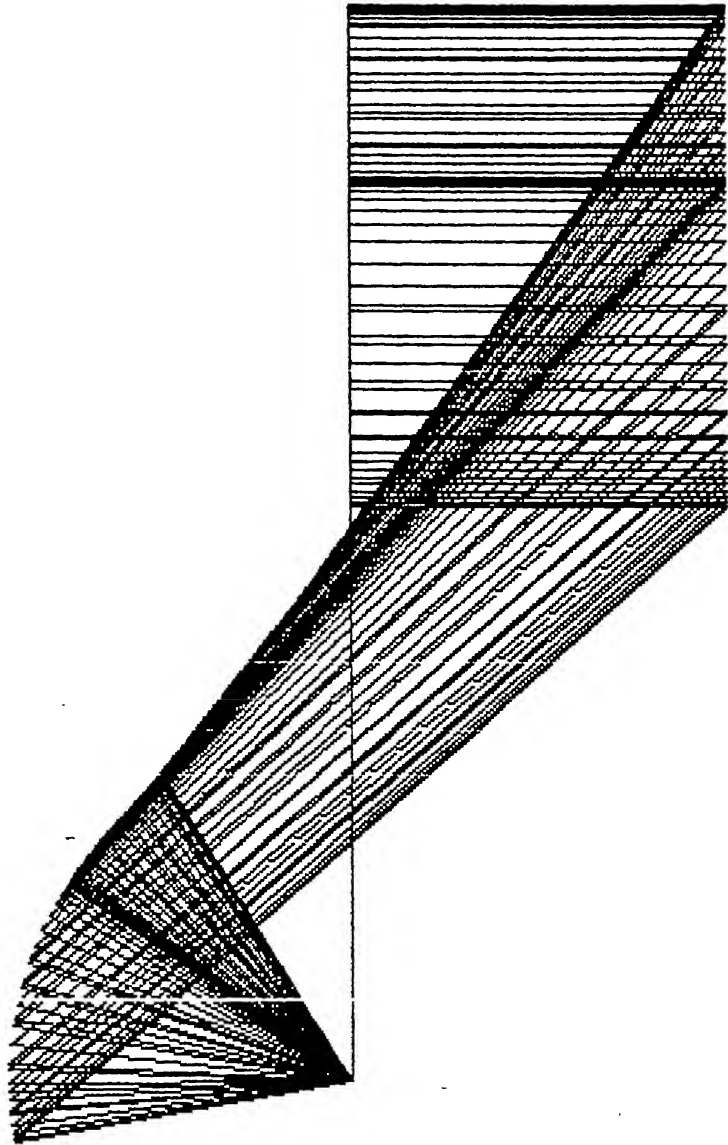


Fig 3.5. Display of 'Y' linkage throughout the input motion range. ( Prob. 1 )

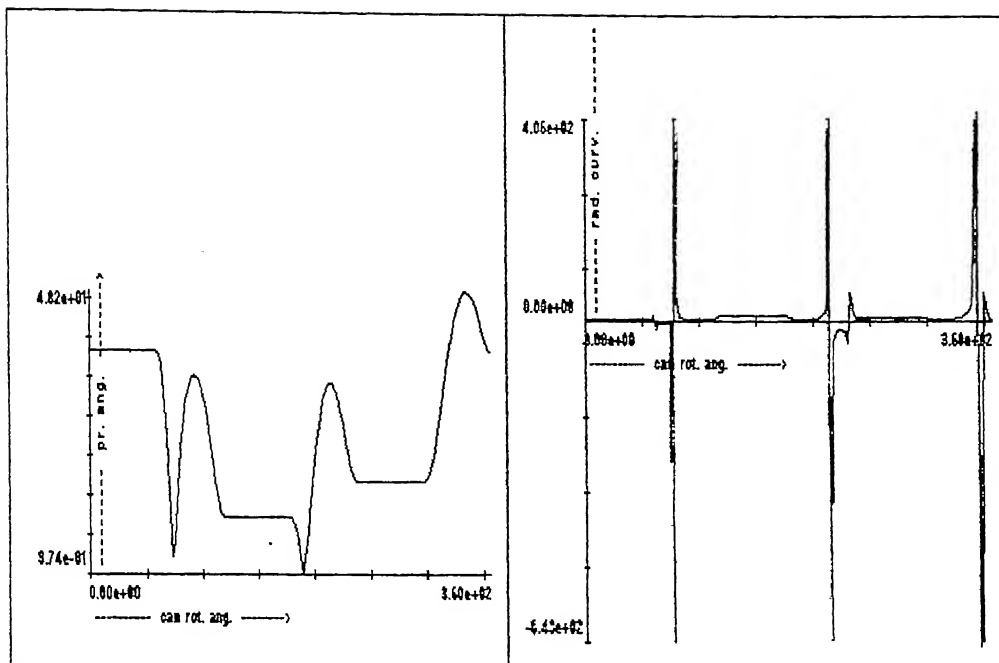


Fig 3.10 Pressure angle plot for cam 'X'. (Prob. 1)

Fig 3.11 Radius of curvature plot for cam 'X'. (Prob. 1)

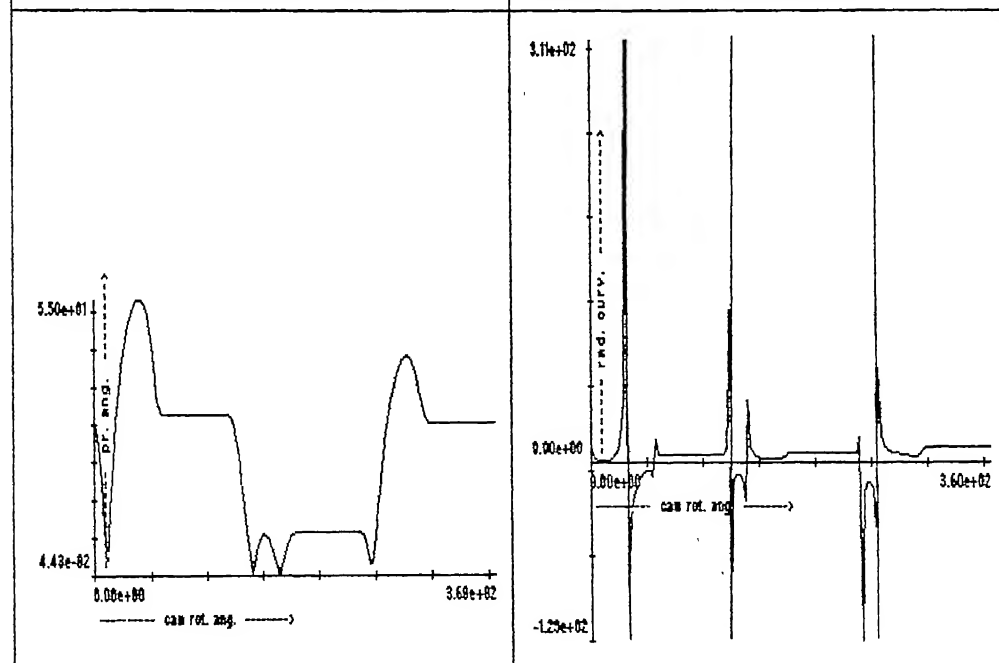
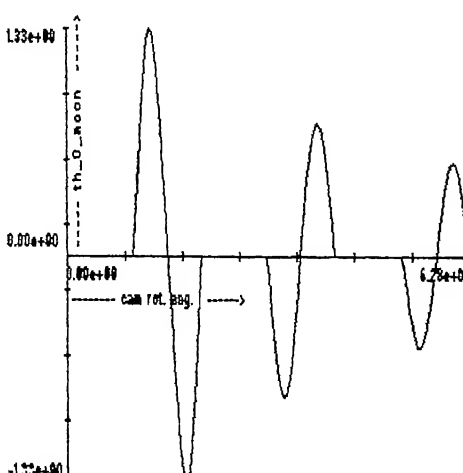
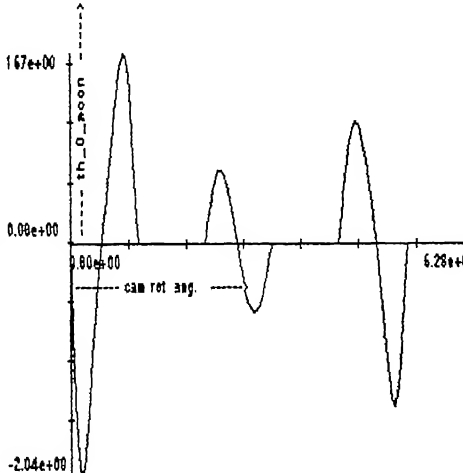


Fig 3.12 Pressure angle plot for cam 'T'. (Prob. 1)

Fig 3.13 Radius of curvature plot for cam 'T'. (Prob. 1)

|   |   |
|---|---|
|    | <p>Optimized follower parameters:</p> <ol style="list-style-type: none"> <li>1. Centre to centre distance 9.92</li> <li>2. Follower arm length 5.04</li> <li>3. Roller radius 1.04</li> <li>4. Min. angle of follower disp. 34.03 deg.</li> </ol> <p>Size of the cam:</p> <ol style="list-style-type: none"> <li>5. Base circle radius 5.83</li> </ol> <p>Operational constraints:</p> <ol style="list-style-type: none"> <li>6. Minimum radius of curvature 3.014</li> <li>7. Maximum pressure angle 42.99 deg.</li> </ol> |
| <p>Fig.3.14 Accela. plot for the i/p link - 'X' linkage. (Prob. 1)</p>              | <p>Table 3.5. Cam - follower data - 'X' cam. (Prob 1)</p>   |
|  | <p>Optimized follower parameters:</p> <ol style="list-style-type: none"> <li>1. Centre to centre distance 9.90</li> <li>2. Follower arm length 5.06</li> <li>3. Roller radius 1.06</li> <li>4. Min. angle of follower disp. 39.99 deg.</li> </ol> <p>Size of the cam:</p> <ol style="list-style-type: none"> <li>5. Base circle radius 5.79</li> </ol> <p>Operational constraints:</p> <ol style="list-style-type: none"> <li>6. Minimum radius of curvature 1.05</li> <li>7. Maximum pressure angle 54.99 deg.</li> </ol>  |
| <p>Fig.3.15 Accela. plot for the i/p link - 'Y' linkage. (Prob. 1)</p>              | <p>Table 3.6. Cam - follower data - 'Y' cam. (Prob 1)</p>   |

based on these values, and the profile generated for both the directions is shown in Figs 3.7 and 3.9. It is seen that the cam size is not extraordinarily large.

Analysis of the mechanism in both the directions is done, and the results are presented in Figs 3.10 through 3.15.

### 3.6 Application to a continuous curve. (Example 2)

The CML type mechanical robots form an ideal choice when the motion in two directions exists inherently in a resolved form. It is shown in the present section how it becomes possible to generate a series of continuous curves known as the Lissajous figures. The principle can be applied to various types of time variations of the output displacement.

Consider the harmonic variation  $x = a \sin(\omega t)$ , where  $\omega$  is the frequency of the wave. If this wave is coupled with a wave in the  $y$  direction having a frequency which is some multiple of that in the  $x$  direction, viz.,  $y = b \sin(r\omega t)$ , then these constitute the Lissajous figure as shown in Fig. 3.16. In the present example,  $r$  is taken as 2.

The variations of the end effector motion in the  $x$  and  $y$  directions are shown in Figs 3.17 and 3.18 along with the amplitudes and frequencies that were used. It can again be seen that the ranges of displacements in both, the  $x$  and  $y$  directions make it infeasible to use a simple cam mechanism. In fact, if just a simple cam mechanism be used for the motion in the  $y$  direction, one of the possible smooth profiles is shown in Fig. 3.19. However, the base circle radius of this cam turns out to be excessively large. Fig. 3.20 shows a possible reduction in the size through optimization, but is still not practicable. A similar phenomenon may be observed in the  $x$  direction also. The solution to this is the use of

linkages, since relatively larger dimensions of the links are practicable.

Tables 3.8 and 3.9 show the input and output motion ranges to be coordinated by the linkages in the  $x$  and  $y$  directions. The resulting linkages are presented in Figs 3.21 and 3.22. A reduction in the link lengths may be possible, with different combinations of the input motion range and mean value. However, generally with large displacements at the output end, large link lengths are unavoidable.

The assembler that is used here is of the  $x$ - $y$  projection type (Sect. 4.1.2) which makes it possible to have an RRRP joint combination for both  $x$  and  $y$  directions. Cams for both the directions are of the oscillating roller follower type and are presented along with the displacement diagrams in Figs 3.23 through 3.26.

Analysis of motion for the mechanism, and profile analysis of the cam surface to find the pressure angle and radius of curvature distribution were done, and are presented in Fig. 3.27 through 3.32.

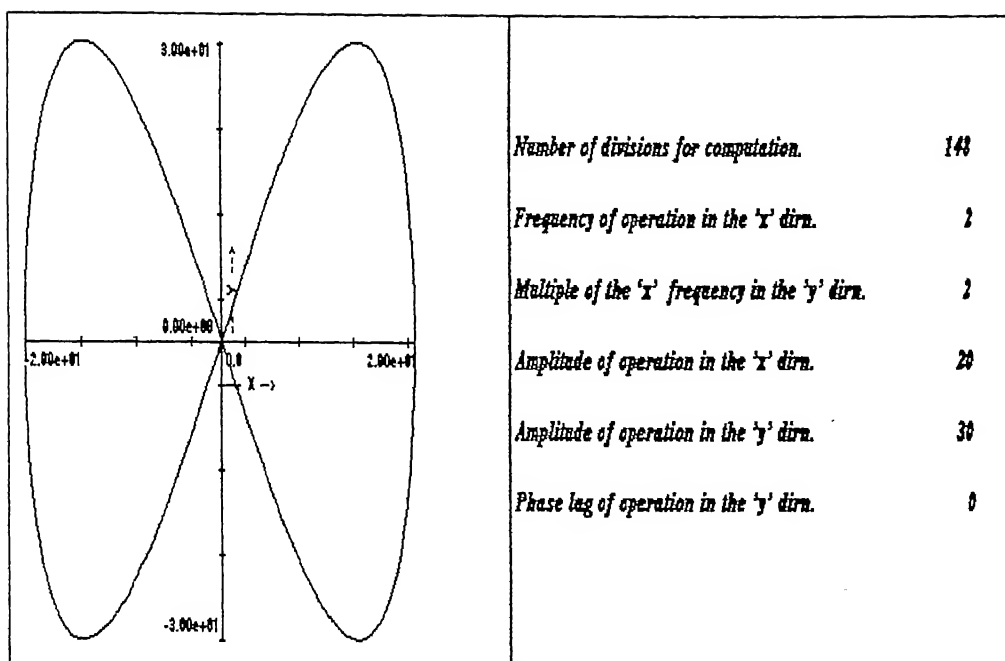


Fig. 3.16. Trajectory. ( Prob. 2 )

Table 3.1 Input data for trajectory. ( Prob. 2 )

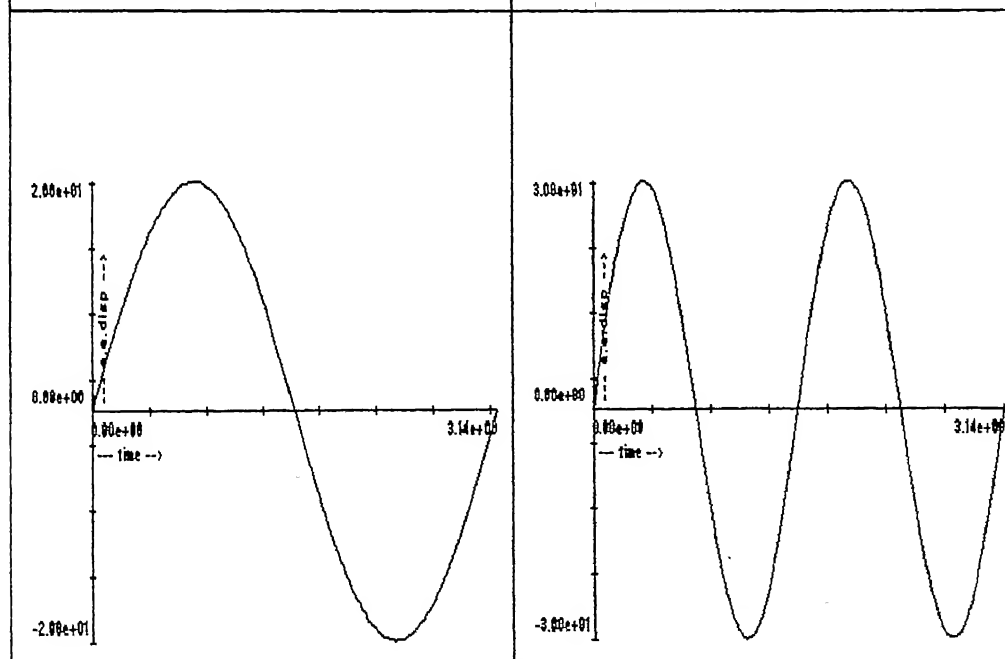


Fig. 3.17. 'X' displacement variation. ( Prob. 2 )

Fig. 3.18. 'Y' displacement variation. ( Prob. 2 )

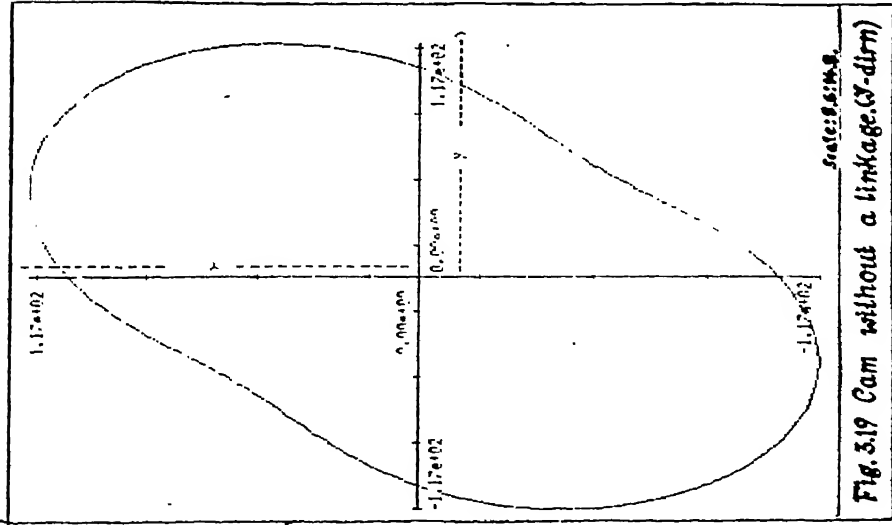


Fig. 3.19 Cam without a linkage (V-dlm)

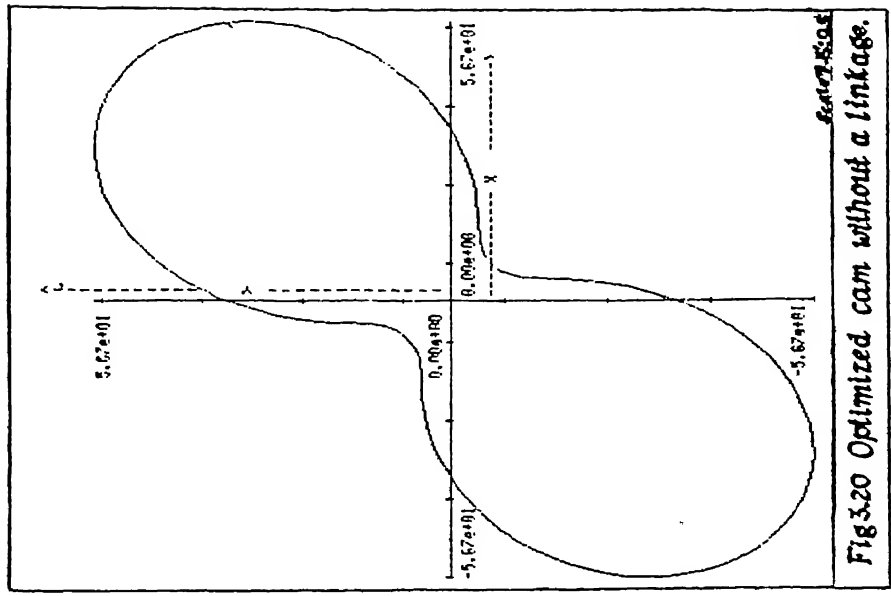


Fig. 3.20 Optimized cam without a linkage.

Linkage type: RRRP

Variables to be synthesised:

$l_0$  driving link  
 $l_1$  coupler  
 $th_1$  secondary variables

Constant parameter

$l_2$  offset 10.00

Input - Output coordination:

Output motion range: 40.0  
 Input motion range: 40.0 deg.

| Config. | Output | Input      |
|---------|--------|------------|
| 1.      | 10.00  | 80.00 deg. |
| 2.      | 50.00  | 40.00 deg. |

Initial values of variables:

link lengths:

$l_0$  30.00  
 $l_1$  20.00

secondary variables:

$theta_{1_1}$  -70.00 deg.  
 $theta_{1_2}$  -10.00 deg

Output:

$l_0$  36.20  
 $l_1$  25.92

Linkage type: RRRP

Variables to be synthesised:

$l_0$  driving link  
 $l_1$  coupler  
 $th_1$  secondary variables

Constant parameter

$l_2$  offset 10.00

Input - Output coordination:

Output motion range: 60.0  
 Input motion range: 50.0 deg.

| Config. | Output | Input       |
|---------|--------|-------------|
| 1.      | 10.00  | 190.00 deg. |
| 2.      | 70.00  | 140.00 deg. |

Initial values of variables:

link lengths:

$l_0$  40.00  
 $l_1$  40.00

secondary variables:

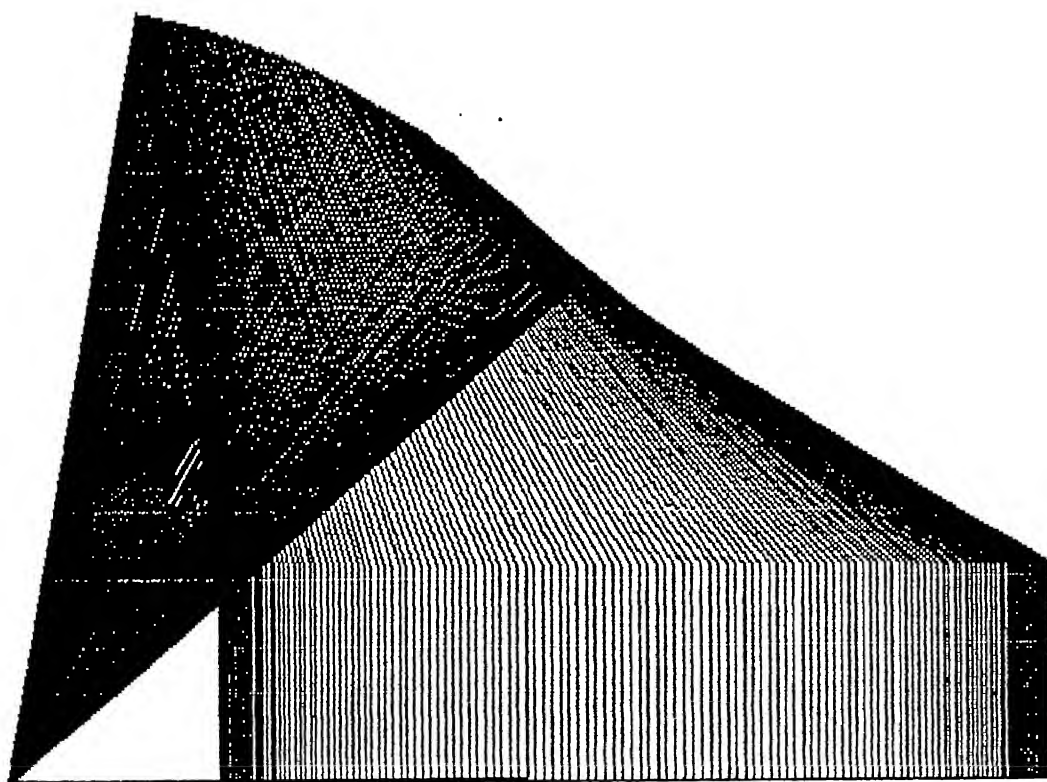
$theta_{1_1}$  20.00 deg.  
 $theta_{1_2}$  80.00 deg

Output:

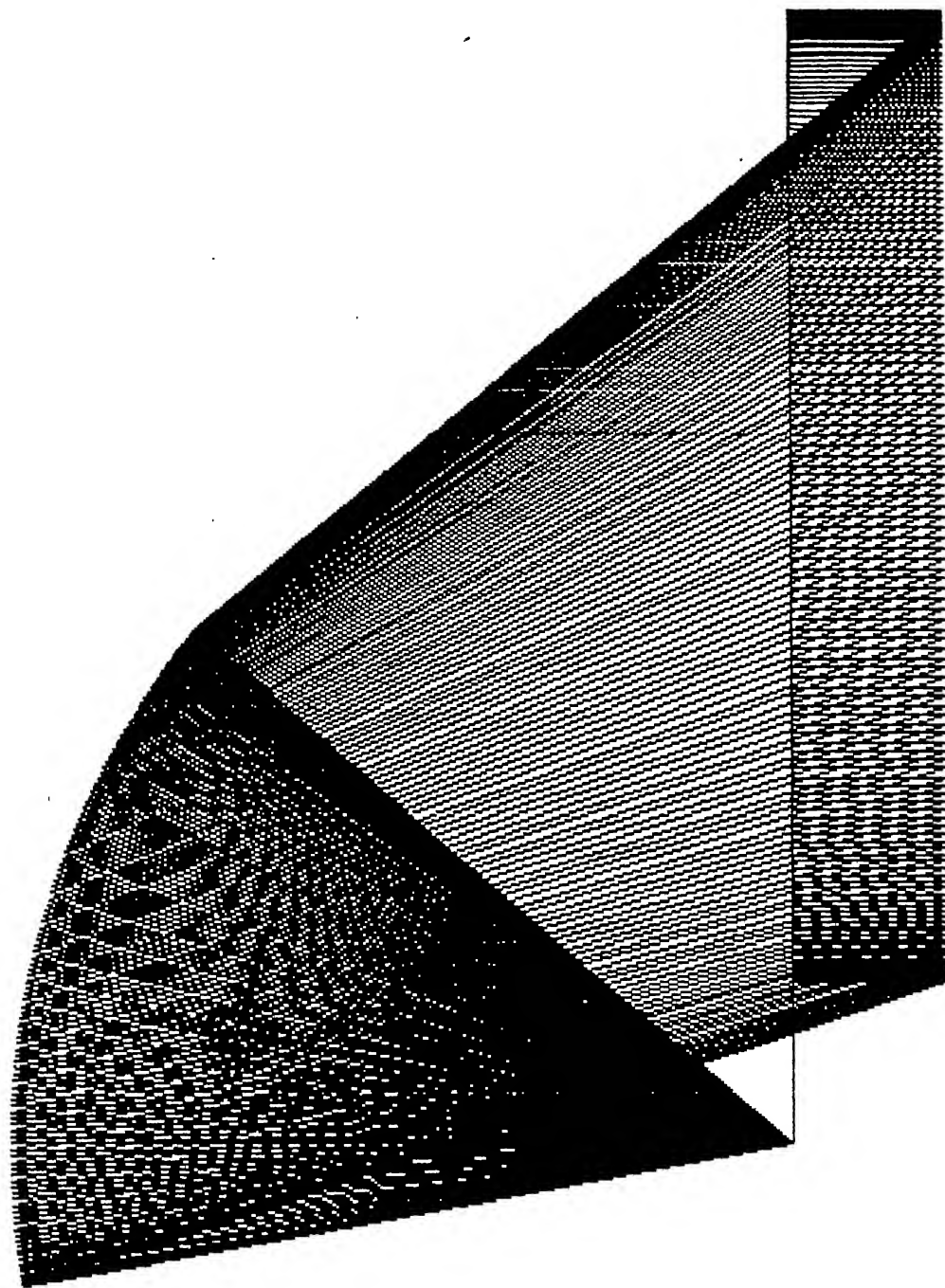
$l_0$  49.06  
 $l_1$  61.18

Table 3.8. 'X' linkage data. (Prob 2)

Table 3.9. 'Y' linkage data. (Prob 2)



3.21 Display of 'X' linkage throughout the input motion range. ( Prob. 2 )



*Fig 3.22. Display of 'Y' linkage throughout the input motion range. ( Prob. 2 )*

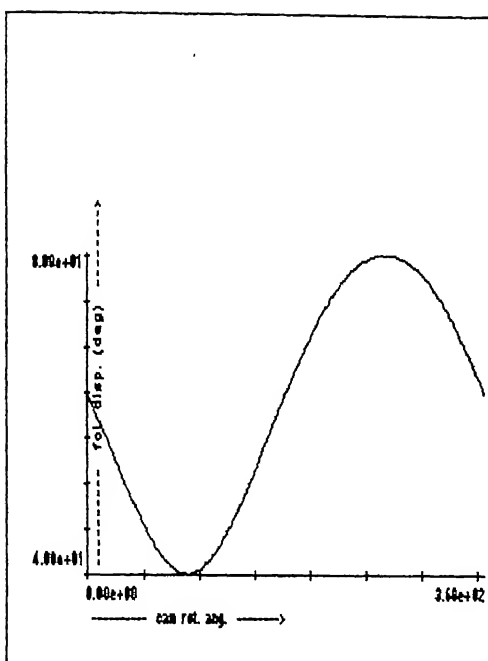


Fig.3.23. Follower disp. variation for 'X' cam. (Prob. 2)

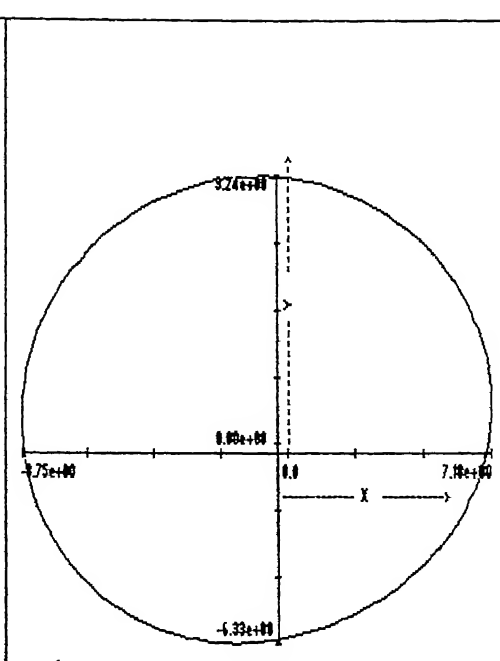


Fig.3.24. Cam for the motion in the 'X' dirn. (Prob. 2)

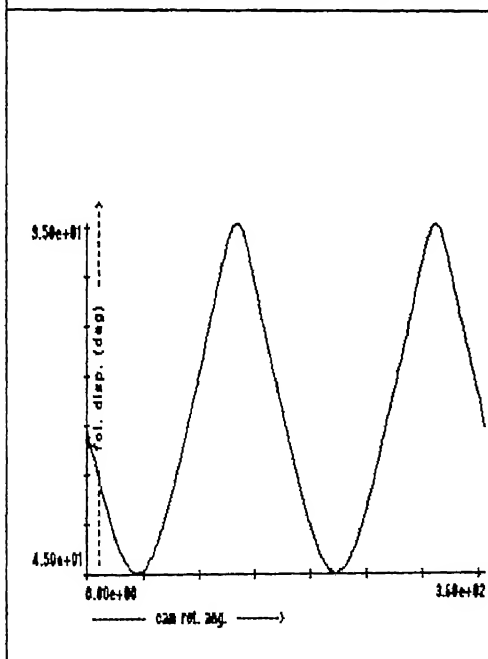


Fig.3.25. Follower disp. variation for 'Y' cam. (Prob. 2)

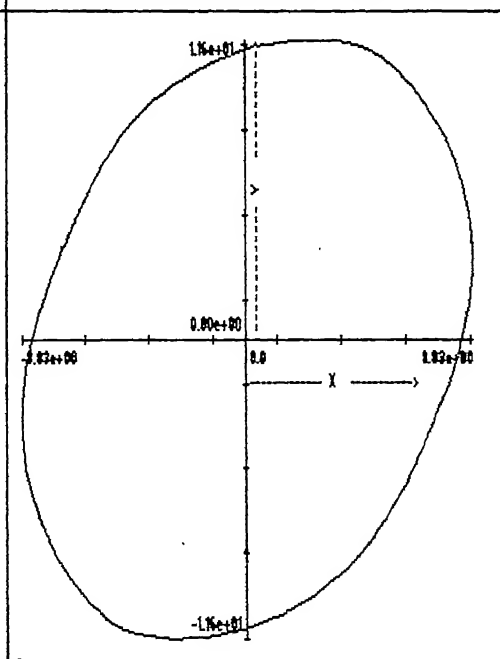


Fig.3.26. Cam for the motion in the 'Y' dirn. (Prob. 2)

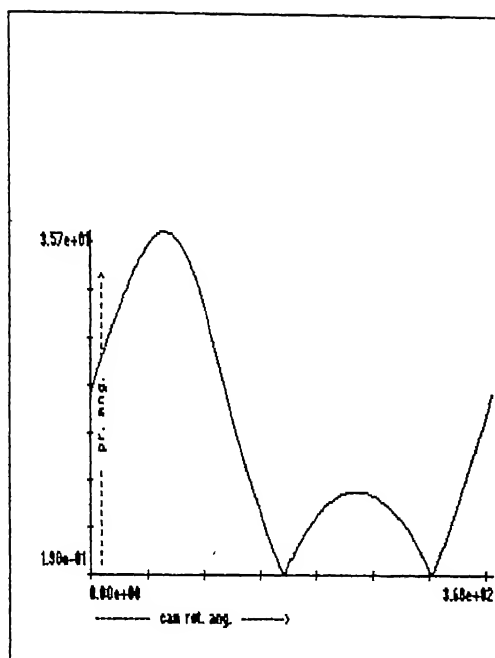


Fig.5.27 Pressure angle plot for 'X' cam. (Prob. 2)

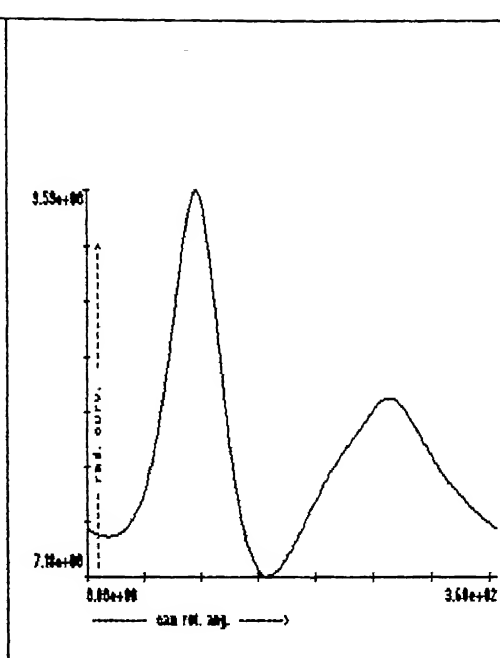


Fig.5.28 Radius of curvature plot for 'X' cam. (Prob. 2)

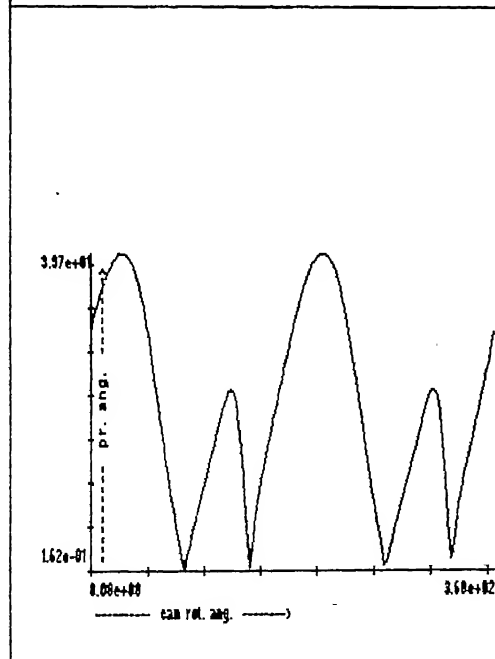


Fig.5.29 Pressure angle plot for 'Y' cam. (Prob. 2)

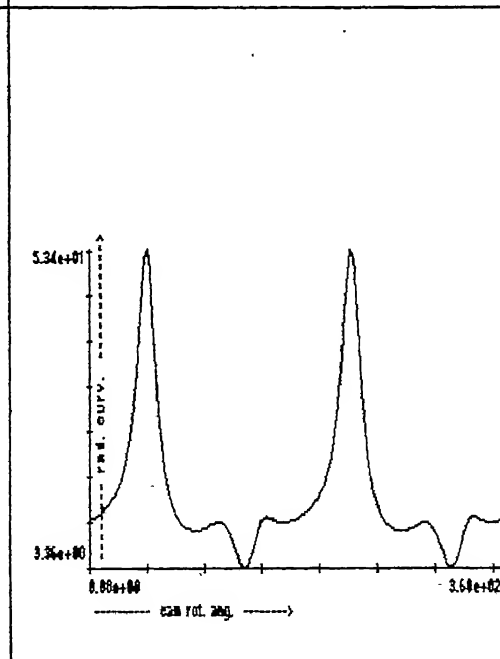
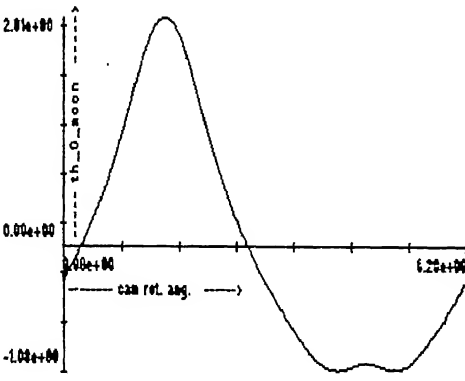
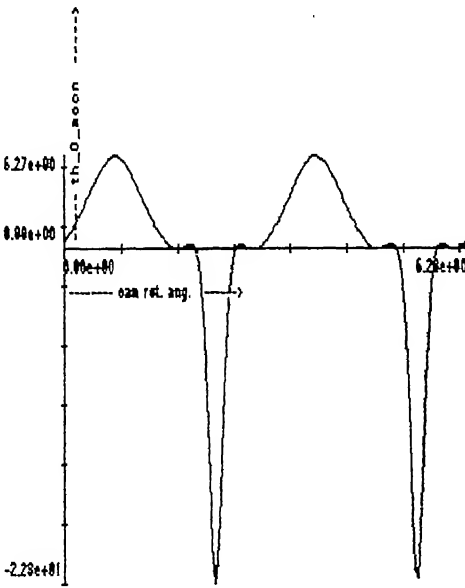


Fig.5.30 Radius of curvature plot for 'Y' cam. (Prob. 2)

|  |   |
|--|---|
|   | <p>Optimized follower parameters:</p> <ol style="list-style-type: none"> <li>1. Centre to centre distance 10.00</li> <li>2. Follower arm length 5.00</li> <li>3. Roller radius 1.00</li> <li>4. Min. angle of follower disp. 40.00 deg.</li> </ol> <p>Size of the cam:</p> <ol style="list-style-type: none"> <li>5. Base circle radius 5.96</li> </ol> <p>Operational constraints:</p> <ol style="list-style-type: none"> <li>6. Minimum radius of curvature 7.18</li> <li>7. Maximum pressure angle 35.70 deg.</li> </ol> |
| <p>Fig.3.51 Acceln. plot for input link - 'X' dirn. ( Prob. 2 )</p>                | <p>Table 3.10 Cam - follower data. - 'X' cam. ( Prob. 2 )</p>   |
|  | <p>Optimized follower parameters:</p> <ol style="list-style-type: none"> <li>1. Centre to centre distance 12.00</li> <li>2. Follower arm length 5.00</li> <li>3. Roller radius 1.20</li> <li>4. Min. angle of follower disp. 45.00 deg.</li> </ol> <p>Size of the cam:</p> <ol style="list-style-type: none"> <li>5. Base circle radius 8.17</li> </ol> <p>Operational constraints:</p> <ol style="list-style-type: none"> <li>6. Minimum radius of curvature 3.36</li> <li>7. Maximum pressure angle 39.70 deg.</li> </ol> |
| <p>Fig.3.52 Acceln. plot for input link - 'Y' dirn. ( Prob. 2 )</p>                | <p>Table 3.11 Cam - follower data. - 'Y' cam. ( Prob. 2 )</p>   |

## chapter 4. PRACTICAL CONSIDERATIONS.

A conceptual development of the mechanism proposed in the present work was shown in the previous chapters. There are other aspects to the practical design of these mechanisms. A few of these are described in the present chapter.

### 4.1 Considerations in the motion assembly.

In the present section, different types of assemblers, which combine motion in different directions, have been dealt with. Also, the effect of the phase difference  $\Phi$  on the output motion coordination is discussed.

#### 4.1.2 Motion assemblers.

An important requirement of the motion assembler is that it should maintain the independency of the motion components along each direction, i.e., the motion along one direction should not affect that in any other direction. This is possible only if the motion along one direction does not alter the configuration of the linkage, or break the cam-follower contact governing the motion along the other direction. There can be various ways in which this can be achieved, and it remains a task of generating innovative mechanisms capable of doing it. A few possibilities of these are discussed here.

#### Movable support type assemblers.

In these, the output end of one of the linkages is not grounded. Instead, it

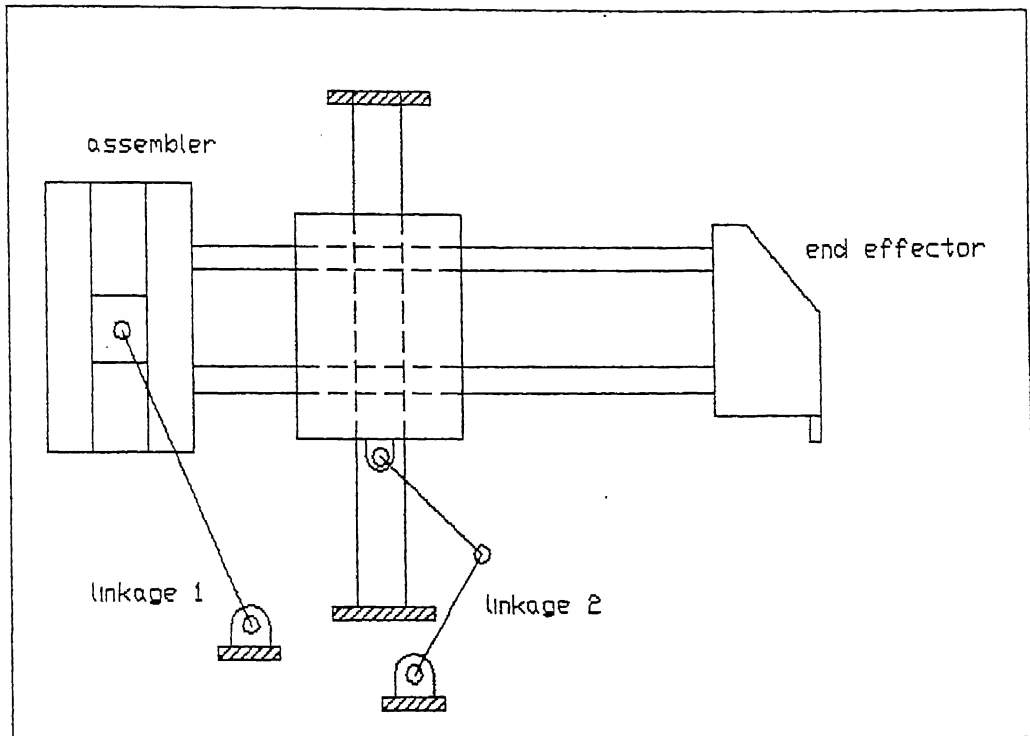


Fig 4.1 Movable support type assembler

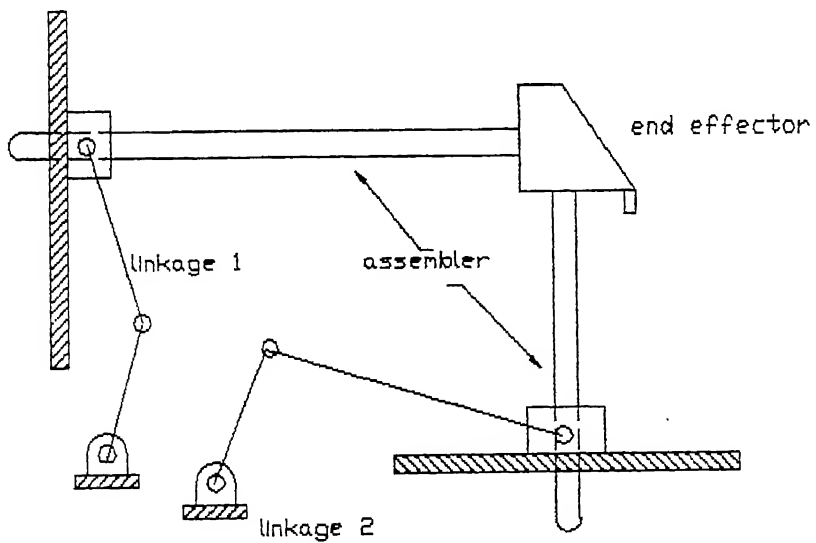


Fig. 4.2 Projection type assembler.

is mounted on the output end of another linkage. Thus, the assembler serves a dual purpose of assembling the motion, and acting as the output link of one of the linkages. ( Fig. 4.1 ). This assembler has to be used with a little discretion though, since the output end of one linkages moves independently of its input and might change the configuration of the linkage. This limits the application of the assembler to only those cases where one linkage is of the RRPP type. Employing an RRPP linkage does not change the output kinematics due to the change in configuration, as can be seen from Fig. 4.1.

#### Projection type assemblers.

Any point on the two dimensional plane can be expressed by the projections of its position vector on the two coordinate axes, viz. the abscissa and the ordinate. A similar principle can be used with an inverted L shaped assembler as shown in Fig. 4.2. This type of assembler has no restriction on the joints of the linkage so far as the output joint of both the linkages is a prismatic joint.

#### Splined shaft type assemblers.

These are used with  $2\frac{1}{2}$  degrees-of-freedom motion and are explained in section 4.2.1.

#### Cable type motion assemblers.

In these, the end effector is mounted on the output end of one of the linkages, and its motion in the other direction is governed by means of a cable connected to the output end of the other linkage. Springs may be used to maintain tension in the cable. This assembler can be used in mechanisms generating a

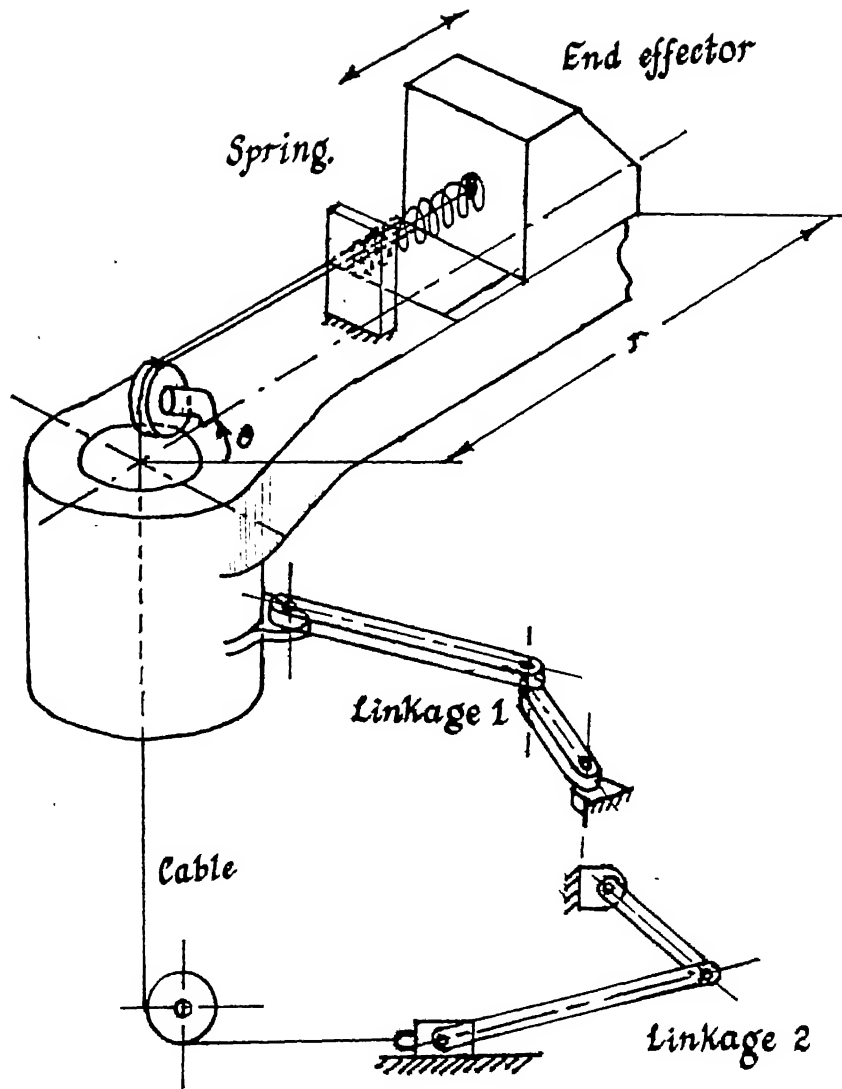


Fig 4.4. Cable type motion assembler.

planar motion with the polar variables  $r$  and  $\theta$ . This is illustrated in Fig. 4.3. The independency of the motions is maintained through the fact that for small rotations of the angle  $\theta$ , the twist produced in the cable is small enough to keep its length unchanged. This type of assembler cannot be used for large angular displacements, if accuracy is to be maintained, and in fact is useless when continuously increasing output is needed.

#### 4.1.3 Motion coordination.

It was mentioned earlier that the phase angle of each cam governs the coordination of the motion between two CMLs. This angle is defined as the angle of cam rotation at time,  $t = 0$ . (denoted by  $\theta_{c0}$ ) Then, the cam angle of rotation at any time instant  $t$  can be given as:

$$\theta_c = \theta_{c0} + \omega t.$$

where  $\omega$  is the rotational speed of the cam. The phase difference between two cams  $p$  and  $q$  is given by:

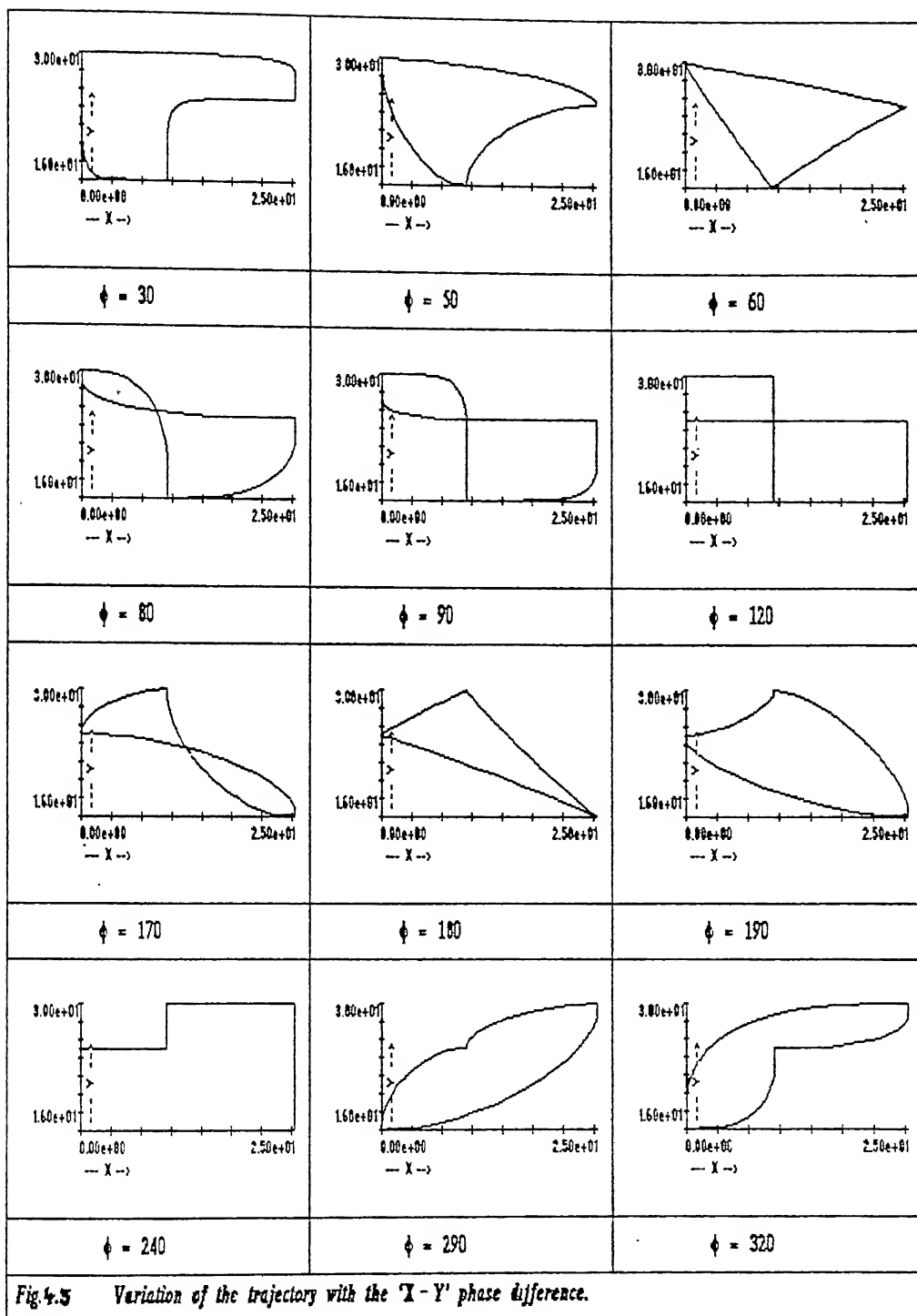
$$\Phi_{pq} = \theta_{c0p} - \theta_{c0q}$$

where the notation  $\Phi_{pq}$  implies that the cam  $p$  leads cam  $q$  by an angle  $\Phi_{pq}$ . For perfect motion coordination,

$$\Phi_{pq} = 0.$$

There will be distortions in the the trajectory if this angle deviates from zero.

It is an interesting observation to see the effect of the variation of this angle on the trajectory. It may become useful when the existing trajectory has to be slightly changed, or some dwell periods have to be added or reduced. These effects can be easily achieved by manipulating the phase difference. The spatial positions of the end effector change drastically with larger values of the phase difference. Fig 4.4 shows the variation in the trajectory of example problem 1 in



chapter 3 ( Fig. 3.1 ) with the phase difference  $\Phi = \Phi_{yx}$  . It is seen that the shapes generated turn out to be very much different from the original shape for which the cams were designed, and from each other.

It may be noted that these different shapes of the trajectory are possible from the designed cam profiles without any change in the kinematic characteristics ( like the cycle time, peak values of the acceleration, velocity, and the extremes of the pressure angle, etc. ) of the mechanisms governing the motion in either direction. This fact may be made use of to extract some flexibility from the system in view of changes in the trajectory. The dwell characteristics can also be similarly manipulated. For example, there were no dwell periods in the original trajectory, whereas with the triangular trajectory in Fig 4.4, (  $\Phi = 60, 180$  ), at all the three vertices of the triangle, there occurs a dwell of 2 seconds each.

Whatever be the phase difference, it needs to be accurately maintained to ensure adherence to the desired performance.

## 4.2 Generation of higher degrees-of-freedom motion.

Most of the discussion in the earlier chapters was related to two degree-of-freedom motion systems. In the present section, the possibility of generation of motion with higher degrees-of-freedom, based on the same working principle is explored.

### 4.2.1 Two and half dimensional motion.

By  $2\frac{1}{2}$  D motion, we mean the motion which can be expressed in terms of two planar variables, but is 3 dimensional in nature. Essentially, it refers to a motion on the surface of a circular cylinder, achievable by the combination of angular

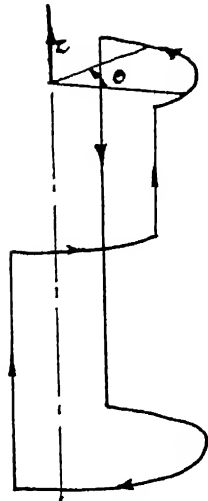


Fig 4.5. 2½-D Trajectory.

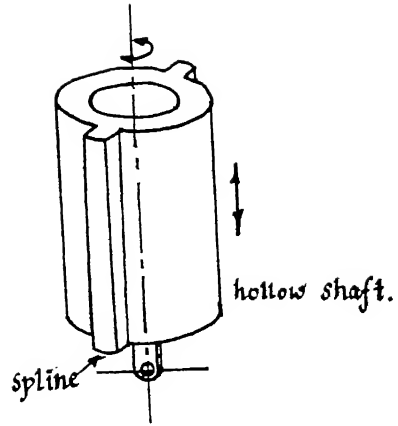


Fig 4.7. Splined shaft type motion assembler.

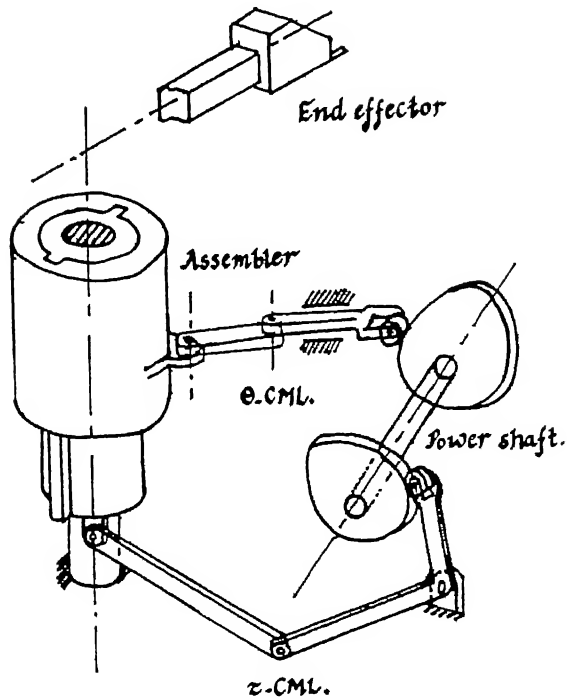


Fig 4.6. Mechanism generating a 2½-D trajectory.

motion with linear motion along its axis. Truly speaking, this motion consists of only two degrees-of-freedom, but has been treated separately on account of its 3 dimensionality. This type of motion is illustrated in Fig. 4.5. The trajectory is produced using two variables -  $\theta$  and  $z$ , as shown. The mechanism which can generate such a trajectory is shown in Fig. 4.6.

Splined shaft type motion assembler has been used here, and is shown in Fig. 4.7. The shaft is hollow, and is free to slide on the axle, and can also undergo a rotational motion about it. The splines make the linear motion independent of the angular motion.

Whenever angular motion at the output end is required, a [P/R][P/R][P/R]R mechanism may be used for input output coordination. For small angular motions, an oscillating follower may directly be employed.

It may be noted that the two linkages for the two different directions in this case operate in two different planes, and if only disc cams are employed, the follower which has to be in the plane perpendicular to the cam profile plane cannot be an oscillating follower, since it might cause a loss of contact. A sliding follower on the other hand can take motion from the cam in one plane, and can be used as the input link of a linkage in a different plane. Three dimensional (globoidal / cylindrical ) cams can be used in these cases, since the plane of motion of the follower can be perpendicular to the cam axis.

### **Three and more degrees-of-freedom.**

Theoretically, the principle on which the CML type mechanical robots are based, can be used to generate motion with any desired number of degrees-of-freedom. In practice though, it becomes increasingly difficult to combine and

coordinate the motion at the output end. The major hindrance is that of the motion assemblers. The motion generated in different directions cannot be maintained independent of each other with higher degrees of freedom.

It can be seen that the assemblers bring about the desired independency for the applications with two degrees-of-freedom by means of some additional constrained motion between two joints which can be considered to be distinct from the joints in the four bar mechanisms. ( Fig. 4.1, 4.2, 4.3, 4.7. ). This additional constrained motion for three degrees-of-freedom, turns out to be a planar motion, which is nothing but the projection of the 3-d motion on to a coordinate plane. Physical systems exhibiting such a situation can be practicable only if this projection is very small.

If the motion with the third or higher degree-of-freedom be used for the purpose of other actuation, like effecting the movement of a gripper, etc. then using a third CML might become feasible.

#### 4.3 Summary.

Though a continuous planar motion can be generated using only one CML, many a times, the cam profiles so designed are not practicable. Also, non differentiable paths are not feasible with these owing to the appearance of cusps on the cam profile.

The major limitation involved in the use of the proposed mechanisms lies in the fact that these lack reprogrammability, and hence can be used for only those trajectories for which they are designed. This low flexibility makes them inapplicable where the path to be traced by the end effector changes frequently. Wherever these changes are limited to a small number, different cams could be

designed with the same linkage for different possible trajectories, and used for the corresponding trajectory. Though, changing the cams might become an undesirable activity, employing these mechanisms still has its advantages cost wise, whenever the number of cams involved is small, and the duration of the operation with one trajectory is large enough.

The assemblers in some cases may turn out be very cumbersome. The dynamics of the assemblers plays an important role in determining the performance of these mechanisms, and should not be excessively large. This limits the range of output motion possible from these mechanisms to as far as the mass of the assemblers remains within practicable values.

It may be noted that these mechanisms are applicable chiefly to those cases where a continuous control over the output kinematics is needed throughout the motion cycle. For point to point control, linkages will prove to be better.

## chapter 5. OPTIMUM DESIGN OF CAM-FOLLOWER SYSTEMS.

### 5.1 Introduction.

Profile synthesis of a cam involves the generation of a space curve which when traced out by a constrained follower point, produces a desired motion of the follower point. Basic purpose of cam design is fulfilled with the generation of such a curve. However, this does not guarantee an efficient motion transmission from the cam to the follower. Other operational constraints also need to be satisfied for this. These could be classified into kinematic and dynamic operational constraints. Two important kinematic constraints are : (i) the kinematic efficiency of motion transfer at the higher pair should be as large as possible, and (ii) the contact stress at the point of contact should be minimum possible.

It is seen that both these kinematic operational constraints can be measured in terms of critical performance parameters. The pressure angle determines the kinematic efficiency, whereas the radius of curvature of the cam profile determines the contact stress at the point of contact. Thus the smoothness of operation of the cam-follower system can be ensured if the values of these performance parameters are within some critical limits. Most commonly, the maximum value of the pressure angle, and the minimum value of the radius of curvature depends on the displacement characteristics of the follower. However, when the follower motion is mapped on the cam profile, structural and other parameters like the cam-follower pivot-to-pivot distance, the radius of the roller, the minimum

the cam-follower pivot-to-pivot distance, the radius of the roller, the minimum displacement of the follower, etc., also play important roles in determining these values. In the present work, a scheme has been developed in which the values of these physical parameters can be selected in a way so as to satisfy the operational constraints in an optimum manner, and at the same time, keep the cam size as small as possible.

The current practice in cam design involves checking the values of these critical performance parameters with reference to some nomograms, charts, or graphs, previously determined for an exhaustive set of values, and has been brought out in many publications. Jensen [6], Chen [11], Ganter and Vicker [4] etc have explained various ways of providing the necessary checks. Essentially, the underlying principle is the selection of a suitable displacement curve and then the determination of the range for the best performance, with the help of the charts for this displacement curve. These methods have a limitation in that they are applicable to a particular curve only, and when the actual curve to be traced is different, or is a combination of standard curves, these procedures become laborious and inaccurate. Maggiore and Meneghetti [9] have optimized the cam-follower behaviour by means of a suitable selection of a displacement curve parameters. Dhande and Kale [2] have developed a method in which a number of combinations of design parameters are generated, and finally those are selected which yield the minimum size of the cam.

In the present work, a more formal perspective has been taken and the problem is formulated as a classical optimization problem. The cam size is treated as the objective function to be minimised with the constraints on the maximum pressure angle and minimum radius of curvature. The Zoutendijk's method of feasible directions for nonlinear optimization has been employed (explained later).

The procedure developed is applicable to any displacement curve and has been implemented in the form of an interactive computer programme. Only kinematic operational constraints have been presently considered. Examples relating to disc cam mechanisms are presented. The principle, however, is applicable to other types of cam mechanisms as well.

## 5.2 Formulation of the optimization problem of cam-follower systems.

It is possible to restrict the extremal values of the performance parameters within a certain critical limit, but only at the expense of a larger cam size. In most of the applications, the designer aims at keeping this to a minimum, since it further reduces the weight, balancing problems, space occupied, cost, etc.. Hence, the objective function used in the problem is the cam size. By the size of the cam is meant the base circle radius. Throughout the work, the terms 'base circle radius', and 'cam size' are treated as synonymous, since the size of the cam can be represented by the base circle radius.

Let  $(a_1, a_2, \dots, a_n)$  be the cam follower system parameters (physical) which have to be designed. Since the size of the cam depends on these, let

$$r_b = f(a_1, a_2, \dots, a_n) \quad (5.1)$$

be the size of the cam. This is our objective function. Let the pressure angle be represented as :

$$\psi = g_1'(a_1, \dots, a_n, s, \dot{s}); \quad (5.2a)$$

and the radius of curvature as :

$$\rho = g_2'(a_1, \dots, a_n, s, \dot{s}, \ddot{s}); \quad (5.2b)$$

where  $s$ ,  $\dot{s}$ , and  $\ddot{s}$  are the follower displacement, and its first and second derivatives respectively.

Now,

$$s = h_1(\theta_c) \quad ; \quad \dot{s} = h_2(\theta_c) \quad ; \quad \text{and} \quad \ddot{s} = h_3(\theta_c) \quad ; \quad (5.3)$$

where

$$\theta_c = h(t) \quad (5.4)$$

is the cam rotation angle. (Usually,  $\theta_c = \frac{t}{\omega}$ ;  $\omega$  = uniform rotational speed of the cam.)

Thus, eliminating  $s$ ,  $\dot{s}$ , and  $\ddot{s}$  from equations 5.2,

$$\psi = g_1''(a_1, \dots, a_n, \theta_c); \quad (5.5a)$$

$$\rho = g_2''(a_1, \dots, a_n, \theta_c). \quad (5.5b)$$

Since we are interested in the extremum values of these functions which can be obtained as -

$$\frac{d\psi}{d\theta_c} = \frac{dg_1''}{d\theta_c} = 0; \quad \frac{d\rho}{d\theta_c} = \frac{dg_2''}{d\theta_c} = 0 \quad (5.6a)$$

$$\frac{d^2g_1''}{d\theta_c^2} < 0; \quad \frac{d^2g_2''}{d\theta_c^2} > 0. \quad (5.6b)$$

If the value of  $\theta_c$  could be found from these equations in terms of  $(a_1, a_2, \dots, a_n)$ , and substituted in equations (5.4), we obtain

$$\psi_{\max} = g_1'''(a_1, \dots, a_n); \quad (5.7a)$$

$$\rho_{\min} = g_2'''(a_1, \dots, a_n); \quad (5.7b)$$

It is desired that

$$\psi_{\max} \leq \psi^* \quad \text{and} \quad \rho_{\min} \geq \rho^* \quad (5.8)$$

where  $\psi^*$  and  $\rho^*$  are the critical values.

Let  $(a_{1l}, \dots, a_{nl})$  and  $(a_{1u}, \dots, a_{nu})$  be the lower and upper bounds on the parameters  $(a_1, \dots, a_n)$ . Then, the problem can be stated as:

Minimise

$$r_b = f(a_1, a_2, \dots, a_n) \quad (5.9)$$

subject to

$$\psi_{max} = g_1'''(a_1, \dots, a_n) \leq \psi^* \quad (5.10a)$$

$$\rho_{min} = g_2'''(a_1, \dots, a_n) \geq \rho^* \quad (5.10b)$$

and

$$\begin{aligned} a_{1l} &\leq a_1 \leq a_{1u} \\ a_{2l} &\leq a_2 \leq a_{2u} \\ &\vdots \\ a_{nl} &\leq a_n \leq a_{nu}. \end{aligned} \quad (5.10c)$$

or in a more generalised manner as:

Minimise

$$r_b = f(a_1, a_2, \dots, a_n) \quad (5.11)$$

subject to

$$g_j(a_1, a_2, \dots, a_n) \leq 0, \quad j = 1, \dots, 2n+2 \quad (5.12)$$

where  $n$  = number of variables.

In words, the problem is stated as follows :

"Given the critical values of the pressure angle and the radius of curvature, to determine a set of parameters ( $a_1, a_2, \dots, a_n$ ) which while remaining within given bounds, will keep the pressure angle and radius of curvature constraints satisfied, and at the same time yield the minimum cam size."

### 5.3 Solution of the optimization problem.

Since the objective function as well as the constraints are nonlinear, there is no method which can give the optimum solution in a deterministic manner. What instead has to be done is to start from an initial point at which all the constraints are satisfied, and go on improving the value of the objective function in an iterative manner. Thus the knowledge of an initial feasible point becomes

necessary. It is obvious that the dependency of the objective function on the various parameters be comprehended before the current values of the parameters are altered. In fact, for any family of curves, the direction of the gradient is the direction along which the values of the curve constants change at the fastest rate. Hence the direction of the negative gradient is always the best direction, since we are interested in minimising the function.

We may move along this direction as long as no constraint gets violated, or a minima occurs.(Fig 5.1) If a minima occurs, then again the negative gradient direction may be determined at that point. If, however, a constraint is violated, this direction becomes infeasible for a further search. At this point then, there could be a possibility of finding another direction along which the objective function reduces, may be at a little lesser rate, but without violating any constraints. Thus, this direction should be such that

- (i) the objective function reduces along it ; and
  - (ii) a finite step in the feasible range can be taken along this direction.
- i.e. it should steer away from the constraint boundary.

In general there could be several such directions, and we would like to find the best one of these. The requirement on this direction - as stated above - is that (Fig 5.2) the  $\angle \gamma_1$  should be as small as possible, and  $\angle \gamma_2$  as large as possible. Thus the direction finding problem itself becomes an optimization problem.

The step taken along any direction could be either till a constraint is violated, or a minima is reached. It is impracticable to directly solve for the point of intersection between the line of the direction of search, and the constraint. Hence, in practice, what can be done is to take a step till a minima is reached, and then to check if the constraints are violated. If any of the constraints is violated, then to recede back and modify the step till the constraint boundary is hit. To

find the step which takes us to a minima, some one dimensional optimization technique has to be employed.

When we see that at a stage either no direction remains along which the search can be continued, or when the step size reduces to zero, we can assume that we have reached the optimal solution.

#### 5.4 Zoutendijk's method for nonlinear optimization.

The above discussion forms the philosophy of the Zoutendijk's method of feasible directions.(Ref. [10] for details.) In the method of feasible directions, a direction is declared as a usable-feasible direction if it satisfies the following conditions :

$$\bar{S}^T \nabla f(A) \leq 0 \quad ; \quad i = 1, \dots, n. \quad (5.13)$$

$$\bar{S}^T \nabla g_j(A) \leq 0 \quad ; \quad i = 1, \dots, n ; \quad j = 1, \dots, m. \quad (5.14)$$

where

$f$  = objective function,

$g_j$  = constraints,

$\bar{S}$  = direction of search,

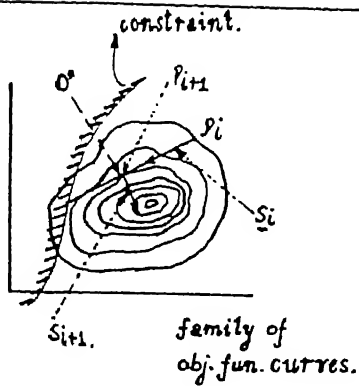
$\bar{S}^T$  = transpose of  $\bar{S}$ ,

$\bar{A}$  = position vector of the current point,

$n$  = number of variables,

$m$  = number of active constraints.

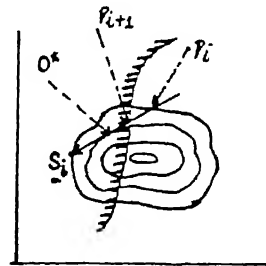
Geometrically, this means that the angle between the gradient direction of the objective function and the search direction should be an obtuse angle, since only in this direction will the objective function reduce. The second condition



$S_i \equiv$  Current Search Direction  
 $S_{i+1} \equiv$  Next Search Direction.

(a)

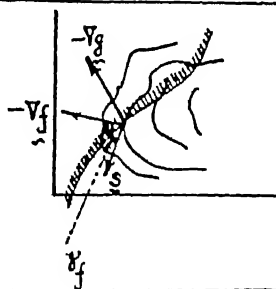
Fig 5.1. Optima before violation.



$O^*$  - Optimal point through 1-d search.  
 $P_i$  - Current Point.  
 $P_{i+1}$  - Next Point.

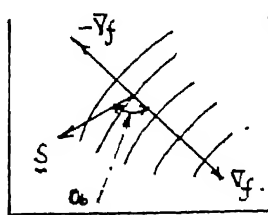
(b)

Violation prior to optima.



$$-\nabla f \hat{\cdot} S \equiv \nabla g.$$

Fig 5.2. Optimization of the search direction.



$O_b \nrightarrow$  Obtuse angle.

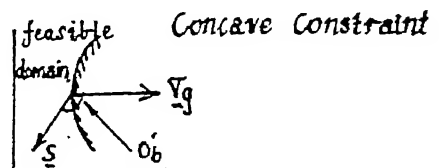
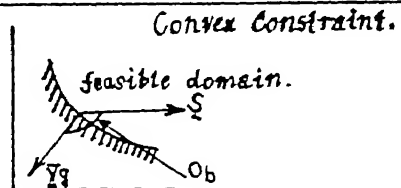


Fig 5.3. Usable-feasible direction.

specifies a similar condition to ensure that we are always in the feasible range. This is illustrated in the Fig. 5.3.

Going a step further, since we wish to go as close to the negative gradient direction as possible, (i.e. as away from the direction of the positive gradient as possible) we impose the constraint that

$$S^T \nabla f(A) \leq -\alpha ; \quad (5.15)$$

where  $\alpha$  is a scalar greater than zero.

And similarly since we want to steer away from the constraint to the maximum extent, we impose the condition that

$$S^T \nabla g_j(A) \leq -\mu_j \alpha ; \quad (5.16)$$

where  $\mu_j$  are some scalar multiples of  $\alpha$ . Now we see that if we try to increase the value of  $\alpha$ , then at its maximum possible value we get the locally best direction.

Then the direction finding problem can be stated as :

Minimise (  $-\alpha$  )

subject to

$$S^T \nabla f(A) \leq 0 \quad (5.17)$$

$$S^T \nabla g_j(A) - \mu_j \alpha \leq 0 \quad (5.18)$$

where  $(a_1, a_2, \dots, a_n)$  are constants.

If this be solved for  $(s_1, s_2, \dots, s_n, \alpha)$ , we shall get the optimal direction. An important point to note here is that the above constraints are all linear in nature, and so is the objective function. In addition to these, we introduce constraints that

$$-1 \leq s_i \leq 1 ; \quad i = 1, \dots, n. \quad (5.19)$$

which normalise the search direction. This ensures that the value of  $\alpha$  remains finite. Any linear optimization technique can be used to solve this.

The determination of the step size can be similarly done by any one

dimensional unconstrained minimisation technique. After finding the optimal step along this direction, it may be iteratively modified if needed to bring the next to current point in the feasibility range.

Again the search is continued till the Kuhn-Tucker conditions are satisfied [10] which determine the existence of an optimal solution of constrained optimization problems. In fact it so happens that when these conditions are satisfied, the value of  $\alpha$  turns out to be zero. (Ref. [10]) Physically this means that there no longer remains any direction in which the search can be continued. Hence the procedure is terminated. The algorithm of the Zoutendijk's method is presented in the form of a block diagram in fig. 5.4 .

## 5.5 Application of the Zoutendijk's procedure to the cam-follower optimization problem

The application dependent issues of the Zoutendijk's method are as follows :

1. Selection of an initial feasible point.
2. Objective function
  - evaluation
  - determination of the gradient.
3. Constraint
  - evaluation
  - determination of the gradient.
4. Linear optimization technique used for direction search.
5. One dimensional unconstrained minimisation technique for step size determination.
6. Technique used for the modification of the step size.

All these are discussed in detail in the following sections.

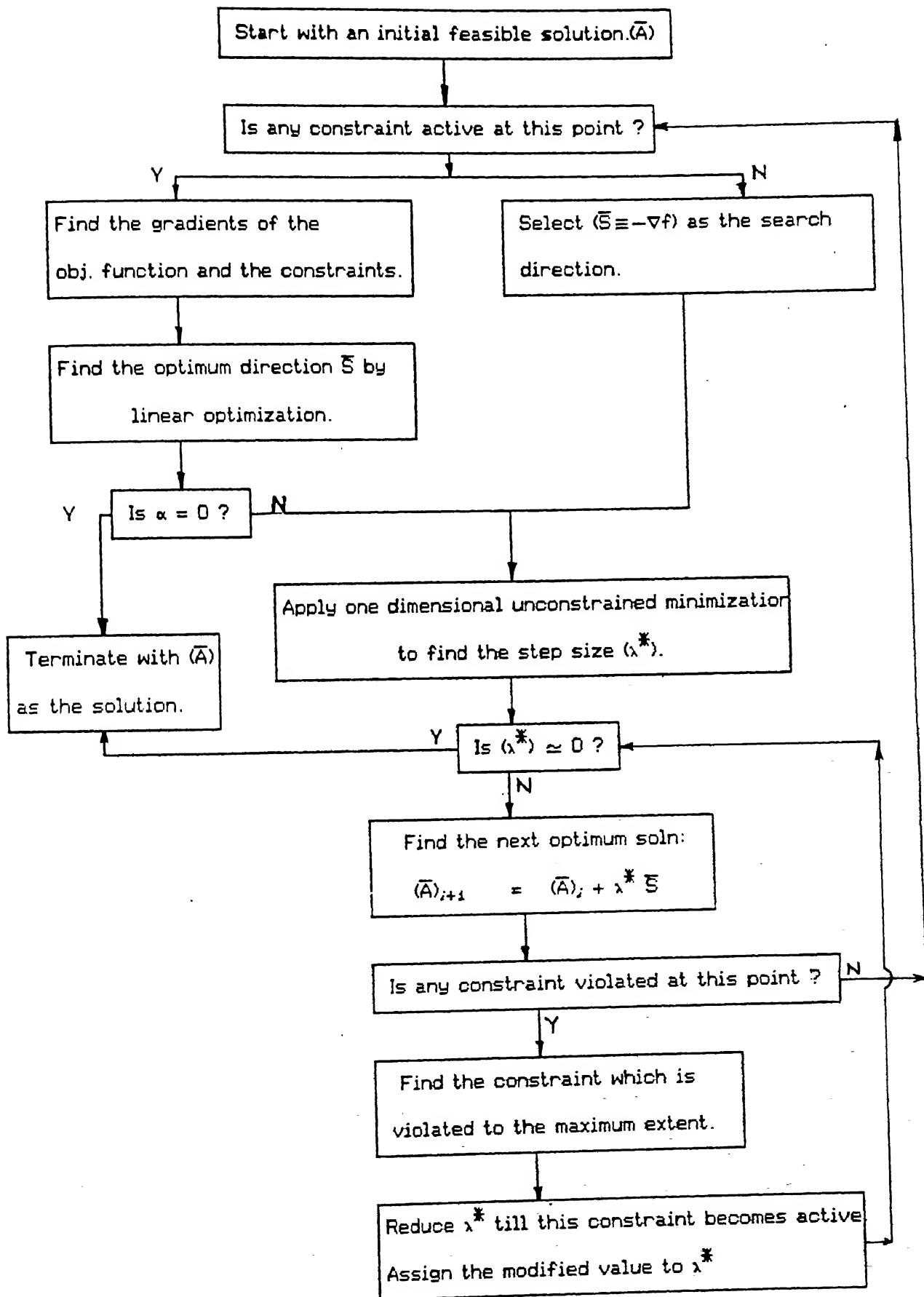


Fig.5.4. Algorithm of the Zoutendijk's method.

**5.5.1 Initial feasible point:** An initial feasible point is one which has to be selected before the Zoutendijk's procedure is invoked. This should be such that all the constraints are critically or otherwise satisfied. In our case this point i.e the value of each parameter of design should (i) be within the range of bounds specified for it; and (ii) evaluate to extremal pressure angle and radius of curvature values which are also in the desired limits.

We know that for any given cyclic follower kinematics (displacement, velocity and acceleration) if the cam size is increased, the maximum value of the pressure angle decreases and the minimum value of the radius of curvature increases. ([1], [6]) Thus if initially the size of the cam is made its maximum possible within the given bounds on the parameters, all the constraints should be satisfied. If they are not, then obviously they cannot be satisfied for any set of values of parameters which gives rise to a lesser cam size. To continue with the optimization procedure in such a situation, either the bounds on the values of the parameters or the critical values of the pressure angle and radius of curvature have to be modified.

### 5.5.2 Objective function.

The base circle radius is used as the objective function. The analytical expression used varies with the type of cam follower. The maximum magnitude of the radius vector of the point of contact may also be considered to represent the cam size. When the follower displacement values are not very large, however, this will give results similar to the one with base circle radius. In all types of cam-follower systems, the base circle radius can be determined in terms of the follower parameters by means of analytical expressions not very complex in nature. Hence once an analytical expression of the objective function is

formulated, evaluating it for a specified set of parameters and determining the gradient remain simple tasks.

### 5.5.3 Constraints.

As far as the constraints putting bounds on the values of the parameters are concerned, determination of the value and the gradient of each constraint is fairly easy. Issues become involved when the pressure angle and radius of curvature constraints come into picture. These can be stated as :

$$g_1 = \psi_{max} (a_1, \dots, a_n) - \psi^* \leq 0 \quad (5.20a)$$

and 
$$g_2 = \rho^* - \rho_{min} (a_1, \dots, a_n) \leq 0 \quad (5.20b)$$

To evaluate the value of the constraint, we need to find  $\psi_{max}$  and  $\rho_{min}$  for a given set of  $(a_1, \dots, a_n)$  on the basis of equations 5.5. We see that the evaluation of the gradients itself forms an one dimensional optimization problem. viz., for a given set of parameters to determine (i) the location (in terms of the cam rotation angle) of the extremum values of the pressure angle and radius of curvature ; and (ii) the values of these at the location found in (i). Also a check becomes necessary to determine whether the obtained value is a maxima or a minima.

Broadly speaking, there are two ways in which the search can be undertaken. One is the elimination method in which the uncertainty interval in which the solution lies is reduced by the elimination of sub-intervals from the range. Other is the interpolation method in which the objective function is approximated as some simpler polynomial in the expected range of solution and this polynomial function is optimized. This procedure is repeated till a satisfactory minimum is reached. In most of the methods which can be classified into the above two categories, some heuristics or approximations are used to quickly arrive at the solution. An elimination method called as the 'exhaustive search method' however uses no

heuristics. It is a so called 'brute force method' in which the objective function is evaluated at every point in the interval and the minimum selected. This method has been implemented in the present algorithm for reasons explained below.

All other methods are superior to this method only in the view that they involve a much lesser number of evaluations of the objective function (or its derivative) thus saving computational time and effort. However, this advantage may be outweighed in this particular case by other computations involved in the search. e.g. the interpolation of the objective function in the interpolation method, or the calculations determining the next range of uncertainty to be eliminated in the elimination methods.

Secondly, all these methods though yield a quick solution, never guarantee a global extremum unless the objective function is a convex function of the independent variable. In most of the cam profiles, this will not be so. We are interested in the global extremums only, since otherwise the results will be of no significance. The method of exhaustive search guarantees a global extrema provided that the step size with which the search is undertaken is small enough.

Since the interval of the search is finite (viz.  $360^\circ$  of cam rotation), we can afford to evaluate the objective function at every interval. In the implementation, it was seen that this method produces results quickly enough, and in fact the entire optimization procedure gets over in real time.

Actually, the exhaustive search method could be used as a 'first guess method' to locate approximately the stationary point, and then in the vicinity of this value the other techniques could have been used. However, it was again found that the exhaustive search method with a reduced step size produces quick and accurate results.

Thus to determine the extremum, the following procedure is adopted.

1. Approximate location of the extremum by the exhaustive search method using a relatively larger step size.
2. Precise location using a reduced step size. (Reduced to approximately 10% of the earlier step size.)

Now let us come to the determination of the gradient of these constraints. Again, since the constraint itself exists as a one dimensional optimization problem, it is almost impossible to analytically determine its gradient. Hence again a numerical technique is adopted. Our purpose is to find the vector

$$\nabla g_j = \left( \frac{\partial g_j}{\partial a_1}, \dots, \frac{\partial g_j}{\partial a_n} \right)^T \quad (5.21)$$

Each component of this vector, i.e.  $\left( \frac{\partial g_j}{\partial a_i} \right)$  is obtained by numerical partial differentiation, i.e. by varying  $a_i$  by a small amount on either sides of the current value, - the other parameters maintained constant - and evaluating the gradient at those points. This finite difference technique is found to give the gradient, again in real time.

### 5.5.3 Linear optimization for direction search.

The direction search problem can be stated as follows :-

Minimise  $(-\alpha)$

subject to

$$s_1 \frac{\partial g_1}{\partial a_1} + \dots + s_n \frac{\partial g_1}{\partial a_n} + \mu_1 \alpha \leq 0 ;$$

$$: \quad : \quad :$$

$$s_1 \frac{\partial g_1}{\partial a_1} + \dots + s_n \frac{\partial g_n}{\partial a_n} + \mu_1 \alpha \leq 0 ; \quad (5.22)$$

$$s_1 \frac{\partial f}{\partial a_1} + \dots + s_n \frac{\partial f}{\partial a_n} + \alpha \leq 0 ; \quad (5.23)$$

$$s_1 - 1 \leq 0,$$

:

$$s_n - 1 \leq 0 ; \quad (5.24)$$

$$-1 - s_1 \leq 0,$$

:

$$-1 - s_n \leq 0 ; \quad \text{and} \quad (5.25)$$

$$\alpha \geq 0 \quad (5.26)$$

$n$  = number of parameters,  $m$  = number of active constraints.

The best method for linear optimization presently is the simplex method, and the same has been implemented here. However, to ensure nonnegativity of the variables used in the simplex method, new variables are introduced, since the present variables can take values from  $-1$  to  $+1$ . These new variables are  $(t_1, \dots, t_n)$  which substitute  $(s_1, \dots, s_n)$  according to the following rule :

$$t_i = s_i + 1 ; \quad i = 1, \dots, n. \quad (5.27)$$

Then the problem becomes:

$$t_1 \frac{\partial g_1}{\partial a_1} + \dots + t_n \frac{\partial g_1}{\partial a_n} + \mu_1 \alpha \leq \sum_{i=1..n} \left( \frac{\partial g_1}{\partial a_i} \right) ;$$

:

:

$$t_1 \frac{\partial g_1}{\partial a_1} + \dots + t_n \frac{\partial g_n}{\partial a_n} + \mu_2 \alpha \leq \sum_{i=1..n} \left( \frac{\partial g_i}{\partial a_i} \right) \quad (5.28)$$

$$t_1 \frac{\partial f}{\partial a_1} + \dots + t_n \frac{\partial f}{\partial a_n} + \alpha \leq \sum_{i=1..n} \left( \frac{\partial f}{\partial a_i} \right) \quad (5.29)$$

$$\begin{aligned} t_1 &\leq 2, \\ &: \\ t_n &\leq 2; \end{aligned} \quad (5.30)$$

$$\begin{aligned} t_1 &\geq 0, \\ &: \\ t_n &\geq 0; \quad \text{and} \end{aligned} \quad (5.31)$$

$$\alpha \geq 0. \quad (5.32)$$

This problem can now be very easily solved by the simplex algorithm. to give the variables  $(t_1, \dots, t_n, \alpha)$  from which either the optimality can be checked ( $\alpha = 0$ ) or the direction of search obtained ( $s_i = t_i - 1$ ). In the implementation, all the values ' $\mu_j$ ' are taken to be unity to give equal importance to all the constraints.

#### 5.5.4 One dimensional unconstrained minimisation for step size determination.

Let

$$r_b = f(a_1, a_2, \dots, a_n) \quad (5.33)$$

be the objective function in 'n' variables  $(a_1, a_2, \dots, a_n)$ .

If  $\bar{S} = (s_1, \dots, s_n)^T$  is the direction of search and  $\lambda$  is the step size, then the next point can be written as :

$$\bar{A}_{i+1} = \bar{A}_i + \lambda \bar{S} = (a_1 + \lambda s_1, \dots, a_n + \lambda s_n)^T. \quad (5.34)$$

and the objective function as :

$$r_b = f(a_1 + \lambda s_1, \dots, a_n + \lambda s_n) \quad (5.35)$$

where  $(a_1, a_2, \dots, a_n)$  and  $(s_1, \dots, s_n)$  are constants.

This is a single variable function in  $\lambda$  which needs to be optimised without any constraints.

As previously stated, one dimensional methods can be of the interpolation or elimination type. The interpolation methods are based more on mathematical approximations of the functions than numerical heuristics, and they converge after a finite number of steps to the real solution (Ref [10]). They are also more efficient than the elimination methods. Hence it will be better to use one of the interpolation methods. Since in our case, there are possibilities of finding one optimal solution close to the previous one, a method which gives quick results in close vicinities of the current point is necessary. The direct root method is one such method. It also works out well for long distance searches though with a little lower efficiency. In this method, the derivative of the objective function is approximated as a straight line and the point at which it becomes zero is found. Then this becomes the new optimal point. This procedure is repeated till a satisfactory value is obtained. This is nothing but determination of the root of the equation

$$\frac{\partial r_b}{\partial \lambda} = \frac{\partial f( (a_1+\lambda s_1), \dots, (a_n+\lambda s_n) )}{\partial \lambda} = 0 ; \quad (5.36)$$

by the Regula – Falsi technique.

### 5.5.5 Step size modification.

On taking an optimal step along the optimal direction, if any of the constraints get violated, then the step size is reduced till the constraint boundary is reached. The maximum violated constraints is first considered, and the

process repeated till all the constraints are finally satisfied. The procedure uses a simple linear interpolation between the feasible and the infeasible point; every time evaluating the gradient to check whether the value becomes zero.

If the  $r$ th constraint is violated at  $\lambda = \lambda^*$ ,

$$g'_r = g_r |_{\lambda = \lambda_1} = g_r(\bar{A}_i) \leq 0 \quad \dots\dots\dots \text{satisfied at } \lambda = \lambda_1 (= 0, \text{ initially}) \quad (5.37)$$

$$g''_r = g_r |_{\lambda = \lambda^*} = g_r(\bar{A}_i + \lambda^* \bar{S}) \geq 0 \quad \dots\dots\dots \text{violated at } \lambda = \lambda^* \quad (5.38)$$

Then, assuming a linear variation of  $g_r$  w.r.t.  $\lambda$ ,

$$g_r(\lambda) = p_1 + p_2 \lambda \quad (5.39)$$

where

$$p_1 = g'_r, \quad \text{and} \quad p_2 = \frac{g'_r - g''_r}{\lambda^*} \quad (5.40)$$

The approximate value of  $\lambda$  which makes  $g_r(\lambda) = 0$  is the desired value of the modified step.

$$\text{Then, } p_1 + p_2 \lambda = 0 \quad \Rightarrow$$

$$\lambda = \frac{-p_1}{p_2} = \frac{-g'_r}{g'_r - g''_r} \lambda^* \quad (5.41)$$

Using this value, a new point can be found which may be in the feasible or infeasible region. A similar interpolation as above can then be continued till the next point lies on the constraint boundary. i.e.

$$g_r(\lambda) |_{\lambda = \lambda^*} \approx 0 \quad (5.42)$$

## 5.6 Limitations of the Zoutendijk's method .

Though the Zoutendijk's method appears to work out efficiently, there are certain drawbacks. These may be listed as follows :

1. It involves a lot of computation in finding the optimal direction owing to

the linear optimization.

2. It requires the evaluation of the gradient of the constraints and the objective function increasing the computation further.
3. Similar to other nonlinear optimization techniques, a global optimum is not guaranteed by the Zoutendijk's procedure and it needs to be repeated with different initial points.

In spite of this, the direct approach used in this method which relies on the dependence of the search direction on the nature of the objective function and the constraints, the method works out efficiently.

In the following chapter we shall discuss how it has been applied to typical cam-follower mechanisms.

## chapter 6. APPLICATION TO TYPICAL CAM-FOLLOWERS.

### 6.1 Preliminaries.

In the application of the method developed in the previous chapter to any specific cam-follower mechanism, the following issues are important.

1. Identification of the design variables.
2. Formulation of the objective function.
  - (a) Evaluation of the function value.
  - (b) Evaluation of the function gradient.
  - (c) Evaluation of the function derivative for single dimensional optimization.
3. Formulation of the constraints.
  - (d) Evaluation of the constraint value.
  - (e) Evaluation of the constraint gradient.

The objective function as previously mentioned will always be the radius of the base circle of the cam, and the design variables will be those which decide this base circle radius. Analytical expressions for all the three (a), (b), and (c) listed above will be used; which will be typical of the cam under consideration. To have a generality in the evaluation of the pressure angle and radius of curvature constraints, the 'transmission angle' instead of the pressure angle has been used. This is nothing but the complement of the pressure angle and is defined as:

$$\tau = \left( \frac{\pi}{2} - \psi \right) \quad \text{and} \quad (6.1)$$

$$\tau_{min} = \left( \frac{\pi}{2} - \psi_{max} \right) \quad (6.2)$$

where  $\psi$  is the pressure angle.

Then the value of the pressure angle constraint will be

$$\tau^* - \tau_{min} \leq 0; \quad (6.3)$$

where

$$\tau^* = \left( \frac{\pi}{2} - \psi^* \right) \quad (6.4)$$

is the critical value of the transmission angle.

Similarly, the radius of curvature constraint will be

$$\rho^* - \rho_{min} \leq 0. \quad (6.5)$$

It may be noted that the critical value of the radius of curvature here refers to the positive value of the radius of curvature. For the negative value of the same, the condition is that the absolute value should be greater than the radius of the roller ( for roller followers ), or should never be reached. (Flat faced followers). This may be incorporated as another constraint, or checked with the final solution obtained.

It is always necessary to delimit the range of permissible values that the variables would take during any stage of the optimization, for at times the variables will take values which will have no physical significance, or impossible to arrive at. Hence for each parameter, the upper and the lower bounds on the values need to be imposed. These act as additional constraints during the procedure of optimization; and are evaluated as follows:

$$a_{iU} - a_i \leq 0, \quad \text{and} \quad (6.6)$$

$$a_i - a_{iL} \leq 0. \quad (6.7)$$

A fact to be noted is that all constraints evaluate to a value lesser than zero when satisfied, and to a value greater than zero when violated. The gradients of the constraints forming the bounds on the values will obviously be

$$\nabla g_i = (0, 0, \dots, z, \dots, 0)^T \quad (6.8)$$

where  $z$  will have a value  $\pm 1$  depending upon whether the constraint under consideration is the upper or lower bound on the value of the variable.

The gradients of the pressure angle and the radius of curvature will be evaluated by the finite difference method as explained below.

Let  $(\Delta a_1, \dots, \Delta a_n)^T$  be the steps taken on either side of the current values  $(a_1, \dots, a_n)^T$ , respectively, for this finite differentiation. Then for a constraint  $g_j$  the gradient will be given as:

$$\begin{bmatrix} : \\ : \\ \frac{g_j(a_1, \dots, (a_i + \Delta a_i), \dots, a_n) - g_j(a_1, \dots, (a_i - \Delta a_i), \dots, a_n)}{\Delta a_i} \\ : \\ : \end{bmatrix} \quad (6.9)$$

Each term of this vector demands two evaluations of the constraint, and in all for one evaluation of the gradient,  $2n$  evaluations of the constraint will be necessary. This means that the pressure angle or the radius of curvature needs to be evaluated  $2n(N + N_p)$  times where  $N$  = the number of divisions on the cam surface, and  $N_p$  = the number of evaluations done for the precise location of the extremum. This figure though alarming, in practice turns out to be negligible as will be seen from the time taken for one iteration of the complete procedure.

The following sections illustrate this idea in relation to typical cam follower mechanisms. In the presentation of the results, the following format for the input and output has been followed. The input to any problem will be in terms of the following:

1. An initial feasible point.
2. Upper and lower bounds on the values of each variable.

3. The critical values of the pressure angle and radius of curvature.
4. The step size necessary for each parameter to evaluate the gradient of the constraints.

Output of the procedure will be in the form presented in tables 6.4 and 6.6. The first column shows the values of the parameters with which the iteration was started. This will always be a feasible point, and the values of the constraints at this point are shown in the next column. The third column shows the direction of search from this point, and the fourth one, the optimal step that should be taken in this direction to find an one dimensional minimum of the objective function. However, at the resulting point (shown in the next column) the constraints may be violated, (Values of the constraints at this point are shown in the next column.) and therefore, the step has to be reduced to a value shown in the column 'modified step'. The resulting point is shown in the first column of the next row, and the values of the constraint in the third row. Finally, the last column shows the time in seconds at the end of each iteration.

We shall now consider the various cam-follower mechanisms.

## 6.2 Translating roller follower mechanism.

In this section the principle of optimisation as applied to a translating roller follower mechanism has been explained. (Fig 6.1).

### 6.2.1 Selection of design variables.

The base circle radius of a cam is determined by the minimum follower displacement, the roller radius and the offset. Hence, these are selected as the

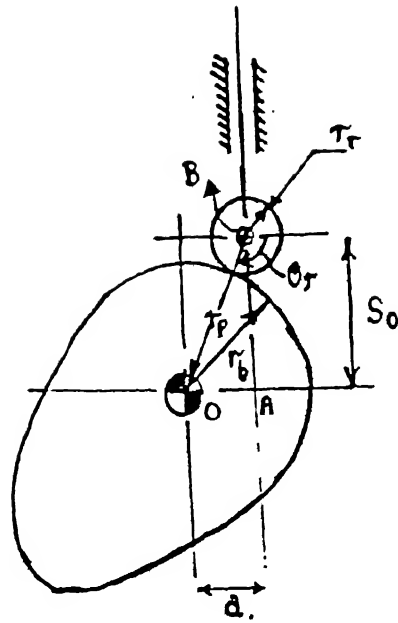


Fig 6.1 Parameters of the reciprocating roller follower.

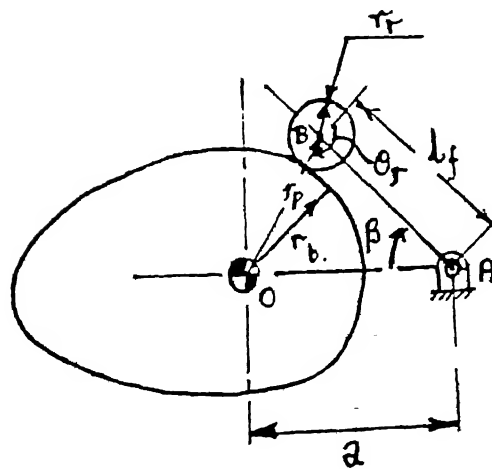


Fig 6.2 Parameters of the oscillating roller follower.

design variables. In actual practice one of these may be a constant depending upon the application of the cam. In such cases these constant values may be assigned to the corresponding parameters, and the cam optimized for the remaining ones. Typically, the radius of the roller is most of the times decided by constraints other than the pressure angle and the radius of curvature, for e.g. - the force transmitted, the minimum pin radius, etc. Here all of these have been considered for the purpose of generality.

## 6.2.2 Formulation of the objective function.

At the minimum follower displacement, the roller follower will be tangential to the base circle of the cam. The prime circle radius will then be

$$r_p = \sqrt{a^2 + s_0^2} \quad (6.10)$$

and the base circle radius

$$r_b = \sqrt{a^2 + s_0^2} - r_r \quad (6.11)$$

The gradient can be obtained by differentiating this w.r.t.  $a$ ,  $s_0$  and  $r_r$ . If  $\lambda$  is the step size along the direction  $(d_0, d_1, d_2)$  then,

$$r_b = \sqrt{(a+\lambda d_1)^2 + (s_0+\lambda d_0)^2} - (r_r+\lambda d_2) \quad (6.12)$$

When differentiated w.r.t.  $\lambda$ , we get  $r_b'(\lambda)$ .

All the resulting expressions are shown in Table 6.1. The objective function reflects that the cam size increases with increasing ' $s_0$ ' and ' $a$ ' and decreases with increasing ' $r_r$ '. However, with a reduced roller radius, the permissible value of the minimum radius of curvature may have to be reduced, ( since  $(r_b + \rho_{min})$  should be always less than  $r_r$  ) or  $r_b$  may have to be decreased. This may result in a reduced cam size which may violate the pressure angle and / or radius of curvature constraints.

The radius of the prime circle could also have been used as the objective

table 6.1 EXPRESSIONS USED FOR TRANSLATING ROLLER FOLLOWER.

Design variables:

|                               |       |
|-------------------------------|-------|
| minimum follower displacement | $s_0$ |
| follower offset               | $a$   |
| roller radius                 | $r_r$ |

Objective function:

value:

$$r_b = \sqrt{s_0^2 + a^2} - r_r.$$

gradient:

$$\left[ \frac{s_0}{\sqrt{s_0^2 + a^2}}, \frac{a}{\sqrt{s_0^2 + a^2}}, -1 \right]^T$$

single variable function for 1\_dimensional optimization:

$$r_b(\lambda) = \sqrt{(s_0 + \lambda d_0)^2 + (a + \lambda d_1)^2} - (r_r + \lambda d_2).$$

$$r_b'(\lambda) = \frac{(s_0 + \lambda d_0)d_0 + (a + \lambda d_1)d_1}{\sqrt{(s_0 + \lambda d_0)^2 + (a + \lambda d_1)^2}} - d_2.$$

function, especially in the cases where the roller radius is decided beforehand, or when the lower and the upper bounds on the roller radius are very narrow.

### 6.2.3 Pressure angle and radius of curvature constraints.

The cam follower geometry has been analysed (Appendix B) and the expressions for these have been determined analytically. It is seen that the pressure angle is independent of the roller radius. This is due to the fact that the actual point of contact of the cam and the follower i.e. the  $\angle\theta$ , (Fig 6.1) is governed by the offset and the minimum follower displacement only. The expression for the radius of curvature reflects the complexity involved, and it is seen that the nonlinearity of the various terms make it almost impossible to comprehend the precise effect of the variation of any one of the parameters on the minimum radius of curvature.

### 6.2.4 Solution of an example problem.

The input given to the example problem demonstrating the optimization of a translating roller follower is shown in table 6.2. Practical values have been selected. Generally, the pressure angle values for such a follower should not exceed  $30^\circ$  to  $35^\circ$ . The minimum radius of curvature should be such that the minimum prime curve radius turns out to be more than the roller radius. The step sizes inputted to the problem are based on judgement. Generally, it turns out that these produce satisfactory results if selected to be about 1 to 2 % of the average possible value of the variable in that range. The range of the permissible values again depends upon the application.

The output / results of this are presented in table 6.4. The cam size has

|  |          |  |           |
|--|----------|--|-----------|
| Step sizes:                                    |          | Step sizes:                                    |           |
| 1.Min. follower displacement ( $s_0$ )         | 0.1      | 1.Pivot-to-centre distance ( $a$ )             | 0.1       |
| 2.Offset ( $a$ )                               | 0.1      | 2.Follower arm ( $l_f$ )                       | 0.1       |
| 3.Roller radius ( $r_r$ )                      | 0.1      | 3.Roller radius ( $r_r$ )                      | 0.1       |
|  |          | 4.Min follower displacement ( $\beta$ )        | 0.2       |
| Bounds on values:                              |          | Bounds on values:                              |           |
|  | $l$ $u$  |  | $l$ $u$   |
| 1.Min. follower displacement ( $s_0$ )         | 3.0 20.0 | 1.Pivot-to-centre distance ( $a$ )             | 5.0 25.0  |
| 2.Offset ( $a$ )                               | 0.0 10.0 | 2.Follower arm ( $l_f$ )                       | 5.0 25.0  |
| 3.Roller radius ( $r_r$ )                      | 0.5 4.0  | 3.Roller radius ( $r_r$ )                      | 1.0 4.0   |
|  |          | 4.Min follower displacement( $\beta$ )         | 15.0 40.0 |
| 5.Min. radius of curvature                     | 1.0      | 5.Min. radius of curvature                     | 1.0       |
| 6.Max. pressure angle                          | 35.0     | 6.Max. pressure angle                          | 37.5      |
| Initial values.                                |          | Initial values.                                |           |
| 1.Min. follower displacement ( $s_0$ )         | 10.0     | 1.Pivot-to-centre distance ( $a$ )             | 10.0      |
| 2.Offset ( $a$ )                               | 5.0      | 2.Follower arm ( $l_f$ )                       | 5.0       |
| 3.Roller radius ( $r_r$ )                      | 1.0      | 3.Roller radius ( $r_r$ )                      | 1.2       |
|  |          | 4.Minimum follower displacement ( $\beta$ )    | 40.0      |
| Note: All angles in degrees.                   |          | Note: All angles in degrees.                   |           |
| Table 6.2 Input data for translating follower. |          | Table 6.3 Input data for oscillating follower. |           |

| Opt.step | Next      | point    |          | Constraints       | Mod.step | Time |
|----------|-----------|----------|----------|-------------------|----------|------|
|          | s_zero    | offset   | r_radius | pr.ang. rad.curv. |          | sec  |
| 87.2922  | (-45.2084 | -22.6042 | 62.7249) | (34.3090 -3.6212) | 1.4595   | 2    |
| 1.3538   | ( 10.4307 | 3.1847   | 2.9315)  | (26.9674 5.0517)  | 1.3538   | 4    |
| 18.0000  | ( -1.7425 | -0.5320  | 15.6594) | (89.9733 -0.2294) | 1.5111   | 6    |
| 4.5324   | ( 4.8764  | -1.6598  | 1.1708)  | (49.1757 2.1058)  | 2.7410   | 9    |
| 2.4647   | ( 8.4939  | 2.5963   | 4.7537)  | (28.7066 1.7338)  | 1.7109   | 12   |
| 3.4604   | ( 4.4751  | -1.6178  | 1.9233)  | (50.8392 1.0065)  | 1.5284   | 14   |
| 2.5816   | ( 8.2362  | 2.8959   | 5.6644)  | (30.6424 0.6219)  | 0.9172   | 16   |
| 2.8365   | ( 4.2205  | -1.6050  | 2.3591)  | (52.0005 0.3563)  | 0.7064   | 20   |
| 0.6683   | ( 5.6822  | 1.1933   | 3.0751)  | (33.0575 1.1067)  | 0.6683   | 23   |
| 9.8312   | ( -1.1211 | -0.2354  | 10.0268) | (89.8075 -1.5031) | 0.0801   | 26   |
| 0.5877   | ( 5.0391  | 1.7694   | 2.7722)  | (35.3443 1.0981)  | 0.5535   | 30   |
| 1.5665   | ( 6.6398  | 0.1686   | 4.3181)  | (34.9211 0.4782)  | 0.1512   | 33   |
|          |           | :        |          |                   | :        |      |
| 0.5376   | ( 4.5364  | 2.2721   | 2.6428)  | (40.5239 1.0720)  | 0.0006   | 56   |

| No. | Current point |        |          | Constraints |           | Size  | Search Direction |         |     |
|-----|---------------|--------|----------|-------------|-----------|-------|------------------|---------|-----|
|     | s_zero        | offset | r_radius | pr.ang.     | rad.curv. |       | s_zero           | offset  | r_r |
| 0.  | (10.0000      | 5.0000 | 1.0000)  | (34.3736    | 6.7967)   | 10.18 | (-0.6325         | -0.3162 | 0.  |
| 1.  | ( 9.0769      | 4.5385 | 2.0320)  | (34.9999    | 4.9844)   | 8.12  | ( 1.0000         | -1.0000 | 0.  |
| 2.  | (10.4307      | 3.1847 | 2.9315)  | (26.9674    | 5.0517)   | 7.97  | (-0.6763         | -0.2065 | 0.  |
| 3.  | ( 9.4088      | 2.8726 | 4.0000)  | (27.8103    | 3.1812)   | 5.84  | (-1.0000         | -1.0000 | -0. |
| 4.  | ( 6.6678      | 0.1317 | 2.2891)  | (35.0000    | 2.5282)   | 4.38  | ( 0.7409         | 1.0000  | 1.  |
| 5.  | ( 7.9355      | 1.8426 | 4.0000)  | (26.6256    | 2.1206)   | 4.15  | (-1.0000         | -1.0000 | -0. |
| 6.  | ( 6.4071      | 0.3142 | 3.0828)  | (35.0000    | 1.5243)   | 3.33  | ( 0.7085         | 1.0000  | 1.  |
| 7.  | ( 7.0569      | 1.2315 | 4.0000)  | (28.7703    | 1.3703)   | 3.16  | (-1.0000         | -1.0000 | -0. |
| 8.  | ( 6.3505      | 0.5250 | 3.5913)  | (34.1888    | 1.0000)   | 2.78  | (-1.0000         | 1.0000  | -0. |
| 9.  | ( 5.6822      | 1.1933 | 3.0751)  | (33.0575    | 1.1067)   | 2.73  | (-0.6920         | -0.1453 | 0.  |
| 10. | ( 5.6268      | 1.1817 | 3.1317)  | (33.3138    | 1.0000)   | 2.62  | (-1.0000         | 1.0000  | -0. |
| 11. | ( 5.0734      | 1.7351 | 2.7932)  | (35.0000    | 1.0892)   | 2.57  | ( 1.0000         | -1.0000 | 0.  |
| 12. |               |        |          |             |           |       |                  |         |     |
| 13. |               |        |          |             |           |       |                  |         |     |
| 14. |               |        |          |             |           |       |                  |         |     |
| 15. |               |        |          |             |           |       |                  |         |     |
| 16. |               |        |          |             |           |       |                  |         |     |
| 17. |               |        |          |             |           |       |                  |         |     |
| 18. | ( 5.0740      | 1.7345 | 2.8826)  | (34.9939    | 1.0000)   | 2.48  | (-1.0000         | 1.0000  | -0. |
| 19. | ( 5.0734      | 1.7351 | 2.8823)  | (35.0000    | 1.0001)   | 2.48  | XXXXXXXXXXXX     |         |     |

**Table 6.4. Optimization of the translating follower.**

reduced from 10.18 to 2.48 in 19 iterations. Many a times this minimum value itself might turn out to be so low that it is impracticable. In such cases, when the size is determined by other constraints like the minimum shaft diameter etc., the minimum permissible value of the size as regards those constraints may be safely assumed.

It is seen that the values of the pressure angle and the radius of curvature are critically satisfied. In some cases the constraints may be satisfied - critically or otherwise - even at the lowest possible cam size. Such a condition should always be checked before the optimization procedure is invoked, since in these case it will not be necessary to optimize at all. The optimization can, however be tried with the constraints tightened or the bounds on the values changed.

It is seen that the direction of search in most of the cases is found by the linear optimization technique. (Reflected from the fact that  $\sum d_i^2 \neq 1$ ) This shows that the constraints were critically satisfied at that point. It will be seen from the step size in the preceeding iteration, that the optimum step size has been modified to take into account the constraint value. Wherever no constraint was violated, the optimum and modified step sizes are equal. The table shows that most of the time the constraints were violated. The modified step shows them to be satisfied.

A look at the last column shows that the total time taken for the 19 iterations was 56 seconds. The results were taken on Apollo-Nexus 3000 terminals, which are considered to be moderately fast machines. Thus we see that the large number of evaluations of pressure angle and radius of curvature, on the whole, become negligible.

Fig 6.5 shows the variation of the pressure angle for one complete rotation

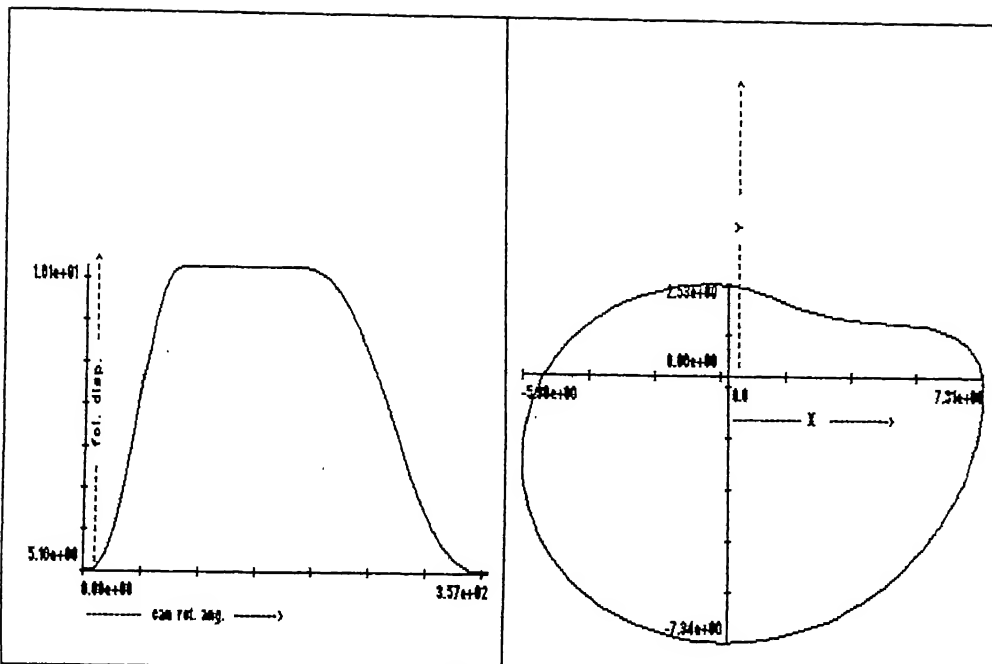


Fig. 6.3 Displacement variation (Translating follower)

Fig. 6.4 Optimized cam profile. (Translating follower)

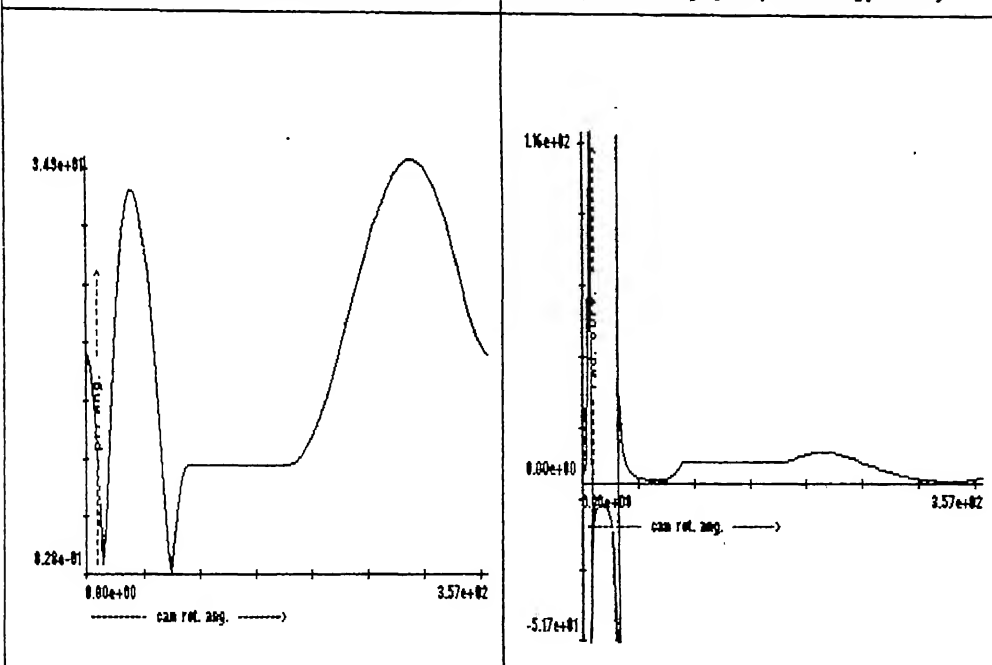


Fig. 6.5 Pressure angle plot. (Translating follower)

Fig. 6.6 Radius of curvature plot. (Translating follower)

of the cam designed on these results. The radius of curvature variation and the cam profile are shown in the figures 6.6 and 6.4 respectively.

### 6.3 Oscillating roller follower mechanism.

In this section the optimization procedure as applied to an oscillating roller follower mechanism has been explained. Ref Fig. 6.2.

#### 6.3.1 Selection of the design variables.

The base circle radius for the cam here is determined by the cam-follower pivot to pivot distance 'a', the follower arm length 'l<sub>f</sub>', the roller radius 'r<sub>r</sub>' and the minimum follower displacement 'β'. Again, one or more parameters may have preassigned values. This can be taken care of in a manner mentioned earlier.

#### 6.3.2 Formulation of the objective function.

At the minimum follower displacement, the roller is tangential to the base circle. From ΔAOB we get

$$r_p^2 = a^2 + l_f^2 - 2 a l_f \cos \beta \quad (6.13)$$

$$r_b = r_p - r_r = \sqrt{a^2 + l_f^2 - 2 a l_f \cos \beta} - r_r. \quad (6.14)$$

This forms the objective function for this particular type of follower. The gradient can be obtained by differentiating this w.r.t. a, l<sub>f</sub>, β, and r<sub>r</sub>. Resulting expressions and the expressions for single variable optimization are shown in Table 6.5. The cam size is seen to increase with a, l<sub>f</sub>, and β (when β ≤  $\frac{\pi}{2}$ ). However it reduces with the follower radius.

The prime circle also could have been used as the objective function if the roller radius was preassigned, or its range was narrow. If the value of β could be

TABLE 6.5,  
EXPRESSIONS USED FOR OSCILLATING ROLLER FOLLOWER.

Design variables:

|                               |         |
|-------------------------------|---------|
| pivot-to-cam-centre distance  | $a$     |
| follower arm length           | $l_f$   |
| roller radius                 | $r_r$   |
| minimum follower displacement | $\beta$ |

Objective function:

value:

$$r_b = \sqrt{l_f^2 + a^2 - 2 l_f a \cos \beta} - r_r.$$

gradient:

$$\begin{bmatrix} \frac{a - l_f \cos \beta}{\sqrt{l_f^2 + a^2 - 2 l_f a \cos \beta}} \\ \frac{l_f - a \cos \beta}{\sqrt{l_f^2 + a^2 - 2 l_f a \cos \beta}} \\ -1 \\ \frac{a l_f \sin \beta}{\sqrt{l_f^2 + a^2 - 2 l_f a \cos \beta}} \end{bmatrix}$$

Single variable function for 1-dimensional optimization:

$$r_b(\lambda) = \sqrt{(l_f + \lambda d_0)^2 + (a + \lambda d_1)^2 - 2(l_f + \lambda d_0)(a + \lambda d_1) \cos(\beta + \lambda d_2)} - (r_r + \lambda d_2)$$

$$r_b'(\lambda) = \frac{(l_f + \lambda d_0)d_0 + (a + \lambda d_1)d_1 - p}{\sqrt{(l_f + \lambda d_0)^2 + (a + \lambda d_1)^2}} - d_2.$$

where  $p = l_f d_2 \sin(\beta + \lambda d_2) - (d_0 l_f + a d_1) \cos(\beta + \lambda d_2)$ .

fixed up from other considerations, then an expression similar to that of the reciprocating follower would have been obtained.

### 6.3.3 Pressure angle and radius of curvature constraints.

The pressure angle unlike in the previous case is not independent of the roller radius. This is due to the fact that the direction of velocity at the point of contact on the follower depends on the roller radius of the follower. The expressions again are nonlinear in nature, and do not reflect any direct conclusions regarding the dependency of the pressure angle and radius of curvature on the design variables.

### 6.3.4 Solution of an example problem.

Input to the problem is shown in Table 6.3 . Normally, the permissible values of the pressure angle for an oscillating follower are more than that for a translating follower. Values of  $\beta$  are accepted in degrees, but during optimization are calculated in radians. The step size for the gradient evaluation for each parameter is consistent to the mean value variation.

The output / results are presented in Table 6.6. Cam size has reduced from 5.76 to 2.48 in 54 iterations. This low reduction in size is chiefly due to the presence of the parameter  $\beta$  in the objective function and as one of the design variables. The difference of scales in the values of  $\beta$  and the other parameters restrict the step size to a very low value since a larger step violates the constraints. The objective function also gets distorted due to these disparities in scale. This could be taken care of by normalising and rescaling the variables. If dimensionless parameters of some sort be used, and all the variables normalised,

| No. | Current point |        |        |         | Constraints |           | Size | Search Direction |         |         |        |
|-----|---------------|--------|--------|---------|-------------|-----------|------|------------------|---------|---------|--------|
|     | a             | l_f    | r_r    | beta    | pr.ang.     | rad.curv. |      | a                | l_f     | r_r     | beta   |
| 0.  | (10.0000      | 5.0000 | 1.2000 | 0.6981) | (37.3375    | 4.3999)   | 5.76 | (-1.0000         | 1.0000  | -1.0000 | -1.000 |
| 1.  | ( 9.9963      | 5.0037 | 1.1963 | 0.6945) | (37.5000    | 4.3859)   | 5.74 | (-1.0000         | 1.0000  | 1.0000  | 0.334  |
| 2.  | ( 9.9854      | 5.0146 | 1.2073 | 0.6981) | (37.2692    | 4.3702)   | 5.73 | (-1.0000         | -1.0000 | -1.0000 | -1.000 |
| 3.  | ( 9.9813      | 5.0106 | 1.2033 | 0.6941) | (37.5000    | 4.3600)   | 5.71 | (-1.0000         | 1.0000  | 1.0000  | 0.333  |
| 4.  | ( 9.9692      | 5.0227 | 1.2154 | 0.6981) | (37.2488    | 4.3428)   | 5.71 | (-1.0000         | -1.0000 | -1.0000 | -1.000 |
| 5.  | ( 9.9648      | 5.0183 | 1.2109 | 0.6937) | (37.5000    | 4.3315)   | 5.69 | (-1.0000         | 1.0000  | 1.0000  | 0.333  |
| 6.  | ( 9.9514      | 5.0316 | 1.2243 | 0.6981) | (37.2258    | 4.3126)   | 5.68 | (-1.0000         | -1.0000 | -1.0000 | -1.000 |
| 7.  | ( 9.9466      | 5.0268 | 1.2194 | 0.6933) | (37.5000    | 4.3002)   | 5.66 | (-1.0000         | 1.0000  | 1.0000  | 0.332  |
| 8.  | ( 9.9320      | 5.0413 | 1.2340 | 0.6981) | (37.2001    | 4.2795)   | 5.65 | (-1.0000         | -1.0000 | -1.0000 | -1.000 |
| :   |               |        |        |         |             |           | :    |                  |         |         |        |
| 36. | ( 9.2354      | 5.4074 | 1.6001 | 0.6981) | (35.9391    | 3.1051)   | 4.57 | (-1.0000         | -1.0000 | -1.0000 | -1.000 |
| 37. | ( 9.2074      | 5.3794 | 1.5721 | 0.6701) | (37.5000    | 3.0209)   | 4.43 | (-1.0000         | 1.0000  | 1.0000  | 0.286  |
| :   |               |        |        |         |             |           | :    |                  |         |         |        |
| 53. | ( 8.0582      | 5.9829 | 2.1755 | 0.6092) | (37.5000    | 1.0006)   | 2.48 | (-1.0000         | 1.0000  | 1.0000  | 0.208  |
| 54. | ( 8.0577      | 5.9834 | 2.1761 | 0.6093) | (37.4915    | 1.0000)   | 2.48 | *****            |         |         |        |

Table 6.6. Optimization of the oscillating follower.

| Opt.step | Next point |        |        |          | Constraints |           | Mod.step | Time |
|----------|------------|--------|--------|----------|-------------|-----------|----------|------|
|          | a          | l_f    | r_r    | beta     | pr.ang.     | rad.curv. |          |      |
| 0.7627   | (9.2373    | 5.7627 | 0.4373 | -0.0646) | (89.9877    | 0.0076)   | 0.0037   | 19   |
| 0.5722   | (9.4242    | 5.5758 | 1.7685 | 0.0856)  | (28.7586    | 3.7979)   | 0.0110   | 26   |
| 0.5796   | (9.4057    | 4.4350 | 0.6277 | 0.1185)  | (78.8991    | 2.2639)   | 0.0040   | 52   |
| 0.5717   | (9.4096    | 5.5823 | 1.7750 | 0.0846)  | (28.7860    | 3.7730)   | 0.0121   | 57   |
| 0.5803   | (9.3889    | 4.4424 | 0.6351 | 0.1179)  | (78.9409    | 2.2265)   | 0.0044   | 76   |
| 0.5676   | (9.3972    | 5.5859 | 1.7786 | 0.0827)  | (28.7791    | 3.7497)   | 0.0133   | 81   |
| 0.5809   | (9.3706    | 4.4507 | 0.6434 | 0.1173)  | (78.9740    | 2.1870)   | 0.0048   | 99   |
| 0.5655   | (9.3811    | 5.5923 | 1.7850 | 0.0812)  | (28.7981    | 3.7215)   | 0.0146   | 104  |
| 0.5815   | (9.3505    | 4.4599 | 0.6525 | 0.1166)  | (79.0099    | 2.1453)   | 0.0053   | 124  |
| :        |            |        |        |          |             |           |          | :    |
| 0.6059   | (8.6295    | 4.8015 | 0.9941 | 0.0922)  | (80.3177    | 1.2154)   | 0.0280   | 430  |
| 0.5671   | (8.6403    | 5.9465 | 2.1392 | 0.8328)  | (30.7368    | 2.4682)   | 0.0976   | 435  |
| :        |            |        |        |          |             |           |          | :    |
| 0.5377   | (7.5205    | 6.5206 | 2.7132 | 0.7220)  | (35.5961    | 0.5092)   | 0.0005   | 528  |
| ***      | *****      |        |        |          | *****       |           | ***      | ***  |

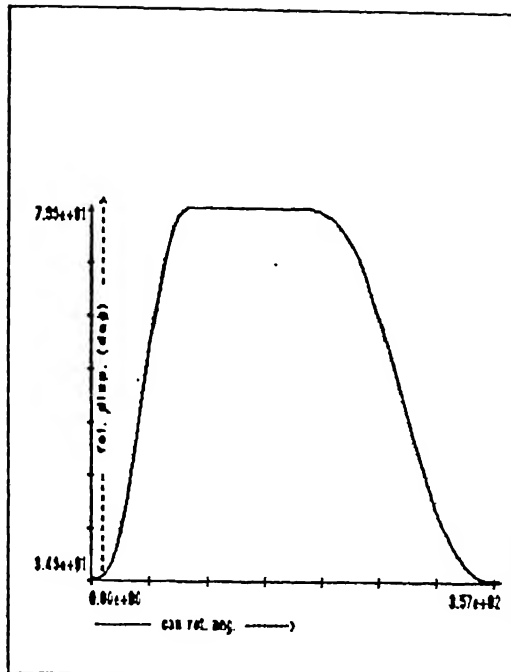


Fig 6.7. Displacement variation (Oscillating follower)

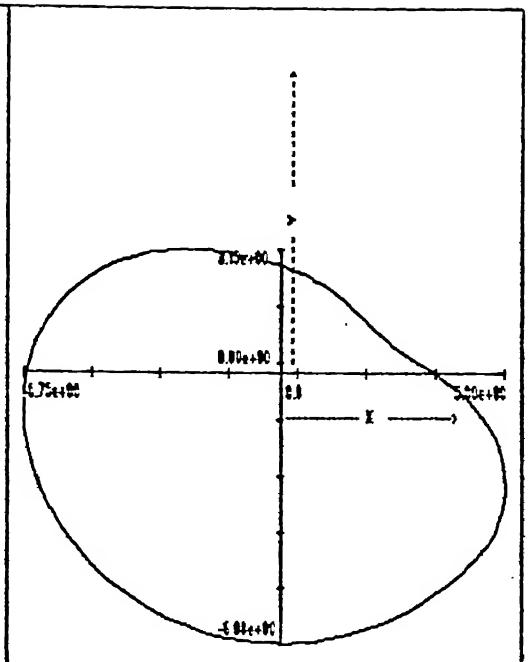


Fig 6.8. Optimized cam profile (Oscillating follower)

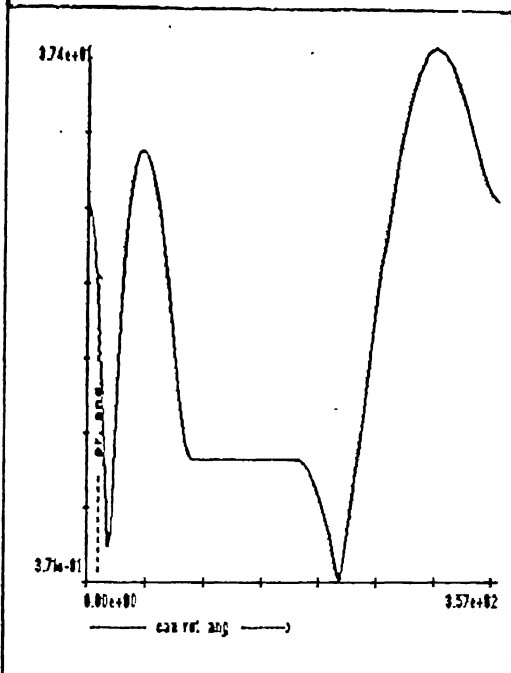


Fig 6.9. Pressure angle plot (Oscillating follower)

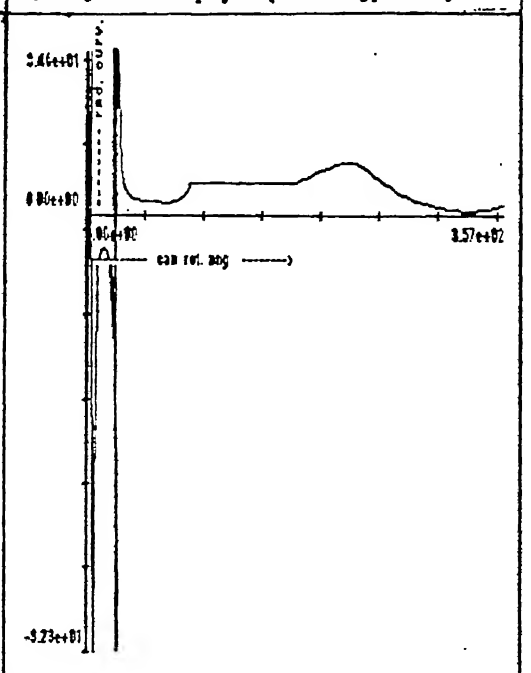


Fig 6.10. Radius of curvature plot (Oscillating follower)

1. Specification of initial values, bounds and step sizes.
2. Effects of different displacement curves.
3. Methods of improving the algorithm.

#### 6.5.1 Specification of the data.

##### (i) Initial values of the variables.

As already mentioned, it is necessary to give an initial feasible solution to start the process of optimization. In most of the cases, this will be selected as the one yielding the maximum possible cam size. A little trial and error may be necessary before these values are finalised. An important point is that the solution obtained is always dependent on the initial point specified. However, this dependence might not be always predictable. The only alternative is to use different initial points and obtain different results if possible; and use the best one. It is to be noted that the solution obtained will not necessarily be a global optimum.

##### (ii) Bounds on variables.

Practical constraints do generally put some bounds on the values of the variables. In cases where such bounds are not precisely defined, arbitrary bound values may be specified, but the procedure does not distinguish between loose bounds and tight bounds. i.e. no distinction between flexible and rigid constraints is made. All constraints are treated as rigid, and are not allowed to be violated. Practical situations may be different, and the bounds may be loosened or tightened accordingly.

Generally, lower bounds on the variable values will be rigid owing to physical limitations. Upper bounds will mostly be placed in view of size reduction, and will have to be varied if the constraints ( pressure angle and radius of curvature ) are not satisfied.

(iii) Number of divisions for constraint evaluation.

The accuracy to which the constraint gets evaluated depends on the number of divisions of the cam. Generally, 80 - 100 divisions of the 360° at the cam centre prove to be a good choice. This depends on the application, and larger cams may demand larger number of divisions.

(iv) Step size for gradient evaluation.

In evaluating the gradient by finite differentiation method, the step sizes ( defined as the vector  $( \Delta a_1, \dots, \Delta a_n )^T$  ) play an important role. If the step size is too small, the value of that gradient component will turn out to be zero. If too large, it will yield incorrect directions. A little judgement in this view is necessary before these values can be properly decided. Generally a step size of 1 - 2 % of the mean value of the variable in the specified range works well.

## 6.5.2 Consideration of different displacement curves.

The values of the constraints obtained at any stage will be to some extent dependent on the type of the displacement curve used. However, these are not of much significance if the second derivative, viz. the the acceleration is continuous. Otherwise, the radius of curvature values become very small yielding cusps, and sharp corners on the cam profile. Displacement curves having smooth acceleration

variation yield the best cam surface characteristics and therefore, the radius of curvature.

### 6.5.3 Methods of improving the algorithm.

(i) Using heuristics for locating the extremum values of the pressure angle and radius of curvature: This is done in view of reducing the computation during the cyclic evaluation of the constraints. One possible heuristic will be to search for the extremum in the vicinity of the location at which it occurred in the previous search, and use some quick search technique to locate it precisely.

(ii) Using other techniques for step modification: Since the point at which the line of the search direction intersects the constraint boundary is found by iterative interpolation, it takes much computational time. Using an accelerated step technique, or fitting a quadratic might yield a better solution in some cases.

(iii) Checking the order of constraint evaluation: If the constraint which would be most commonly violated is known, then this constraint should always be evaluated first during the modification of the step size. Any other constraint should be checked for violation only if this constraint is satisfied.

## chapter 7. IMPLEMENTATION.

The theory regarding the design of the cam modulated linkage type mechanical robots, followed by the optimization procedure to minimize the cam size was explained in the previous chapters. A software incorporating these two has been developed and implemented on the Apollo-Nexus 3000 ( b & w ) workstations. Details regarding the implementation are described in this chapter.

The system has been developed in C, and primitive graphic resources provided on the Apollo workstations have been used for all the graphics involved. The system developed is interactive in nature, and provides user control at all stages of design.

### 7.1 Scope and assumptions.

The procedure of optimization is included in the system as a part of the design of the CMLs. However, the optimization procedure can also be invoked independently.

It is assumed that the specified trajectories will always be two variable, two dimensional trajectories, in the x-y plane. Though mechanisms for more than 2 dimensional trajectories can be designed, they will not be displayed in three dimensions. Instead, they will appear as x-y plots in 2 dimensions.

The cams that can be used are of the disc type, with oscillating and reciprocating, and roller and flat faced follower combinations. Four bar linkages ( prismatic or revolute joints ) with the number of vectors upto eight forming the

loop can be designed. ( More than eight vectors will almost never be needed. ) Optimization of the cam-follower systems is based on the objective of cam size, and is made possible for reciprocating and oscillating roller follower types. Optimization is not necessary for flat faced followers.

The Zoutendijk's method of nonlinear optimization is used for the design of the follower parameters, and the Newton-Raphson's algorithm for the synthesis and analysis of linkages.

The assembly includes the design of the assembly dependent follower parameters. The type of assembler used has been given no consideration, and the user needs to decide the nature of the joints in the linkage based on the type of the assembler he chooses to use.

## 7.2 Data structures.

The important data structures used in the system comprise those for the representation of the trajectory, linkages and cam-follower mechanisms.

The trajectory is stored as a linked list of motion sections. The structure representing each motion section contains information about the type of space curve followed by the end effector in that section, ( i.e. a straight line, circular path, etc ) the time variation of this space curve, ( linear, harmonic, cycloidal, etc. ); the end points of the trajectory in terms of the x and y coordinates, and the starting and the terminating time instant of that section. Obviously, the terminating instant of the last motion section of the trajectory represents the cycle time needed to trace this trajectory.

The kinematics of the end effector at small time intervals throughout the motion cycle, is stored in terms of the resolved components of motion in x and y

direction, each in an array of structures, with each structure representing the kinematics at one instant of time. This may also be directly filled by the user without forming the linked list of the motion sections.

The linkage is stored as a structure consisting of the following information: the number of the joints with the nature of each ( revolute, prismatic, immovable ); the flags deciding whether the vectors are of constant or variable lengths, and whether the angles between two vectors are fixed or variable; and a configuration of this linkage for reference, to be taken as the initial point during analysis. These fields describe a linkage completely. In addition, the variables of analysis, and the maximum and minimum displacements of the output link are also stored.

During the analysis of the linkage motion, ( that needed for cam profile synthesis, ) a reverse linkage of exactly the same data type as above is formed, and the kinematics at small time intervals around the time cycle is stored in an array of structures representing instantaneous motion as described above. The reason to use arrays here is to permit a quick access to the kinematics at any point since this will be very frequently used, especially during the optimization of the follower parameters. Also, the number of divisions in which the cam surface is divided is usually in the range of 100 - 120.

The structure representing a cam mechanism consists of two fields. The follower parameters form one field, and are stored in arrays with predefined positions for each parameter. The other field is the cam profile, and this is stored as an array of points expressed in their x-y coordinates at small intervals along the cam profile.

A table illustrating these data structures and their fields, is presented in

Trajectory: doubly linked list of motion sections.

Motion section: record.

fields:

- motion section number (id)
- space curve id.
- time curve id.
- space function parameters ( array )
- time function parameters ( array )
- pointer to the previous motion section.
- pointer to the next motion section.

Linkage: record.

fields:

- number of vectors in the loop.
- joint types ( array )
- flag for variable link lengths. ( array )
- flag for variable included angles. ( array )
- configuration for reference.
- information regarding the variables of analysis.
- maximum and minimum output displacements.

linkage configuration: record.

fields:

- link lengths. ( array )
- orientations. ( array )

Cam mechanism: record.

fields:

- follower parameters. ( array )
- cam profile ( array of coordinate points )

End effector kinematics: double array of instantaneous kinematics.  
( number of dimensions X number of divisions )

Follower kinematics: double array of instantaneous kinematics.  
( number of dimensions X number of divisions )

Instantaneous kinematics: record.

fields:

- parameter of motion ( time / cam rotation angle )
- displacement.
- velocity.
- acceleration.

Table 7.1. Primary data structures.

Fig. 7.1.

### 7.3 Programme structure.

The programme is interactive in nature. All the modules are organized in such a way that they form infinite loops embedded one inside another which can be exited at the will of the user.

The programme is divided into four major modules as follows:

- trajectory specification.
- synthesis of the mechanisms.
- analysis of the mechanisms.
- assembly.

Each of these is described in the following sections.

#### Trajectory specification.

This module performs the following three functions.

1. Building up of the trajectory, section by section.
2. Determination of the resolved components of the end effector motion.
3. Display of the generated trajectory, and the end effector kinematics.

Building up of one motion section consists essentially of the identification of the space curve, its time variation, and determining the extent of motion with respect to both of these. Straight lines and circular arcs are possible, while the time variation can be linear, harmonic, or cycloidal. The user can define any other path or time variation if necessary.

Determination of the end effector kinematics is based on the curves, and time variations defined earlier, or direct generation of the values.

## Synthesis.

Synthesis comprises of two sub-modules, viz. Linkage synthesis and cam design.

Linkage synthesis consists of generating the data for the synthesis, and the actual synthesis procedure. Two different modules are used to perform these two functions. The synthesis information collecting module gathers from the user, information regarding the number of variables to be synthesised, the coordinated input and output motion values, etc. The synthesis module processes this data to produce the values of the linkage dimensions.

The cam design also, comprises of two different modules. One generating the values of the follower parameters, and the other designing the cam profile based on this. In the profile design, the follower type is identified, and a number of points along the periphery of the cam are generated.

There are various modules in the follower parameter determination which bring about the optimization of the cam size. An input module takes the data needed for the optimization from the user. ( the initial values of the variables, the step sizes, etc., ) The actual optimization module employs the Zoutendijk's method, and invokes two subprogrammes in this process. One is for the determination of the optimal search direction using the simplex algorithm, and the other is for the step size determination based on the direct root method. There is another module which continuously interacts between the Zountendijk's procedure and the follower optimization data, to determine the objective function, constraints, etc. .

## Analysis.

Here also, we have a subdivision in terms of the linkages, and cams. A linkage configuration analysis algorithm based on the Newton-Raphson's technique is employed to determine the kinematics of the linkage at different time instances. Kinematics of the cam-follower system are based on a similar approach as that of the linkage analysis. The results of the analysis can be viewed in the form of various graphs, and animated displays of the linkage. A graph sketching module using the calls to the primitive graphic resources in the workstation, is employed for this purpose.

## Assembly

Assembly of the mechanisms is governed by two modules. One module determines the assembly dependent follower parameters, and the other determines the location of the cam centre.

A chart illustrating all these modules appears in Fig. 7.2

## 7.4 User interaction.

The system is completely user interactive in nature. At every stage, the user has a large control in deciding the flow of the programme. Various menus appearing at the left hand side of the input pad, prompt the user to take an appropriate action.

## I/O

All input is through the keyboard. However, it is possible for the user to

## TRAJ ( trajectory specification )

- Editing a trajectory. (optional)
  - Motion section addition.
  - Motion section deletion.
  - Refilling a motion section.
- Determination of end effector kinematics.
- Display of trajectory.
  - Path followed in space.
  - Variation of the end effector kinematics over the cycle.

## SYNTHESIS.

- LINKAGE.
  - Specification of the nature of joints.
  - Determination of the dimensions.
    - User specified dimensions.
    - Synthesised dimensions.
      - Specification of input-output coordination.
      - Solution of 2m loop closure equations.
- CAM
  - Determination of the follower parameters.
    - User specified dimensions.
    - Optimized dimensions.
      - Specification of bounds, initial values etc.
      - Application of the Zoutendijk's procedure.
  - Determination of the cam profile coordinates.

## ANALYSIS.

- LINKAGE.
  - plots of the variation of any parameter of the linkage around the cycle. (Disp, vel., accln)
  - Cyclic recursive display. (superimposed)
  - Animated display.
- CAM
  - profile
  - follower kinematics. ( disp., velocity, accln. )
  - Pressure angle.
  - Radius of curvature.

## ASSEMBLY.

- Location of the cam centre.
- Determination of assembly dependent parameters.

|                                   |
|-----------------------------------|
| Table 7.2 Programme organization. |
|-----------------------------------|

enter data from the consol, or a file, or both, intermittently. This facilitates the inputting of numeric data through files, and governing the direction of flow through the consol. The output device is the terminal, and the graphs and other results are displayed on it. It is possible to direct this output to a file, and a printer plot of the displayed figure can also be taken.

### Utilities.

The linkage, trajectory, cam mechanism, or the kinematics of the follower and the end effector, can be stored and saved, so that they can be retrieved later on for a next run of the programme.

Editing facilities have been provided for the trajectory, so that the user can interactively build a trajectory of the desired shape from the coded functions, and other user defined functions. The output is in the forms of sketches and graphs, and numeric tables. All the figures can be scaled, or moved by moving the window. The extent of the graph may also be controlled.

Help regarding the design procedure has been incorporated at different levels of operation, and is displayed in a separate window appearing at the top of the screen. Helpful messages and warnings are also displayed time to time during the run.

### Error handling.

Error handling has been done to ensure a correct input from the user. For this purpose also, the programme is so organized, that it runs in an infinite loop, prompting the user regarding the various possible alternatives, and does not exit the loop unless the proper input is given. This includes taking the input amongst

the valid choices only, and to ensure a proper flow of the programme at certain places, for eg. the trajectory cannot be viewed unless it is built first, and the like. At some places, it is also possible to abort the procedure, and return the control to a higher level.

## 7.5 Programme control flow.

Though the flow of the programme is governed by the user, the processing done from the specification of the trajectory, to the final assembly, is briefly summarized in the present section. This is also illustrated in Fig. 7.3.

The top-most level decides the course to be taken initially. Various possibilities are the specification, synthesis, analysis, or assembly.

Specification of the trajectory is done in the module TRAJ. The user fills the linked list of the motion sections for as many motion sections as desired. Facilities like adding, refilling, and deleting a motion section can be made use of for this. When the trajectory so formed is verified by the user, the end effector kinematics are calculated. The building of the trajectory is optional, and the end effector kinematics can be directly specified. At this stage the user has to decide upon the number of divisions the trajectory has to be divided into for the processing to be done in the succeeding modules. The end effector kinematics, and the trajectory can be viewed, and any modifications if necessary, can be done by going back to the trajectory editor.

Two possible options in the synthesis are that of linkages and cams. Linkages are designed in the LINKAGE\_SYNTHESIS module based on the end effector kinematics. The extremities of the displacement are determined, and are displayed to facilitate the user to specify the coordinated input and output

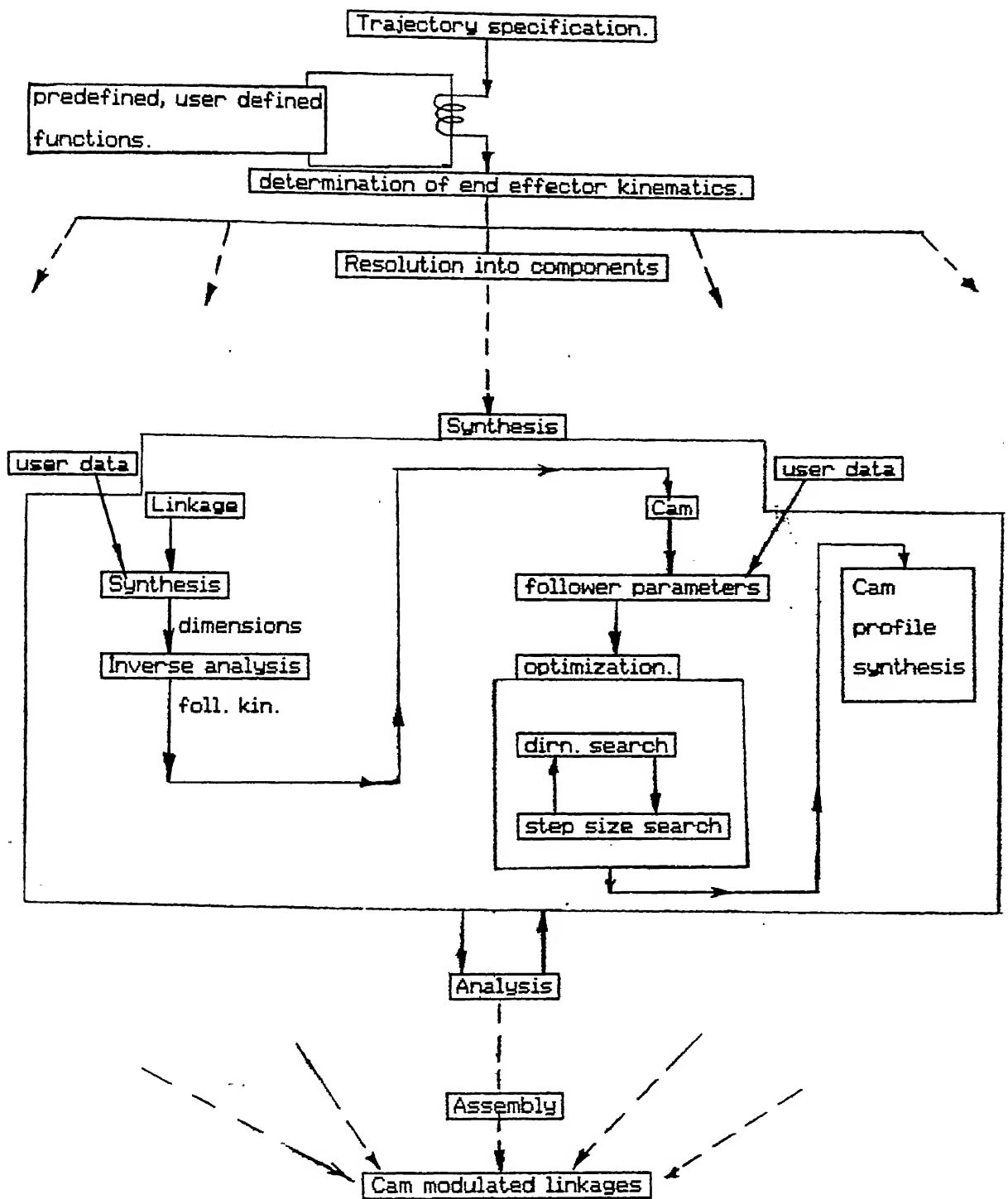


Fig. 7.3. Programme control flow.

values. The type of linkage depending upon the joint configuration is first taken in form the user. This is followed by the specification of the input output coordinated values. The linkage is synthesised on the basis of these data, and the results are presented. If the values are not satisfactory, or a solution is not possible with the specified input, the linkage can be resynthesised with modified input values.

Cam design in the *CAM\_SYNTHESIS* module comprises of the optimization of the follower parameters, and the profile synthesis. Direct specification of the follower parameters is also possible. In the optimization, the input is first accepted regarding the constraints, bounds on variables etc. and the module for the Zoutendijk's method is invoked for the optimization. The cam profile is then designed based on the designed follower parameters, and the follower kinematics.

Various parameters of motion are then analysed in the *ANALYSIS* module, to test the performance of the synthesised mechanism. This consists of the display of various plots like the velocity, acceleration of the different components of the mechanism, pressure angle and radius of curvature of the cam profile, and the profile itself. The linkages can be displayed for the complete motion cycle with one configuration superimposed on another, or in an animated manner.

Any of the designed mechanisms can be resynthesised if their performance is not found to be satisfactory. Finally, the mechanisms in the different directions are assembled in the module *ASSEMBLY*.

## chapter 8. CONCLUSIONS AND FURTHER WORK

### 8.1 Conclusions.

In the first part of this work, issues regarding the kinematic synthesis of a multi degree-of-freedom mechanism to generate a specified trajectory, were studied. A design scheme for this pupose has been developed.

It was seen that it is possible to generate any trajectory, differentiable, or non-differentiable, with these mechanisms, provided the higher derivatives of the components of the motion are differentiable. Cusps appear on the cam profile when a single CML is used to generate a non-differentiable trajectory.

As a part of the design of the CMLs, a generalised formulation of a four bar planar linkage for kinematic synthesis and analysis was done. The linkages were seen to serve purposes of motion magnification and type conversion ( angular to linear and vice-versa ) . It was further observed, that in the absence of the linkages, the cam size in many cases turns out to be impracticably large.

The major hurdle in employing this class of mechanisms for more than two degrees-of-freedom was found to be the limitation on the motion assemblers to maintain the independence of motion in each direction. ( i.e. for each degree of freedom. )

Motion coordination was found to play an important role in determining the final trajectory generated by these mechanisms, and it was also observed that some flexibility in view of having modified trajectories could be extracted by

manipulating the phase angle between two cams.

In the second part, a method for the optimal design of cam-follower systems was proposed. It was seen that it is possible to optimize the size of a cam subject to the pressure angle and radius of curvature constraints. The procedure developed was shown to be applicable to the reciprocating and oscillating roller followers. It was observed that this sort of optimization is not necessary for flat faced followers.

Finally, in the third part, an interactive software was developed incorporating the complete design of CMLs.

## 8.2 Scope for further work.

The present work on the CML type mechanical robots is based on the kinematics of the end effector and other components of the mechanism. However, the range of output motion itself depends on the dynamic characteristics of the various moving members, particularly the assemblers. This fact can be explored by modeling the system designed, from dynamic considerations, and modifying or resynthesising various parameters if necessary.

It was mentioned that the input-output motion relationships in the linkages may help in simplifying the cam profile. In the present work, linkage design is based only on the input-output motion coordination. If it could be done with a view of simplifying the cam profile, the mechanisms can be made applicable to a large number of seemingly difficult trajectories also.

Multiple loop chains and 3-d cams too, could have been used in these mechanisms. The advantages, and limitations of using these can be studied.

An important need is that of developing different types of motion

assemblers so that the principle suggested becomes widely applicable, especially to three and more degrees-of-freedom.

In the optimization of the follower parameters, only disc cam mechanisms have been considered. This principle may be applied to 3-D cams as well. The effects of dynamic limitations along with the kinematic constraints can also be included. Objective functions other than the cam size, for eg. based on the rigidity or dynamic performance characteristics can be considered.

## REFERENCES.

1. Chen F.Y.

**Mechanics and Design of Cam Mechanisms.**

Pergamon Press Inc., New-York, 1982.

2. Dhande S.G. and Chakraborty J.

**Kinematics and Geometry of Planar and Spatial Cam Mechanisms.**

Wiley Eastern Ltd., New-Dehli, 1977.

3. Dhande S.G. and Kale T.G.

**Optimal design of disc Cam Mechanisms.**

Proceedings of the Sixth World Congress on Theory of Machines and Mechanisms, 1983 (p. 1195).

4. Ganter M.A. and Uicker J.J. Jr.

**Design Charts for Disk Cams with Reciprocating Radial Roller Follower.**

Journal of Mechanical Design, July 1979, Vol. 101 (p. 465).

5. Hartenberg R.S. and Denavit J.

**Kinematic Synthesis of Linkages.**

McGraw Hill Publication Company, New-York, 1964.

6. Jenson P.W.

**Cam Design and Manufacture.**

Marcel Dekker Inc., New-York 1983.

7. Ghosh A. and Mallik A.K.

**Theory of Mechanisms and Machines.**

Affiliated East-West Press Private Ltd., New-Dehli, 1976.

8. Kohli D. and Singh Y.P.

**Synthesis of Cam-link Mechanisms for exact path generation.**

Machines and Mechanism Theory, Vol. 16, No. 4 (p. 447).

9. Maggiorie A. and Meneghetti U.

**Optimization of Cam Systems.**

Proceedings of the Seventh World Congress on Theory of Machines and Mechanisms. 1987 (p. 1653).

10. Rao S.S.

**Optimization: Theory and Applications.**

Wiley Eastern Ltd., New-Dehli, 1984.

11. Sandor G.M and Erdman A.G.

**Advanced Mechanism Design: Analysis and Synthesis.**

Prentice-Hall Inc., New-Jersey, 1984.

## appendix A. THE NEWTON-RAPHSON METHOD.

The Newton-Raphson's method is used for the solution of nonlinear simultaneous equations in the linkage synthesis and analysis. A few points are discussed here regarding its application. These are:

1. Brief description of the principle.
2. An initial point needed for the commencement of the algorithm.
3. Criterion which decides the termination of the process.
4. Error checking.

### Principle.

Let

$$\begin{aligned}e_1 &\equiv f_1(x_1, \dots, x_n) = 0, \\&\dots \dots \dots \\e_n &\equiv f_n(x_1, \dots, x_n) = 0,\end{aligned}\tag{A.1}$$

be the  $n$  equations in  $n$  variables. Let  $(x_{10}, \dots, x_{n0})$  be the approximate set of the values of the parameters, and let  $(\Delta x_1, \dots, \Delta x_n)$  be the corrections applied to this approximate set. Then, the equations with the new set of values become:

$$\begin{aligned}f_1(x_1 + \Delta x_1, \dots, x_n + \Delta x_n) &= 0, \\&\dots \dots \dots \\f_n(x_1 + \Delta x_1, \dots, x_n + \Delta x_n) &= 0.\end{aligned}\tag{A.2}$$

Expanding these by the Taylor's theorem, and neglecting the terms in higher powers of the corrections,

$$f_1 + \Delta x_1 \left[ \frac{\partial f_1}{\partial x_1} \right] + \dots + \Delta x_n \left[ \frac{\partial f_1}{\partial x_n} \right] = 0, \tag{A-1}$$

$$f_n + \Delta x_1 \left[ \frac{\partial f_n}{\partial x_1} \right] + \dots + \Delta x_n \left[ \frac{\partial f_n}{\partial x_n} \right] = 0. \quad (A.3)$$

where all the coefficients of the corrections, and the constants, i.e.  $(f_1, \dots, f_n)$  are evaluated at the current approximate values. These form  $n$  linear equations in  $n$  unknowns, and can be evaluated for the values of  $(\Delta x_1, \dots, \Delta x_n)$  by simple matrix transformations. Then, the second approximation can be found, and the process repeated till a satisfactory solution is reached.

#### Initial point.

Most of the time an initial point can be specified in the vicinity of which the solution is expected to lie, on the basis of one of the following.

1. A scaled drawing of the possible solution.
2. Approximate calculations neglecting a few terms.
3. Judgement based on the past experience.

The solution obtained depends on the initial point specified, and will be the closest possible solution from this point. The possibility of multiple solutions has to be explored through different sets of initial points.

#### Error checking.

This is necessary in view of the following.

1. Divergent solutions: At times due to the nonlinearity of the equations, the next point obtained may lie farther off from the solution than the current point. a check on the maximum number of iterations is necessary to govern such a situation.

2. Singularities: Many a times, the determinant of the coefficients of the variables in the linearized approximation may become zero. This indicates the existence of a singularity and a new initial point may have to be tried.

#### Termination criterion.

The solution is identified when the residual values of the equations being solved become nearly zero. This forms the termination criterion under normal circumstances. The errors mentioned above may occur sometimes, and the procedure needs to be terminated under such circumstances also. It may be retried with a different initial point.

## appendix B. EXPRESSIONS FOR CAM-FOLLOWER DESIGN

The analytical expressions to map the follower motion on the cam profile ( as shown in Sect. 2.4.2 ) are:

$$[M_c]_g (R)_{1c} = [M_f]_g (R)_{1f}. \quad (B.1)$$

$$(R)_{1c} = [M_c]_g^{-1} [M_f]_g (R)_{1f}. \quad (B.2)$$

where

$(R)_{1f}$  = position vector of the contact point in frame  $L_f$ ,

$[M_f]_g$  = transformation matrix from frame  $L_f$  to  $C_G$ .

$(R)_{1c}$  = position vector of the contact point in frame  $C$ ,

$[M_c]_g$  = transformation matrix from frame  $C$  to  $C_G$ .

Analytical expressions for all the terms in the matrix  $[M_c]_g$  are determined in section 2.4.2. The matrix  $[M_f]_g$  and the vector  $(R)_{1f}$  depend on the type of the follower being used, and are determined here for four different types of followers. Since it is possible to get analytical expressions for the  $x$  and  $y$  coordinates of the point on the cam profile, these are determined for each of the case with the help of equation B.2.

Expressions for the pressure angle and radius of curvature for each case based on the following definitions have also been determined.

The pressure angle  $\psi$  is defined as the angle between the direction of the applied force on the follower ( i.e. the common normal to the cam and follower surfaces,  $\underline{g}$  ), and the direction of the velocity vector ( $\underline{v}$ ) of the follower at the

point of contact.

$$\text{Thus,} \quad \cos \psi = \underline{e} \cdot \underline{v}. \quad (\text{B.3})$$

The radius of curvature is defined as the reciprocal of the principal curvature of the cam profile at the point of contact. The curvature for two dimensional curves is given as: [2]

$$\kappa = \frac{N}{G}; \quad (\text{B.4})$$

where N and G are the first and second quadratic forms for planar curves, and for a cam profile are given as:

$$N = \frac{\partial \underline{e}}{\partial \theta_c} \cdot \frac{\partial \underline{R}}{\partial \theta_c}, \quad (\text{B.5})$$

and,

$$G = \frac{\partial \underline{R}}{\partial \theta_c} \cdot \frac{\partial \underline{R}}{\partial \theta_c}. \quad (\text{B.6})$$

where  $\underline{R}$  is the position vector of the contact point. Both  $\underline{e}$  and  $\underline{R}$  need to be expressed in the same frame of reference.

#### Translating flat faced follower.

Ref. Fig. B.1. In the frame of reference  $L_f$ , the velocity of the follower is given as:

$$\underline{v}_f = (0, \omega_c \cdot s_1', 0). \quad (\text{B.7})$$

where,  $s_1 \equiv$  the follower displacement,

$$\text{and} \quad s_1' = \frac{ds_1}{d\theta_c}.$$

The relative velocity between the cam and follower surfaces is given as:

$$\underline{v}_r = \omega_c \{ (s_1 + s_0), (s_1' - \delta - a), 0 \}^T \quad (\text{B.8a})$$

The common normal to the cam and follower surfaces is given as:

$$\underline{e} = (0, 1, 0)^T. \quad (\text{B.8b})$$

Then from equation B.3,

$$\delta = s_1' - a. \quad (B.9)$$

The radius vector on the follower surface can then be written as:

$$(R)_{1f} = (\delta, s_1, 0, 1)^T. \quad (B.10)$$

The matrix  $[M_f]_g$  is given as:

$$[M_f]_g = \begin{bmatrix} 1 & 0 & 0 & a \\ 0 & 1 & 0 & s_0 \\ 0 & 0 & 1 & 0 \\ 0 & 0 & 0 & 1 \end{bmatrix} \quad (B.11)$$

Then, from equation B.2,

$$(R)_{1c} = \begin{bmatrix} \cos\theta_c & \sin\theta_c & 0 & a \cos\theta_c + s_0 \sin\theta_c \\ -\sin\theta_c & \cos\theta_c & 0 & -a \sin\theta_c + s_0 \cos\theta_c \\ 0 & 0 & 1 & 0 \\ 0 & 0 & 0 & 1 \end{bmatrix} \cdot (R)_{1f} \quad (B.12)$$

$$= (x_p, y_p, z_p, 1),$$

$$\text{where, } x_p = (a + \delta) \cos\theta_c + (s_0 + s_1) \sin\theta_c,$$

$$y_p = -(a + \delta) \sin\theta_c + (s_0 + s_1) \cos\theta_c,$$

$$\text{and } z_p = 0. \quad (B.13)$$

From equations B.3, and B.8, we get,

$$\psi = 0. \quad (B.14)$$

Also, expressing  $\underline{g}$  in the frame C, and letting  $\underline{R} = (R)_{1f}$ , from equations B.4, B.8, and B.10, we get,

$$X = \frac{1}{(s_1'' + s_1 + s_0)}, \quad (B.15)$$

and

$$\rho = \frac{1}{X}. \quad (B.16)$$

Translating roller follower.

The procedure is exactly similar to the one described above, and only the expressions involved are given here in reference to Fig. B.2.

The velocity of the follower in the frame of reference  $L_f$ :

$$v_f = (0, \omega_c \cdot s_1', 0). \quad (B.17)$$

$s_1 \equiv$  the follower displacement,

$$s_1' = \frac{ds_1}{d\theta_c}.$$

Relative velocity between the cam and follower surfaces:

$$v_r = \omega_c \{ -(s_1 + s_0 + r_r \sin \theta_r), (-s_1' + r_r \cos \theta_r + a), 0 \}^T \quad (B.18)$$

Common normal to the cam and follower surfaces:

$$g = \{ \cos \theta_r, \sin \theta_r, 0 \}^T. \quad (B.19)$$

Condition of contact.

$$-(s_0 + s_1) \cos \theta_r + (a - s_1') \sin \theta_r = 0. \quad (B.20)$$

$$\theta_r = \tan^{-1} \left( \frac{-(s_0 + s_1)}{-(a - s_1')} \right). \quad (B.21)$$

At  $s_1 = 0$ ,  $\theta_r$  lies in the third quadrant.

Profile.

$$\{R\}_{1f} = \{r_r \cos \theta_r, (s_1 + r_r \sin \theta_r), 0, 1\}^T. \quad (B.22)$$

$$[M_f]_g = \begin{bmatrix} 1 & 0 & 0 & a \\ 0 & 1 & 0 & s_0 \\ 0 & 0 & 1 & 0 \\ 0 & 0 & 0 & 1 \end{bmatrix} \quad (B.23)$$

$$(R)_{1c} = \begin{bmatrix} \cos\theta_c & \sin\theta_c & 0 & a \cos\theta_c + s_0 \sin\theta_c \\ -\sin\theta_c & \cos\theta_c & 0 & -a \sin\theta_c + s_0 \cos\theta_c \\ 0 & 0 & 1 & 0 \\ 0 & 0 & 0 & 1 \end{bmatrix} \cdot (R)_{1f} \quad (B.24)$$

$$= (x_p, y_p, z_p, 1), \quad (B.25)$$

$$x_p = r_r \cos(\theta_r - \theta_c) + a \cos\theta_c + (s_0 + s_1) \sin\theta_c,$$

$$y_p = r_r \sin(\theta_r - \theta_c) - a \sin\theta_c + (s_0 + s_1) \cos\theta_c,$$

$$z_p = 0. \quad (B.26)$$

Pressure angle.

$$\psi = \sin^{-1} \|\sin\theta_r\|. \quad (B.27)$$

Curvature.

$$\chi = \frac{G}{N}, \quad (B.28)$$

$$N = -(1 - \theta_r') [r_r(1 - \theta_r') + (a - s_1') \cos\theta_r + (s_0 + s_1) \sin\theta_r] \quad (B.29)$$

$$G = r_r^2(1 - \theta_r')^2 + (s_0 + s_1)^2 + (a - s_1')^2 + 2 r_r(1 - \theta_r') [(a - s_1') \cos\theta_r + (s_0 + s_1) \sin\theta_r]. \quad (B.30)$$

$$\theta_r' = \frac{s_1''(a - s_1') + s_1'''(s_0 + s_1)}{(s_0 + s_1)^2 + (a - s_1')^2} \quad (B.31)$$

Radius of curvature.

$$\rho = \frac{1}{\chi}. \quad (B.32)$$

Oscillating flat faced follower.

The velocity of the follower in the frame of reference  $L_f$ : (Fig. B.3)

$$\underline{v}_f = \delta \cdot \omega_c \cdot \theta_f' \{ -\sin\theta_f, \cos\theta_f, 0 \}^T. \quad (B.33)$$

$\theta_f \equiv$  the follower displacement,

$$\theta_f' = \frac{d\theta_f}{d\theta_c}.$$

Relative velocity between the cam and follower surfaces:

$$\underline{v}_r = \omega_c(1 + \theta_f') \{ -\delta\sin\theta_f, (\delta\cos\theta_f - a / (1 + \theta_f')), 0 \}^T \quad (B.34)$$

Common normal to the cam and follower surfaces:

$$\underline{e} = \{ \sin\theta_f, -\cos\theta_f, 0 \}^T. \quad (B.35)$$

Condition of contact.

$$\delta(1 + \theta_f') = a \cos\theta_f. \quad (B.36)$$

Profile.

$$\{R\}_{1f} = \{ \delta \cos\theta_f, \delta \sin\theta_f, 0, 1 \}^T. \quad (B.37)$$

$$[M_f]_f = \begin{bmatrix} -\cos\theta_f & \sin\theta_f & 0 & a \\ \sin\theta_f & -\cos\theta_f & 0 & 0 \\ 0 & 0 & -1 & 0 \\ 0 & 0 & 0 & 1 \end{bmatrix} \quad (B.38)$$

$$\{R\}_{1c} = \begin{bmatrix} -\cos(\theta_c + \theta_f) & \sin(\theta_c + \theta_f) & 0 & a \cos\theta_c \\ \sin(\theta_c + \theta_f) & \cos(\theta_c + \theta_f) & 0 & -a \sin\theta_c \\ 0 & 0 & 1 & 0 \\ 0 & 0 & 0 & 1 \end{bmatrix} \cdot \{R\}_{1f} \quad (B.39)$$

$$= \{ x_p, y_p, z_p, 1 \},$$

$$\begin{aligned}
 x_p &= -\cos(\theta_c + \theta_f) \delta + a \cos \theta_c, \\
 y_p &= \sin(\theta_c + \theta_f) \delta - a \sin \theta_c, \\
 z_p &= 0.
 \end{aligned} \tag{B.40}$$

Pressure angle.

$$\psi = 0. \tag{B.41}$$

Curvature.

$$\chi = \frac{(1 + \theta_f')^2}{\theta_f'' \delta + (1 + 2\theta_f')a \sin \theta_f}, \tag{B.42}$$

Radius of curvature.

$$\rho = \frac{1}{\chi}. \tag{B.43}$$

Oscillating roller follower.

Velocity of the follower in the frame of reference  $L_f$ :

$$\underline{v} = \omega_c \cdot \theta_f' \begin{bmatrix} -[l_f \sin \theta_f + r_f \sin(\theta_r + \theta_f)] \\ [l_f \cos \theta_f + r_f \cos(\theta_r + \theta_f)] \\ 0 \end{bmatrix} \tag{B.44}$$

$\theta_f \equiv$  the follower displacement,

$$\theta_f' = \frac{d\theta_f}{d\theta_c}.$$

Relative velocity between the cam and follower surfaces:

$$\underline{v} = \omega_c \begin{bmatrix} (1 + \theta_f') [l_f \sin \theta_f + r_f \sin(\theta_r + \theta_f)] \\ (1 + \theta_f') [l_f \cos \theta_f + r_f \cos(\theta_r + \theta_f)] - a \\ 0 \end{bmatrix} \tag{B.45}$$

Common normal to the cam and follower surfaces:

$$\underline{e} = (\cos(\theta_r + \theta_f), \sin(\theta_r + \theta_f), 0)^T. \tag{B.46}$$

Condition of contact.

$$-(a \sin \theta_r) \cos \theta_r + ((1 + \theta_r') l_r - a \cos \theta_r) \sin \theta_r = 0. \quad (B.47)$$

$$\theta_r = \tan^{-1} \left( \frac{(a \sin \theta_r)}{((1 + \theta_r') l_r - a \cos \theta_r)} \right). \quad (B.48)$$

Profile.

$$\{R\}_{1f} = (l_r + r_r \cos \theta_r, \quad r_r \sin \theta_r, \quad 0, \quad 1)^T. \quad (B.49)$$

$$[M_r]_g = \begin{bmatrix} -\cos \theta_r & \sin \theta_r & 0 & a \\ \sin \theta_r & -\cos \theta_r & 0 & 0 \\ 0 & 0 & -1 & 0 \\ 0 & 0 & 0 & 1 \end{bmatrix} \quad (B.50)$$

$$\{R\}_{1c} = \begin{bmatrix} -\cos(\theta_c + \theta_r) & \sin(\theta_c + \theta_r) & 0 & a \cos \theta_c \\ \sin(\theta_c + \theta_r) & \cos(\theta_c + \theta_r) & 0 & -a \sin \theta_c \\ 0 & 0 & 1 & 0 \\ 0 & 0 & 0 & 1 \end{bmatrix} \cdot \{R\}_{1f} \quad (B.51)$$

$$= (x_p, \quad y_p, \quad z_p, \quad 1),$$

$$x_p = -l_r \cos(\theta_c + \theta_r) - r_r \cos(\theta_r + \theta_c + \theta_r) + a \cos \theta_c$$

$$y_p = l_r \sin(\theta_c + \theta_r) + r_r \sin(\theta_r + \theta_c + \theta_r) - a \sin \theta_c$$

$$z_p = 0. \quad (B.52)$$

Pressure angle.

$$\cos \psi = \frac{l_r \sin \theta_r}{\sqrt{l_r^2 + r_r^2 + 2r_r l_r \cos \theta_r}} \quad (B.53)$$

Curvature.

$$\chi = \frac{-(1 + \frac{k_1}{k_2})}{r_r} \quad (B.54)$$

$$k_1 = [(1 + \theta_r')^2 l_r^2 \cos^2 \theta_r - a^2 \cos^2(\theta_r + \theta_f)]^2 \quad (B.55)$$

$$k_2 = r_r [\theta_r'' l_r \sin \theta_r - \theta_r' a \cos(\theta_r + \theta_f)]$$

$$-\sqrt{k_1} [(1 + \theta_r')^2 (l_r \cos \theta_r + r_r) - a \cos(\theta_r + \theta_f)] \quad (B.56)$$

Radius of curvature.

$$\rho = \frac{1}{X} \quad (B.57)$$

## appendix C. EXPRESSIONS FOR THE ASSEMBLY OF THE CMLs.

Expressions which are used for the location of the cam centre after determination of the follower parameters of each CML, are derived here. Also, a few points as regards the assembly dependent follower parameters are mentioned.

### C.1 Location of the cam centre.

Location of the cam centre depends upon the combination of the follower type that is being used, and expressions for each are determined. Different combinations of oscillating and reciprocating followers are considered. For each case the determination forms a simple geometric point location problem.

#### Two oscillating followers.

The cam centre in this case is decided by the follower pivot to cam centre distance. Locus of the cam centre with respect to the follower pivot of each CML, is a circular arc with centre at the follower pivot, and radius equal to the pivot-to-cam-centre distance. The cam centre should lie at the intersection of the two circular loci.

If  $(x_1, y_1)$  and  $(x_2, y_2)$  are the global coordinates of the follower pivots of the two CMLs, and  $a_1$  and  $a_2$  the corresponding distances from the cam centre, then from simple geometry, the coordinates of the centre can be given as the point of intersection of the two circles:

$$(x - x_1)^2 + (y - y_1)^2 = a_1^2, \quad (C.1)$$

$$\text{and} \quad (x - x_2)^2 + (y - y_2)^2 = a_2^2, \quad (\text{C.2})$$

One oscillating follower and one translating follower.

The pivot-to-cam-centre distance of the oscillating follower, and the offset of the translating follower are the parameters that decide the location of the cam centre. The loci of the cam centre are circular and that of a straight line for the oscillating, and the translating follower respectively.

If  $(x_1, y_1)$  are the global coordinates of the follower pivot of the oscillating follower, and  $(x_2, y_2)$  that of a fixed point in space for the CML with a translating follower, and  $a_1$  and  $a_2$  the pivot-to-cam-centre-distance, and the offset respectively, then as before, the coordinates of the centre can be given as the point of intersection of the circle

$$(x - x_1)^2 + (y - y_1)^2 = a_1^2, \quad (\text{C.3})$$

and the straight line

$$(y - y_2 - a_2 \cos \theta) = \tan \theta (x - x_2 + a_2 \sin \theta), \quad (\text{C.4})$$

where  $\theta$  is the orientation of the line of reciprocation of the follower with respect to the global x axis.

Two translating followers.

In this case, the locus of the cam centre with respect to both the followers is a straight line and the centre should lie at the point of intersection of these. The two straight lines are given as:

$$(y - y_1 - a_1 \cos \theta_1) = \tan \theta_1 (x - x_1 + a_1 \sin \theta_1), \quad (\text{C.5})$$

$$\text{and} \quad (y - y_2 - a_2 \cos \theta_2) = \tan \theta_2 (x - x_2 + a_2 \sin \theta_2). \quad (\text{C.6})$$

In all these cases, the coordinates of the cam centre can be found by solving the two simultaneous equations. The number of solutions obtained can be either two, one or none. If two solutions are obtained, the one forming a more compact assembly may be selected. If no consistent solution is obtained with the two simultaneous equations, the fixed points of both the CMLs may be shifted to other possible locations, and the assembly tried again. It might also become necessary to modify the values of the offset and / or the pivot-to-cam-centre distance.

## C.2 Assembly dependent parameters.

Since the location of the cam centre is determined after the design of the CMLs, it becomes necessary to transfer the temporary cam centre to that position. Since this might change the values of the follower displacement, two parameters, viz. the follower rod length, and the the follower arm angle, are designed at a later stage. The values of these are determined from the coordinates of the reference point on the follower, and the cam centre. (Fig. 2.7, 2.8).

### Discussion.

A common problem in the analysis of linkages is that one obtains geometric inversions of the linkage instead of the real solution at the specified value of the input. This happens since the loop closure equations are satisfied with that configuration also. Actually this inverted configuration is generally not attainable in the motion cycle unless the mechanism is disassembled and reassembled in an inverted manner.

However, with the Newton-Raphson's method, we always get that solution which is in the vicinity of the initial point. Thus, if at every stage a configuration near to the actual solution is used as the initial point, the required solution only will be reached, and not its geometric inversion. For the cyclic analysis, this has the effect of moving the linkage through small discrete steps around the entire motion range of the input as shown in Figs 3.4, 3.5.

However, there are problems when both the geometric inversions are nearly equally close to the initial point. This happens in the case of rocker mechanisms, at points near the dead center of the input link. In such mechanisms, both the inversions are possible with the same linkage assembly - one while approaching the dead center, and the other while reproaching. Physically, the path taken up by the coupler and the output link are determined by their inertias. Generally, they tend to move in a direction in which they were previously moving. Since inertias cannot be modeled in the Newton-Raphson's method, the results obtained may not be true to the real. There is a small computational trick however, which can be used

to overcome this problem.

The fact that both, the coupler, and the output link continue to move in the same direction as before, can be made use of. While specifying the initial point in the vicinity of the extremity, the values of the variables determining the motions of these links may be incremented in the direction of their movement. i.e. if  $s_{prev}$ ,  $s_{cur}$ , and  $s_{next}$  are the previous, current, and next values of the variables, then we know that  $(s_{cur} - s_{prev})$  and  $(s_{next} - s_{cur})$  have the same signs. For small intervals,

$$s_{cur} - s_{prev} \approx s_{next} - s_{cur} \quad (3.7a)$$

or, 
$$s_{next} = 2 s_{cur} - s_{prev}. \quad (3.7b)$$

This can be used as the initial value for the next point, and the loop closure equations solved as before. Using this technique, we can hope to get the real solution.

If however, a dwell occurs at the extreme position of the input, then one would not be certain about the direction in which the coupler and the output link would move, since  $s_{cur} = s_{prev}$ . Physically also, there would be no control over the direction of movement in such situations, since it will be determined by other operation dependent considerations like vibrations, clearances, etc. It is advisable not to use rocking mechanisms with a dwell at the input extremity.

020601

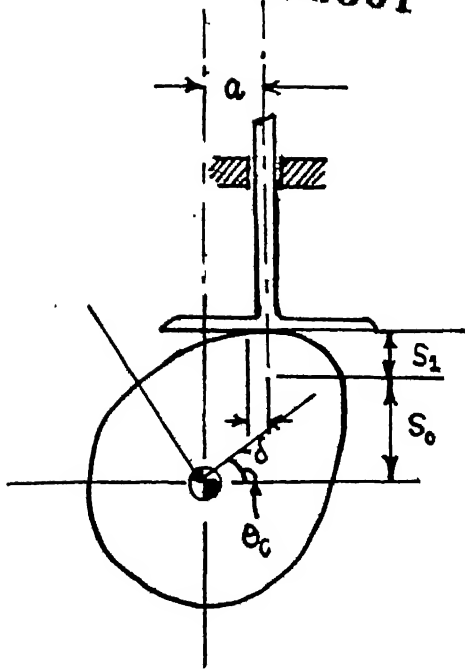


Fig B.1

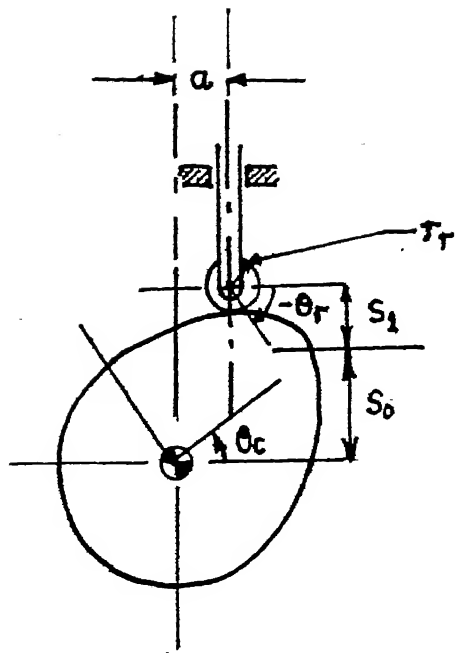


Fig B.2

Fig B.3

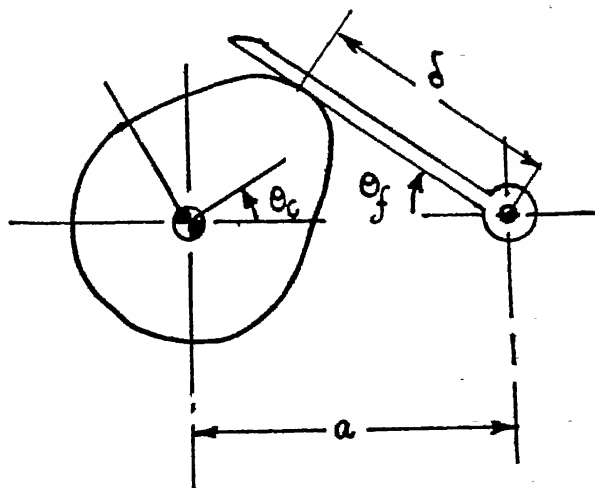


Fig B.4.

